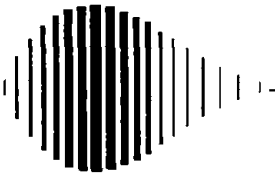

A Semi-Empirical Analysis of Strong-Motion Peaks in Terms of Seismic Source, Propagation Path and Local Site Conditions

by

M. Kamiyama[1], M.J. O'Rourke[2] and R. Flores-Berrones[3]

September 9, 1992

Technical Report NCEER-92-0023

NCEER Project Number 90-3012

NSF Master Contract Number BCS 90-25010
and
NYSSTF Grant Number NEC-91029

1 Visiting Research Professor, Department of Civil and Environmental Engineering, Rensselaer Polytechnic Institute
2 Professor, Department of Civil and Environmental Engineering, Rensselaer Polytechnic Institute
3 Visiting Research Professor, Department of Civil and Environmental Engineering, Rensselaer Polytechnic Institute

NATIONAL CENTER FOR EARTHQUAKE ENGINEERING RESEARCH
State University of New York at Buffalo
Red Jacket Quadrangle, Buffalo, NY 14261

PREFACE

The National Center for Earthquake Engineering Research (NCEER) was established to expand and disseminate knowledge about earthquakes, improve earthquake-resistant design, and implement seismic hazard mitigation procedures to minimize loss of lives and property. The emphasis is on structures in the eastern and central United States and lifelines throughout the country that are found in zones of low, moderate, and high seismicity.

NCEER's research and implementation plan in years six through ten (1991-1996) comprises four interlocked elements, as shown in the figure below. Element I, Basic Research, is carried out to support projects in the Applied Research area. Element II, Applied Research, is the major focus of work for years six through ten. Element III, Demonstration Projects, have been planned to support Applied Research projects, and will be either case studies or regional studies. Element IV, Implementation, will result from activity in the four Applied Research projects, and from Demonstration Projects.

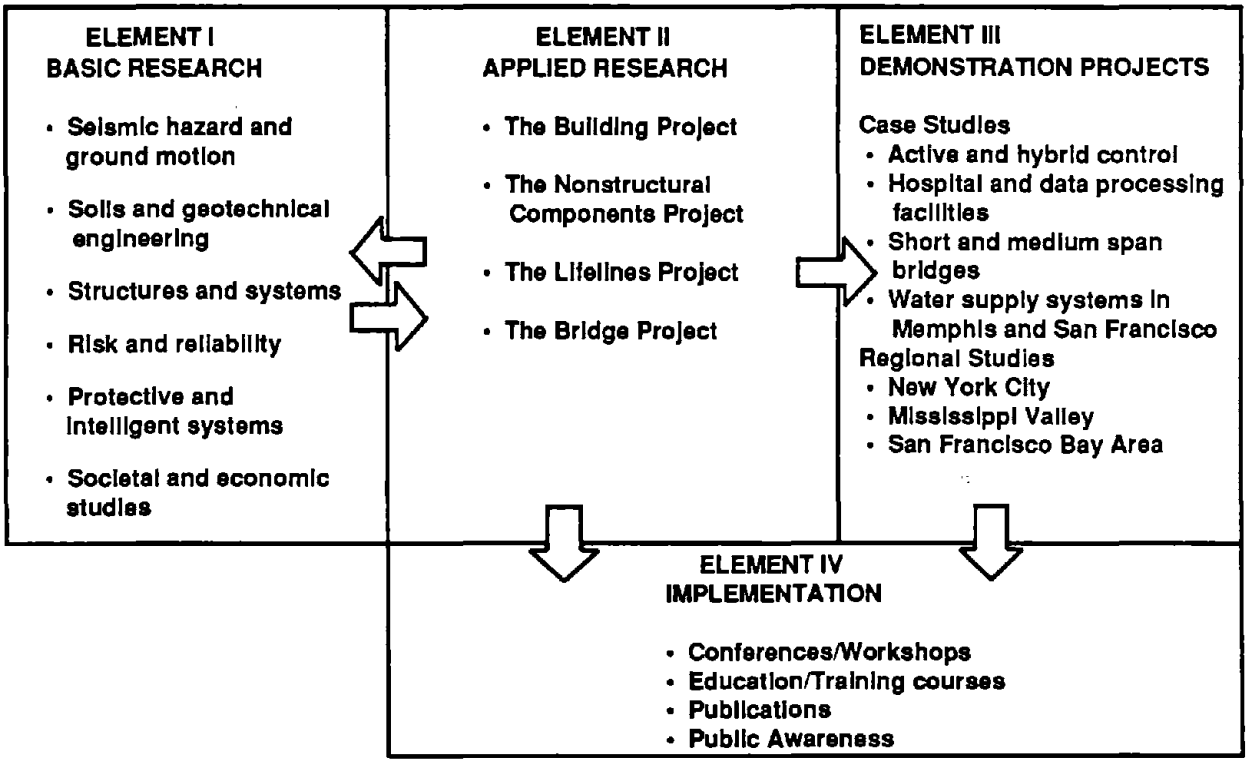

Tasks in Element I, **Basic Research,** include research in seismic hazard and ground motion; soils and geotechnical engineering; structures and systems; risk and reliability; protective and intelligent systems; and societal and economic impact.

The **soils and geotechnical engineering program** constitutes one of the important areas of research in Element I, **Basic Research**. Major tasks are described as follows:

1. Perform site response studies for code development.
2. Develop a better understanding of large lateral and vertical permanent ground deformations associated with liquefaction, and develop corresponding simplified engineering methods.
3. Continue U.S. - Japan cooperative research in liquefaction, large ground deformation, and effects on buried pipelines.
4. Perform soil-structure interaction studies on soil-pile-structure interaction and bridge foundations and abutments, with the main focus on large deformations and the effect of ground failure on structures.
5. Study small earth dams and embankments.

The purpose of this report is to derive a semi-empirical expression for scaling strong-motion peaks in terms of seismic source, propagation path and local site conditions. Peak acceleration, peak velocity and peak displacement are derived by using strong-motion data obtained in Japan. In the derivation, earthquake magnitude (JMA) and hypocentral distance are selected as independent variables and the dummy variables are introduced to identify the amplification factor due to individual local site conditions. The resulting semi-empirical expressions for the peak acceleration, velocity and displacement are then compared with strong-motion data observed during three earthquakes in the U.S. and Mexico. In addition, two methods for predicting the amplification factor at a site are proposed. A simplified method for estimating maximum soil strain is also presented.

ABSTRACT

The purpose of this report is to derive a new type of semi-empirical expression for scaling strong-motion peaks in terms of seismic source, propagation path and local site conditions. Peak acceleration, peak velocity and peak displacement are analyzed in a similar fashion because they are interrelated. However emphasis is placed on the peak velocity which is a key ground motion parameter for lifeline earthquake engineering studies. With the help of seismic source theories, the semi-empirical model is derived using strong motions obtained in Japan. In the derivation, statistical considerations are used in the selection of the model itself and the model parameters. Earthquake magnitude **M** and hypocentral distance **r** are selected as independent variables and the dummy variables are introduced to identify the amplification factor due to individual local site conditions. The resulting semi-empirical expressions for the peak acceleration, velocity and displacement are then compared with strong-motion data observed during three earthquakes in the U.S. and Mexico. This comparison suggests that the proposed semi-empirical model is superior to existing models for strong ground motion peaks. The amplification factors for acceleration, velocity and displacement peaks obtained empirically by the model are found to be period-dependent and related to local soil conditions. In addition, two methods for predicting the amplification factor at a new site are proposed. Finally, a simplified method for estimating maximum soil strain is presented with the aid of the proposed semi-empirical expression for the peak velocity.

ACKNOWLEDGEMENT

We thank the Port and Harbor Research Institute of the Ministry of Transport of Japan and the Public Works Research Institute of the Ministry of Construction of Japan for providing the strong-motion earthquake records used in this study. This study would have been impossible without these valuable strong-motion records. Gratitude is also extended to Toshiyuki Iwamoto of Kubota Copr. and Susumu Nakamura of Sato Corp. for their observed soil strain data. We are grateful that the observed data of strain by Prof.Tsuneo Katayama et al. are available to our study through their papers.

This study was done while the first and third authors were a visiting professor at the Department of Civil and Environmental Engineering, Rensselaer Polytechnic Institute. They have benefited greatly from collaboration and discussion with their colleagues. Especially Prof. Apostolos Papageorgiou offered an opportunity to use the strong-motion data of the 1989 Loma Prieta Earthquake as well as giving numerous suggestions for this study.

TABLE OF CONTENTS

TABLE OF CONTENTS(Cont'd)

LIST OF ILLUSTRATIONS

LIST OF ILLUSTRATIONS(Cont'd)

LIST OF ILLUSTRATIONS(Cont'd)

LIST OF TABLES

SECTION 1
INTRODUCTION

In the assessment of earthquake hazard potential and seismic design of engineering structures, it is fundamental from both technological and economical points of view to have realistic estimates of future strong ground motions. Strong motions are generally complicated functions of time. However, in order to simplify design, they are often characterized by parameters such as peak values (acceleration, velocity and displacement), duration, period characteristics, spectral content, energy related parameters, etc. Although spectral content may give more accurate information about damage potential for various structures, the peak values are often employed as representative design parameters mainly because of their simplicity. However, controversy still remains concerning whether peak acceleration, peak velocity or peak displacement is more important to determine earthquake damage. In particular, it has increasingly become known that peak acceleration, which has been most widely used, is not necessarily adequate to assess the seismic performance of various types of structures[1]. In the field of lifeline earthquake engineering, for example, it is well recognized that peak particle velocity is directly related to ground strain which often controls the behavior of buried systems such as pipelines[2]. In addition, peak displacement may be more significant for the sloshing of tanks whose behavior is closely associated with long-period motions. Thus various peak values of motions are crucial for different systems. Hence a unified assessment of peak acceleration, peak velocity and peak displacement is desirable and reasonable in light of the fact that the peak values are interrelated.

Strong earthquake motions are influenced by three main factors: seismic source, propagation path of waves and local site conditions. Therefore peak ground motion parameters should also be estimated in terms of the three factors. Recent developments in seismic source modeling has enhanced the possibility of theoretical estimates of the parameters, especially, in regions where recorded strong ground motions are limited[3]. However estimates of high frequency peak values are still not reliable because of the complexity of high-frequency motions[4]. In the past, empirical analysis of observed strong ground motion records has been the most common technique. Such analyses have been conducted by a number of researchers worldwide, presenting different expressions for peak values of motions. An extensive review of empirical prediction of strong ground motions has been recently given by Joyner and Boore[5], being preceded by another comprehensive review of Campbell[6] which focussed on strong-motion attenuation relations from a statistical standpoint. Some problems peculiar to empirical prediction of strong motions are

pointed out in these reviews along with methods for overcoming such problems. The greatest obstacle for empirical analysis is the limited availability of observed strong motion data. This obstacle is not easily overcome because new strong motion records accumulate at a slow pace. In order to overcome the difficulties of purely empirical prediction methods, it is necessary to develop a semi-empirical technique which incorporates information from theoretical seismic source models.

The main objective of this report is to present a new type of semi-empirical expression for peak particle velocity in terms of seismic source, propagation path of waves and local site conditions. Although the peak particle velocity, which is needed for lifeline earthquake engineering studies, is the primary target of this paper, semi-empirical relations for peak acceleration and peak displacement are also presented.

As stated above, strong-motion records accumulated to date are limited not only in number but also in type. For example, in the United States near field records from moderate-size earthquakes are relatively available but there are few strong-motion records obtained during large magnitude earthquakes. Conversely in Japan there are fewer records in near field even though there is a comparative abundance of records in the far field for large earthquakes. This motivates a systematic empirical analysis of strong-motion records collected from several countries in an attempt to compensate for the lack of data. Such analyses have been carried out by several workers[7, 8]. Although the method gives a way to extensively apply the resulting empirical expression, it simultaneously creates ineffective separation for the effects of seismic source characteristics, propagation path and local soil conditions because these factors are considered to be remarkably site-specific. Herein we use strong-motion records obtained in Japan with emphasis on the dependence on the three factors, in particular, on local site conditions. We attempt to compensate for the lack of data in the near field with the aid of information from theoretical seismic source models. The resulting semi-empirical expression based solely on Japanese data is then compared with near field data observed in the U.S. and Mexico to confirm its validity.

As described in the reviews by Joyner and Boore[5] and by Campbell[6], many workers have investigated the influence of local site conditions on peak values of strong motions. Almost all of these investigations use a rough classification scheme such as soft soil, intermediate soil, hard soil and rock without detailed soil profiles specific to individual sites. However a number of actual earthquake damage experiences have taught us that the degree of earthquake damage vary markedly from site to site even within the "soft soil" area. This indicates the importance of individual differences in soil properties at each site. In this study we device an empirical technique to obtain

site-specific amplification of peak acceleration, velocity and displacement based on the soil profile at each site.

The proposed semi-empirical technique also provides us with an estimate of peak values of strong motions on "seismic bed rock", which is bed rock for seismic response analysis of surface soils, as well as the site-specific amplification. Since the characteristics of the seismic bed rock are given explicitly, we can apply the results to estimates of several seismic parameters such as soil strain and liquafaction potential of sandy soils. In this report, as an example of the application, we present a simplified method for estimating soil strain, which is significant in soil dynamics and lifeline earthquake engineering, on the basis of the semi-empirical technique.

SECTION 2
MODEL FOR SEMI-EMPIRICAL ANALYSIS

2.1 Parameter Selection for the Model

According to statistical terminology, an empirical expression presents dependent variable as function of independent variables. In our case, peak acceleration, velocity and displacement respectively are the dependent variables. Regarding the independent variables, it is important to select them considering the physics of problem and their convenience in practical use. The dependent variables in our analysis are physically related to seismic source characteristics, propagation path of waves and local site conditions. Consequently we select the independent variables which represent each of these factors. With the aid of recently developed seismic source models, we could select various independent variables representing the seismic source characteristics and propagation path. However practical considerations confine us to select earthquake magnitude and hypocentral distance because they are the only source- and path-parameters available for most of our earthquake data. Hence for the convenience and simplicity of the model, herein we selected earthquake magnitude and hypocentral distance as the independent variables representing the effects of the seismic source and propagation path. We recognize that there are several ways to measure source-to-site distance. One such measure is the closest distance to fault rupture zone. However that distance is not necessarily available for small earthquakes. Herein we simply use hypocentral distance as a representative of source-to-site distance and derive attenuation in terms of that distance and a fault area parameter.

The technique used herein to characterize local site effects is somewhat unique. We define independent variables to represent local effects at each site as opposed to the rough classification schemes used in the past empirical analyses. That is, we introduce independent variables reflecting the effects specific to individual site conditions rather than grouping sites into a rough classification scheme. Kamiyama and Yanagisawa[9] has shown that the concept of dummy variables was effective for individualizing local site effects in their statistical analysis of response spectra. This concept is also used herein. A dummy variable is given a value of **1** when a phenomenon occurs and **0** when it does not occur[10]. Suppose now that strong motions were observed at a total of **N** observation sites during various earthquakes. Then we introduce a dummy variable S_i in order to express the phenomenon of obtaining strong motions at the i-th site during an earthquake so that $S_i=1$ when a record was obtained at the i-th site and $S_i=0$ when a record was not obtained. Such dummy variables are available for all the observation sites and by using these variables we can

quantify the local effects at individual observation sites. It should be emphasized herein that these dummy variables are treated in the same manner as the other independent variables, namely earthquake magnitude **M** and hypocentral distance **r**, in the formulation of the empirical model.

In summary, we start our semi-empirical analysis by assuming the following relationship between the dependent and independent variables.

$$v = f(M, r, S_1, S_2, \cdots, S_j, \cdots S_N) \tag{2.1}$$

where **v** is peak acceleration, velocity or displacement, **M** is the earthquake magnitude, **r** is the hypocentral distance, S_j are the dummy variables related to local site effects, and **N** is the total number of observation sites.

2.2 Statistical Consideration for Earthquake Magnitude M and Hypocentral Distance r

The parameter selection stated in the preceding section is not unusual except for the introduction of the dummy variables but herein we attempt a unique modelling for these parameters using theoretical seismic source results. It is important to give statistical consideration to the parameters **M** and **r** because they are generally correlated and such correlation has generally been ignored in past studies. Many studies in the past similarly have selected **M** and **r** as their independent variables and performed a regression analysis on the data. The resulting relationship from such an analysis typically has the form

$$\log_{10} v = aM + b\log_{10} r + c \tag{2.2}$$

where **a,b** and **c** are regression coefficients.

Eq.(2.2) is a multiple regression model based on the assumption that the two independent variables **M** and **log r** are statistically independent of each other, namely, the correlation coefficient between them is zero. However the earthquake data in the past empirical analyses of strong motions show rather strong correlation between earthquake magnitude **M** and hypocentral distance **r**. For example strong motions for a small magnitude earthquake typically are observed only in a near distance field: i.e. when **r** is small. Needless to say, an empirical analysis which disregards such a correlation gives less reliable results. Since the above correlation is often unavoidable, one

needs alternative techniques for overcoming such inherent difficulty as long as purely empirical analysis is pursued. Joyner and Boore[11] used the so-called two-stage regression procedure partly for this purpose while Fukushima and Tanaka[8] explained a controversial point about Eq.(2.2) with their own method. An explanation of the problem peculiar to Eq.(2.2) is as follows.

After variance analysis, the regression coefficients **a** and **b** of Eq.(2.2) can be shown to be

$$a = \frac{\sigma_{\log v}}{2\sigma_M}\left(\frac{R_{M,\log v} + R_{\log r,\log v}}{1+R_{M,\log r}} + \frac{R_{M,\log v} - R_{\log r,\log v}}{1-R_{M,\log r}}\right) \tag{2.3}$$

$$b = \frac{\sigma_{\log v}}{2\sigma_{\log r}}\left(\frac{R_{M,\log v} + R_{\log r,\log v}}{1+R_{M,\log r}} - \frac{R_{M,\log v} - R_{\log r,\log v}}{1-R_{M,\log r}}\right) \tag{2.4}$$

where $\sigma_{\log v}$, σ_M and $\sigma_{\log r}$ are the standard deviation for **log v**, **M**, and **log r** respectively and $R_{M,\log v}$, $R_{\log r,\log v}$ and $R_{M,\log r}$ are the correlation coefficients between **M** and **log v**, etc. If **M** and **log r** are uncorrelated, that is, $R_{M,\log r}=0$ which would be expected of independent variables, then the regression coefficients **a** and **b** become respectively

$$a = \frac{\sigma_{\log v}}{\sigma_M} R_{M,\log v} \tag{2.5}$$

$$b = \frac{\sigma_{\log v}}{\sigma_{\log r}} R_{\log r,\log v} \tag{2.6}$$

In Eqs. (2.5) and (2.6) the coefficients **a** and **b** are determined only by the correlation between the dependent variable and independent variables and the correlation between the independent variables taken as zero. On the other hand, if **M** and **r** are correlated, the values of **a** and **b** are affected by the degrees of the correlation. In particular the value of **b** is more strongly affected than the value of **a.** Fig.2-1 is a three dimensional scattergram of peak particle velocity in cm/sec, hypocentral distance in kilometer and earthquake magnitude for the strong ground motion data analyzed herein. Note that the correlation coefficient $R_{M,\log r}$ is a positive value close to 1. Hence from Eq.(2.4) the regression coefficient **b** is strongly influenced by the correlation coefficient between these "independent" variables, while the regression coefficient **a** is less strongly influenced. The above discussion suggests that one needs to pay special attention to the attenuation coefficient **b**. Note

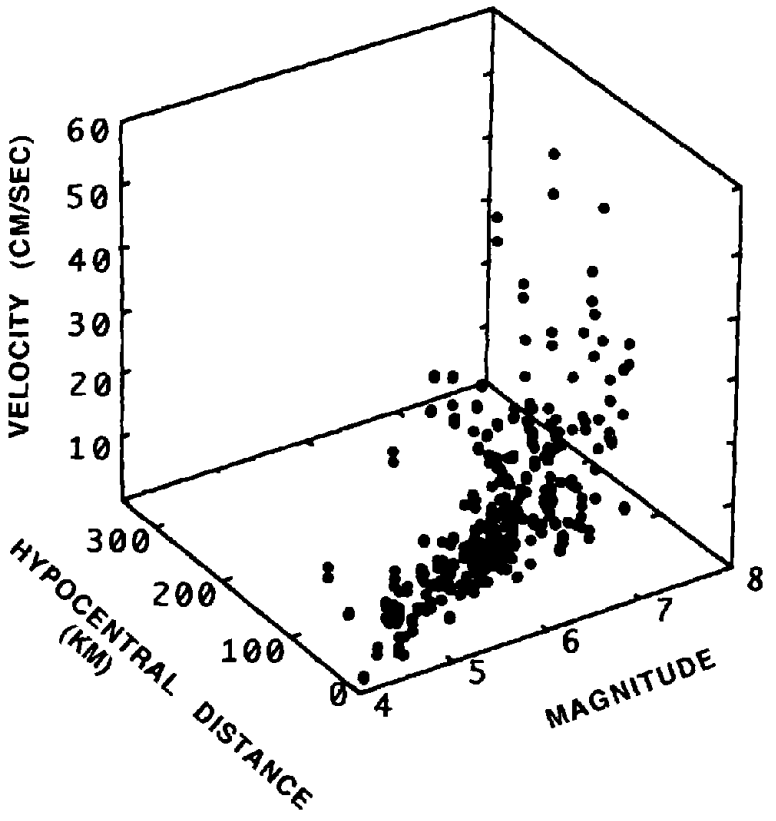

Fig.2-1 Scattergram of Peak Horizontal Velocity in cm/sec, Hypocentral Distance in kilometer and Magnitude for Japanese Earthquakes

for instance that Trifunac[12] employed a standard distance attenuation factor after Richter[13] while Joyner and Boore[11] relied on a geometrical attenuation coefficient derived from wave propagation theory. Herein we use an alternative consideration to avoid the difficulties inherent in the straightforward application of Eq.(2.2).

Although there are several ways of obtaining the attenuation coefficient **b**, we base our attenuation relation on the coefficient which was statistically derived in terms of earthquake magnitude and source-to-site distance using past earthquake data in and around Japan. We need the distance attenuation applied only to the far-field from the seismic source area as will be explained later. From these requirements we adopt the statistical attenuation coefficient of distance obtained by the Japan Meteorological Agency (JMA) which systematically determines the magnitude of earthquakes occurring in and around Japan. The agency has empirically derived the following expression for earthquake magnitude which uses maximum velocity in the vertical direction [14]:

$$M = \log_{10} A_z + 1.64 \log_{10} \Delta + 0.22 \tag{2.7}$$

where Az is the maximum velocity in the vertical direction and Δ is the epicentral distance.
Eq.(2.7) was obtained statistically from the earthquake data which satisfy the conditions of the far-field. Accordingly, we employ the value of 1.64 as the distance attenuation coefficient for our semi-empirical model which targets horizontal motions in terms of hypocentral distance, assuming that there is little difference between vertical and horizontal motions and between epicentral and hypocentral distances. That is, the basic expression of our semi-empirical model is given by

$$\log_{10} v = aM - 1.64 \log_{10} r + c + f(S_1, S_2, \cdots, S_N) \tag{2.8}$$

2.3 Theoretical Seismic Source Considerations

The hypocentral distance used in Eq.(2.8) is not necessarily the best choice to quantify source-to-site distance but it was selected purely because of its simplicity in practical use. In its current form Eq.(2.8) implicitly assumes the earthquake source to be a point. Actually, however, the earthquake source is not a point but consists of a fault with some extended area. Herein we make use of seismic source theory to resolve the problem.

According to recent studies of earthquake faults, earthquakes generally occur in a form of multiple-shocks which are triggered by rupture of sub-faults associated with the so-called barriers or

asperities[15]. In other words, actual earthquakes can be viewed as the result of multiple point-sources, scattered randomly over the entire fault plane. Since such multiple shocks may occur incoherently over the fault plane, one can assume that the peaks of strong motions on or near the fault area are independent of their locations. That is, peak ground motion on and near the fault would be relatively constant. Beyond the immediate fault area, peak motion decreases with distance due to geometric spreading and inelastic phenomena. The model assumed herein for the variation of peak ground motion with hypocentral distance is sketched in Fig.2-2. Hence the remaining problem is the determination of the constant level **c** and transition distance $\mathbf{r_t}$ in Fig.2-2.

Papageorgiou and Aki[16] discussed theoretically the peak values of strong motions in a fault area based on the specific barrier model. They suggested that the average cohesive force distributed on the cohesive zone of their specific barrier model and average slip **D** are determinant parameters for the peaks, and the peak acceleration $\mathbf{a_{max}}$ and peak velocity $\mathbf{v_{max}}$ in a fault area are approximately given by the following expressions from Ida[17].

$$a_{max} \approx \frac{\sigma_c}{\mu} V_r 2 \frac{1}{D} \tag{2.9}$$

$$V_{max} \approx \frac{\sigma_c}{\mu} V_r \tag{2.10}$$

where σ_c is an average cohesive stress in the cohesive zone,
D is the average slip in the cohesive zone , $\mathbf{V_r}$ is the rupture velocity and
μ is the rigidity modulus.

Applying the specific barrier model to earthquakes in California, Chin and Aki[18] estimated empirically the values of σ_c and **D** which are associated with earthquake magnitude. The results show that the logarithmic values of both σ_c and **D** are linearly proportional to earthquake magnitude in a similar manner. This means from Eqs.(2.9) and (2.10) that peak acceleration in a fault zone is independent of earthquake magnitude while the peak of velocity is proportional to earthquake magnitude since $\mathbf{V_r}$ and μ are known to be independent of earthquake magnitude. Such magnitude saturation of peak acceleration has been discussed by other researchers along with debates over its validity. We employ this assumed characteristics of peak acceleration and peak velocity in a fault zone as an important starting point for our semi-empirical model. On the other hand, the fault extent, namely, the transition distance $\mathbf{r_t}$ in Fig.2-2 is identical for both acceleration and velocity and herein assumed to be an increasing function of the earthquake magnitude. This is based on numerous empirical studies which show that earthquake fault length is an increasing function of earthquake magnitude. That is, our semi-empirical models are based on Fig.2-3(a) and

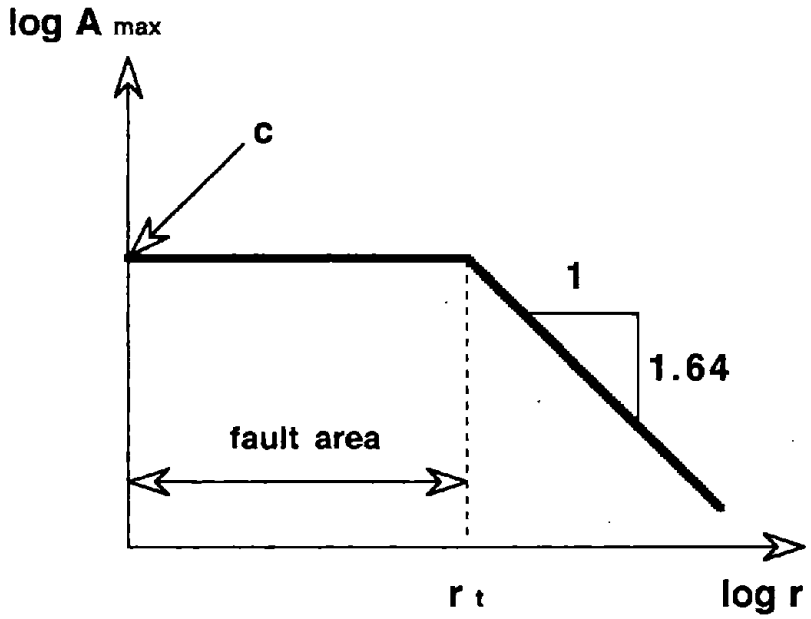

Fig.2-2 **Proposed Model for Variation of Ground Motion Peak with Hypocentral Distance for a Fixed Magnitude**

Fig.2-3(b) for peak acceleration and peak velocity respectively. Note that peak displacement is assumed to behave in a manner similar to peak velocity.

2.4 Empirical Determination of the Model Parameters

The parameters $\mathbf{c_a}$, $\mathbf{c_b}$ and $\mathbf{r_t}$ in Fig.2-3(a) and Fig.2-3(b) are determined empirically in accordance with observed earthquake data. We require that the values of $\mathbf{r_t}$ be common for the acceleration, velocity and displacement models, since they represent earthquake fault size. Fig.2-3(a) and Fig.2-3(b) show clearly that it is easier to first determine $\mathbf{r_t}$ from the acceleration data and then apply the values to the more complicated velocity and displacement models whose peaks in the fault region depend on earthquake magnitude.

Up to this point, the acceleration model is a function of two parameters; $\mathbf{r_t}$ which is a function of earthquake magnitude and $\mathbf{c_a}$ which is a constant. Based upon the results of previous studies, we assume herein that $\mathbf{\log r_t}$ is linearly proportional to earthquake magnitude. A dummy variable concept, described by Kamiyama and Matsukawa[19], is then used to evaluate $\mathbf{r_t}$ and $\mathbf{c_a}$. We use a trial and error procedure incorporating an arbitrary value $\mathbf{r_c}$. This yields a regression model:

$$\log_{10} a_{max} = -1.64R_0 + b_1R_1 + b_2R_2 + c_a \tag{2.11}$$

where

$$R_0 = \begin{cases} 0 & (r \le r_c) \\ \log_{10} r - \log_{10} r_c & (r > r_c) \end{cases} \tag{2.12}$$

$$R_1 = \begin{cases} 0 & (r \le r_c) \\ 1 & (r > r_c) \end{cases} \tag{2.13}$$

$$R_2 = \begin{cases} 0 & (r \le r_c) \\ M & (r > r_c) \end{cases} \tag{2.14}$$

and $\mathbf{b_1}$,$\mathbf{b_2}$ and $\mathbf{c_a}$ are regression coefficients.
The parameter $\mathbf{r_t}$ becomes a function of earthquake magnitude **M** as

$$r_t = r_c \times 10^{\frac{b_1 + b_2 M}{1.64}} \tag{2.15}$$

As shown in Eq.(2.15), the target values $\mathbf{r_t}$ and $\mathbf{c_a}$ determined by the model of Eq.(2.11) are dependent on the selected value for the arbitrary variable $\mathbf{r_c}$. The final determination of $\mathbf{r_t}$ and $\mathbf{c_a}$ is

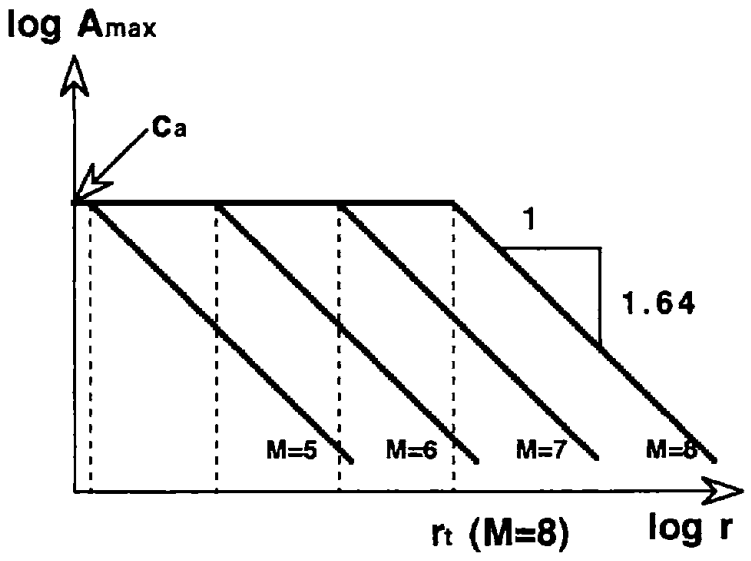

Fig.2-3(a) Proposed Model for Peak Horizontal Ground Acceleration as Function of Hypocentral Distance and Magnitude

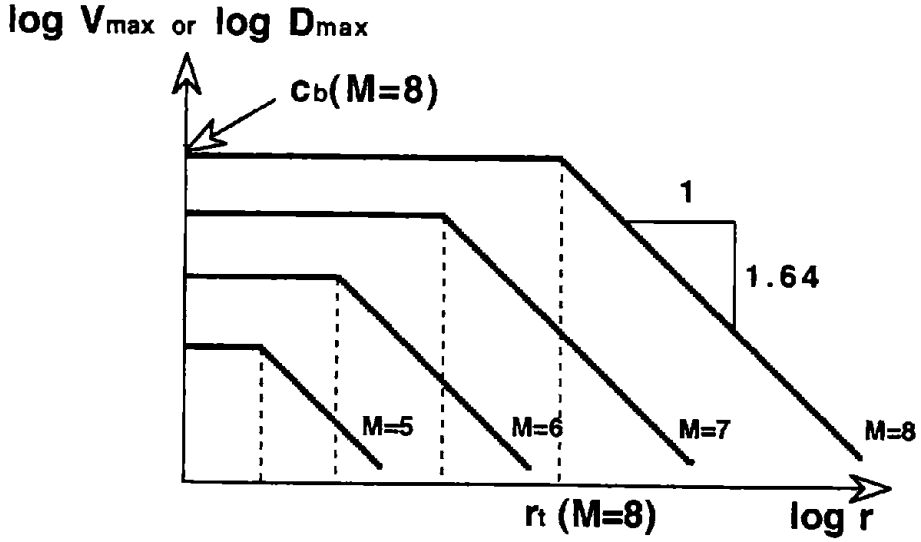

Fig.2-3(b) Proposed Model for Peak Horizontal Ground Velocity and Displacement as Function Hypocentral Distance and Magnitude

based upon the goodness of fit between predicted and observed of $\mathbf{a_{max}}$ for various values of the arbitrary variable $\mathbf{r_c}$, as well as empirical information on earthquake fault size.

The models for peak velocity and displacement in Fig.2-3(b) are constructed by adding another term controlling the magnitude-dependence of the peak in the fault zone and using the regression coefficients $\mathbf{b_1}$ and $\mathbf{b_2}$ in Eq.(2.11) of the acceleration model. Namely, they are given by

$$v_{max} = \alpha M - 1.64R_0 + b_1R_1 + b_2R_2 + c_v \tag{2.16}$$

$$d_{max} = \delta M - 1.64R_0 + b_1R_1 + b_2R_2 + c_d \tag{2.17}$$

where $\mathbf{v_{max}}$ is the peak velocity, $\mathbf{d_{max}}$ is the peak displacement, $\mathbf{M}$ is the earthquake magnitude, and α, δ, $\mathbf{c_v}$ and $\mathbf{c_d}$ are regression coefficients, and

$$R_0 = \begin{cases} 0 & (r \le r_c) \\ \log_{10} r - \log_{10} r_c & (r > r_c) \end{cases} \tag{2.18}$$

$$R_1 = \begin{cases} 0 & (r \le r_c) \\ 1 & (r > r_c) \end{cases} \tag{2.19}$$

$$R_2 = \begin{cases} 0 & (r \le r_c) \\ M & (r > r_c) \end{cases} \tag{2.20}$$

In Eqs.(2.16) and (2.17), only the coefficients α, δ, $\mathbf{c_v}$ and $\mathbf{c_d}$ are determined empirically by regression analysis, since the values $\mathbf{b_1}$ and $\mathbf{b_2}$ are determined from the acceleration model.

2.5 Local Site Effects

Eqs.(2.11), (2.16) and (2.17) are semi-empirical models which consists of seismic source characteristics and propagation path. As described in the foregoing section, an additional term is needed to reflect the individual local site effects. In other words, we express the independent variables $\mathbf{S_1}$, $\mathbf{S_2}$, ----, $\mathbf{S_N}$ in Eq.(2.1) as a concrete functional form so that they represent local soil conditions at each observation site.

Referring to response spectra of strong motions, Kamiyama and Yanagisawa[9] discussed in detail such independent variables in connection with the theory of earthquake response of surface soils and concluded that a linear equation of such variables is sufficient to obtain amplification factors

compatible with the frequency response function physically caused by local surface soils. The peak values of strong motions which is our target, of course, differ from response spectra in character. Particularly, the linear transmission of frequency response functions which is satisfied in the case of spectra can not be directly applied to the peak values of motions. However, it would be almost impossible to constitute a semi-empirical model which exactly reflects such characteristics peculiar to the peak values of motions because of its complexity. As the first approximation, we herein employ the following model, similar to that for response spectra, in order to empirically obtain the effect of individual local sites:

Peak acceleration,

$$\log_{10} a_{max} = -1.64R_0 + b_1R_1 + b_2R_2 + c_a + A_1S_1 + A_2S_2 + \cdots + A_{N-1}S_{N-1} \qquad (2.21)$$

Peak velocity and displacement,

$$\log_{10} v_{max} = \alpha M - 1.64R_0 + b_1R_1 + b_2R_2 + c_v + B_1S_1 + B_2S_2 + \cdots + B_{N-1}S_{N-1} \qquad (2.22)$$

$$\log_{10} d_{max} = \delta M - 1.64R_0 + b_1R_1 + b_2R_2 + c_d + D_1S_1 + D_2S_2 + \cdots + D_{N-1}S_{N-1} \qquad (2.23)$$

where $\mathbf{A_i}$, $\mathbf{B_i}$ and $\mathbf{D_i}$ (i=1-N-1) are regression coefficients.

As seen in Eqs.(2.21) to (2.23), the **N-1** independent dummy variables $\mathbf{S_j}$ are assigned to all observation sites except a reference site. This technique avoids statistical difficulties and obtains local site amplification factors of the peak values with respect to a reference site. When a reference site is selected to satisfy the conditions of the seismic bed rock, the amplification factors thus obtained have physical meaning. An explanation of such amplification factors is described fully in Kamiyama and Yanagisawa[9]. The amplification factors $\mathbf{AMP_i}$ for the peak acceleration, velocity and displacement at the i-th site against a reference site are given by

$$AMP_i = 10^{A_i},\ 10^{B_i} \text{ or } 10^{D_i} \qquad (2.24)$$

SECTION 3
EARTHQUAKE DATA USED FOR THE SEMI-EMPIRICAL ANALYSIS

In this study we focus our attention on earthquake data obtained in Japan. Strong motion observation in Japan dates back to early 1960's when the so-called SMAC accelerograph was developed. Since then numerous useful records have been obtained. Systematic strong-motion observation networks have been established throughout the country by both the Ministries of Transport and Construction. Since our empirical analysis places an emphasis on local site effects as well as the effects of earthquake source and propagation path, it would be desirable to use earthquake data collected as systematically as possible. In other words, we need earthquake data observed at several specific sites during many earthquakes with various magnitudes for the purpose of efficiently separating seismic source, propagation path and local site condition effects. In addition, we need free field accelerograms to avoid unnecessary effects such as soil-structure interaction. A total of 33 observation sites were selected from the Transport and Construction Ministries networks meeting these requirements. Horizontal accelerograms at these sites obtained during a total of 82 earthquakes constitute the data set for our semi-empirical analysis[20, 21]. The total number of the accelerograms is 357. These accelerograms are listed in Table A-1 along with the observation sites, earthquake magnitude, focal depth, epicentral distance, hypocentral distance and peak ground motion parameters. The observation sites are illustrated together with the epicenters of the earthquakes in Fig.3-1. Many of these accelerograms and observation sites are identical to those used in the statistical analysis of response spectra by Kamiyama and Yanagisawa[9], but 7 observation sites were newly added along with new accelerograms. In these accelerograms, two different horizontal components simultaneously obtained at one site for an earthquake are included as an individual to enrich the data set. The earthquake magnitude listed in Table A-1 is the JMA earthquake magnitude determined by the Japan Meteorological Agency. The agency has been determining the magnitude of earthquakes occurring in and around Japan based on various methods[1,14]. These methods are applied depending on earthquake conditions. For example, the magnitude of earthquakes with the focal depth less than or equal to 60 km is determined using the following formula:

$$M = \frac{1}{2}\log_{10}(A_N^2 + A_E^2) + 1.73\log_{10}\Delta - 0.83 \qquad (3\text{-}1)$$

where M is the magnitude, A_N and A_E are the maximum amplitudes of north and east components in micron respectively, and Δ is the epicentral distance in km. Those ground amplitudes are of seismometers with periods of about 5 seconds and of waves shorter than 5 seconds.

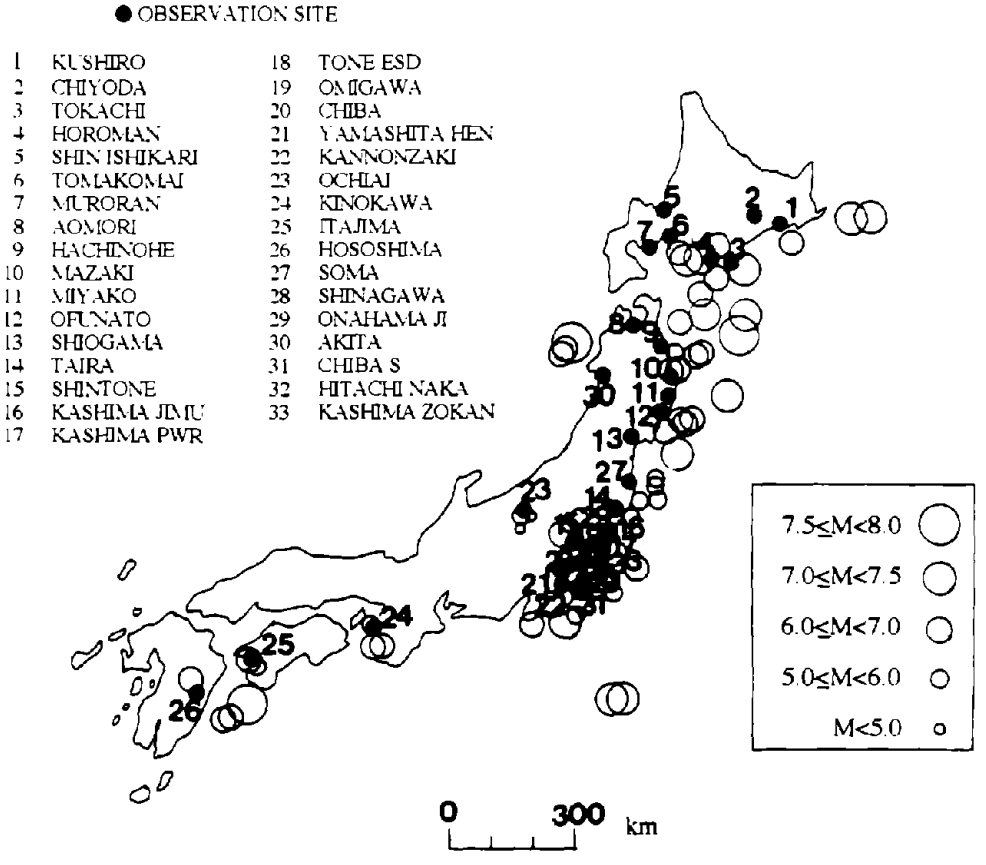

Fig.3-1 Obseravtion Sites and Epicenters

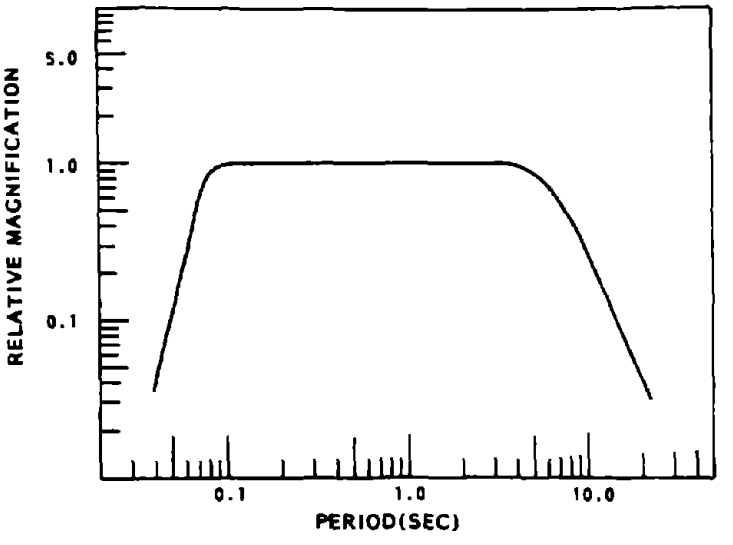

Fig.3-2 Band Pass Filter Used for Corrected Acceleration, Velocity and Displacement Records

The accelerograms in Table A-1 were obtained mostly by the SMAC types of accelerographs. The original accelerograms include several errors resulting from the frequency characteristics of the instrument, digitization processing, etc. We removed the errors by performing a correction according to the frequency characteristics of each instrument as well as by using a band path filter. Based on such correction and filtering, corrected acceleration, velocity and displacement records were numerically obtained together with their peak values which are shown in Table A-1. The frequency characteristics of the band-path filter used herein is shown in Fig.3-2. This filter, proposed by Iai et al.[22] as a standard filter for accelerograms obtained by the Transport Ministry, has a flat part ranging from about 0.09 sec. to about 4.2 sec. This period band should be emphasized when the peak velocity and displacement are examined. An example of corrected acceleration record and the corresponding velocity and displacement time histories obtained by the processing technique are presented in Fig.3-3.

Figs.3-4 and 3-5 describe the range of the independent variables, magnitude and hypocentral distance for the data used in developing the semi-empirical relations. Although the distribution of magnitude is fairly uniform, the hypocentral distance data concentrates in the 50 to 150 kilometer range. Figs.3-6 through 3-8 are histograms for the dependent variables; peak horizontal acceleration, velocity and displacement. The interrelationship between the independent variables, earthquake magnitude and hypocentral distance is shown in the scattergram in Fig.3-9. This figure, which presents information similar to that in Fig.2-1, shows strong positive correlation between the two variables. Hence the data set used herein has some limits from a statistical point of view. These limits provided motivation for the semi-empirical model as stated in the foregoing section.

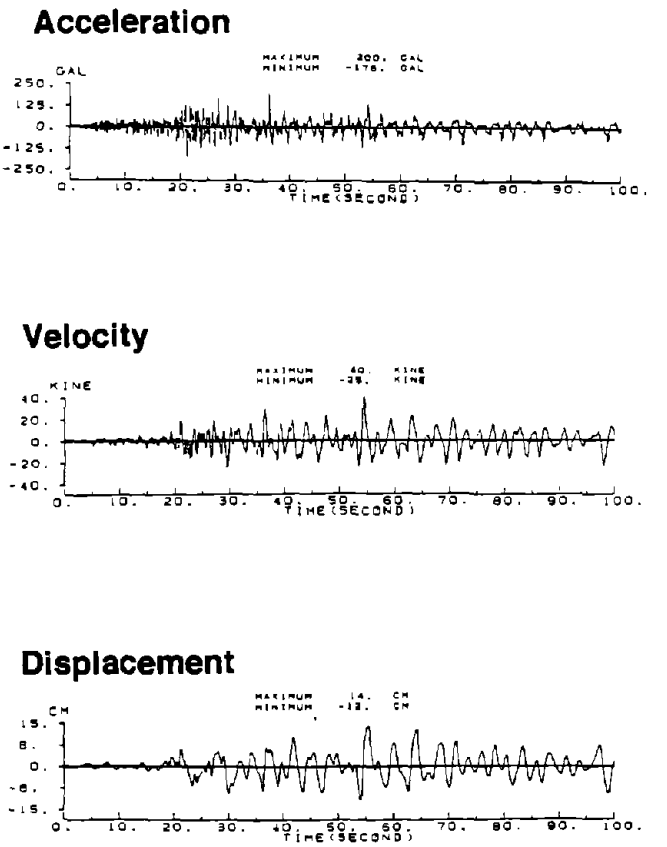

Fig.3-3 Corrected Acceleration Time History, and Corresponding Velocity and Displacement Records for May 16, 1968 Event at Aomori

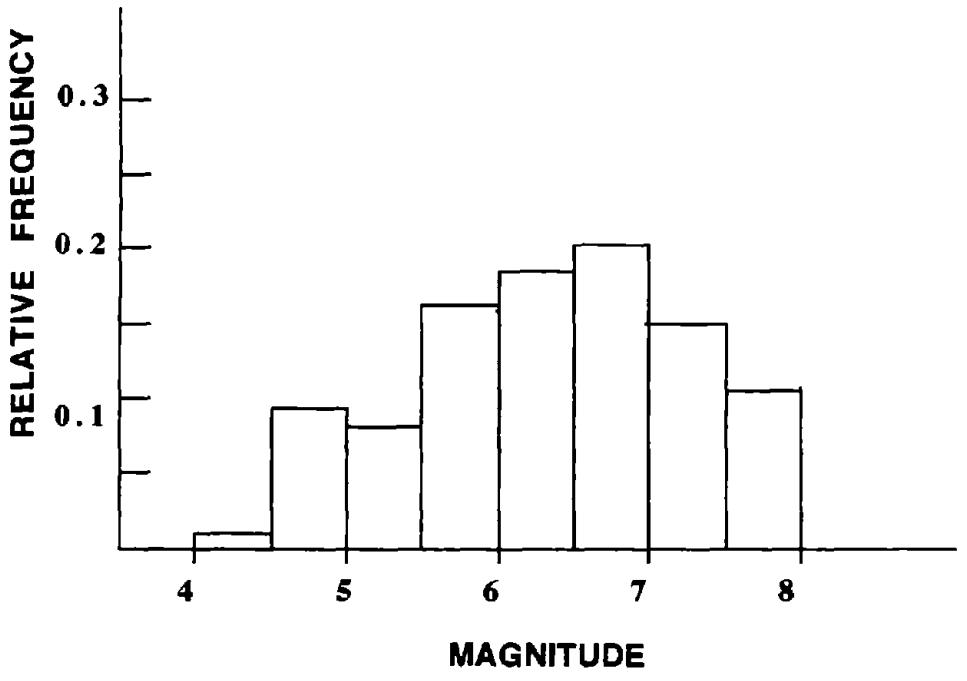

Fig.3-4 Histogram of Earthquake Magnitude Used in the Analysis

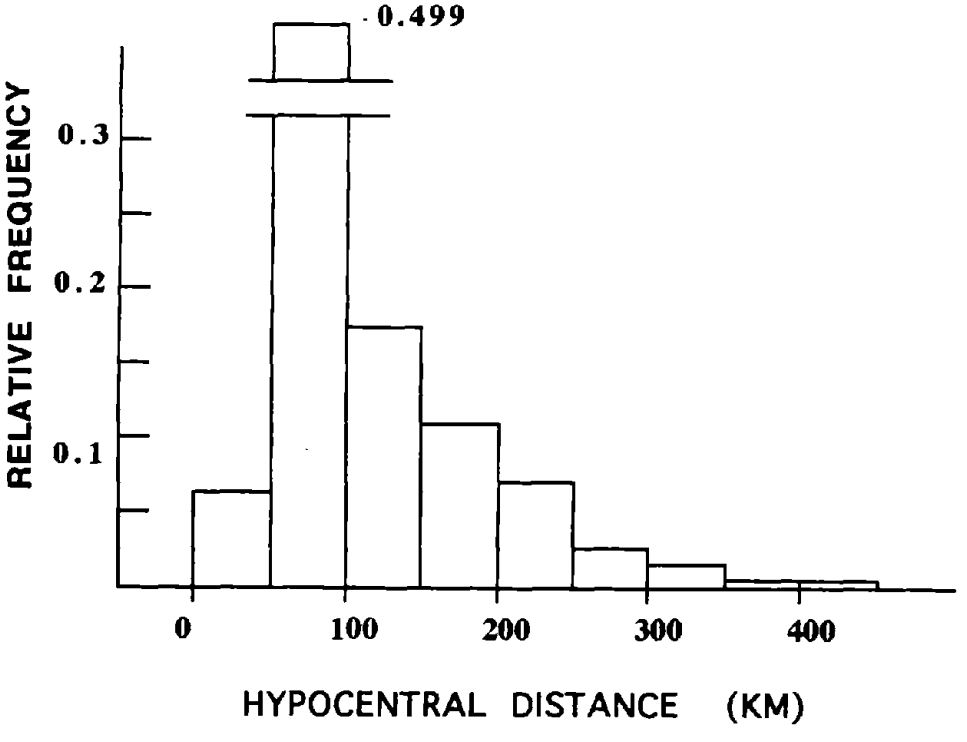

Fig.3-5 Histogram of Hypocentral Distance Used in the Analysis

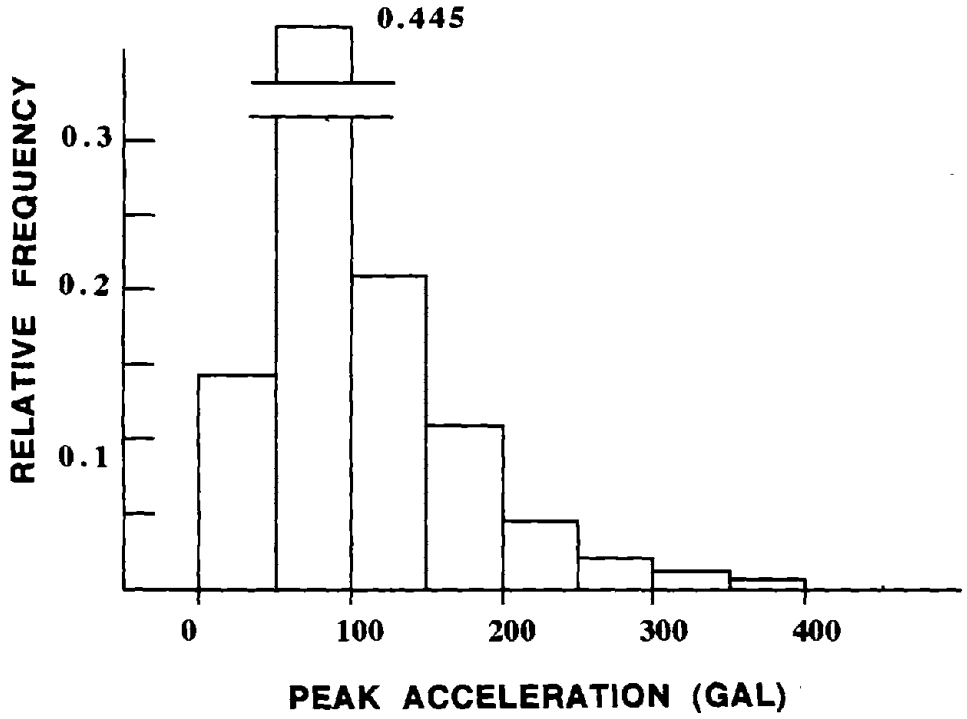

Fig.3-6 Histogram of Peak Horizontal Ground Acceleration Used in the Analysis

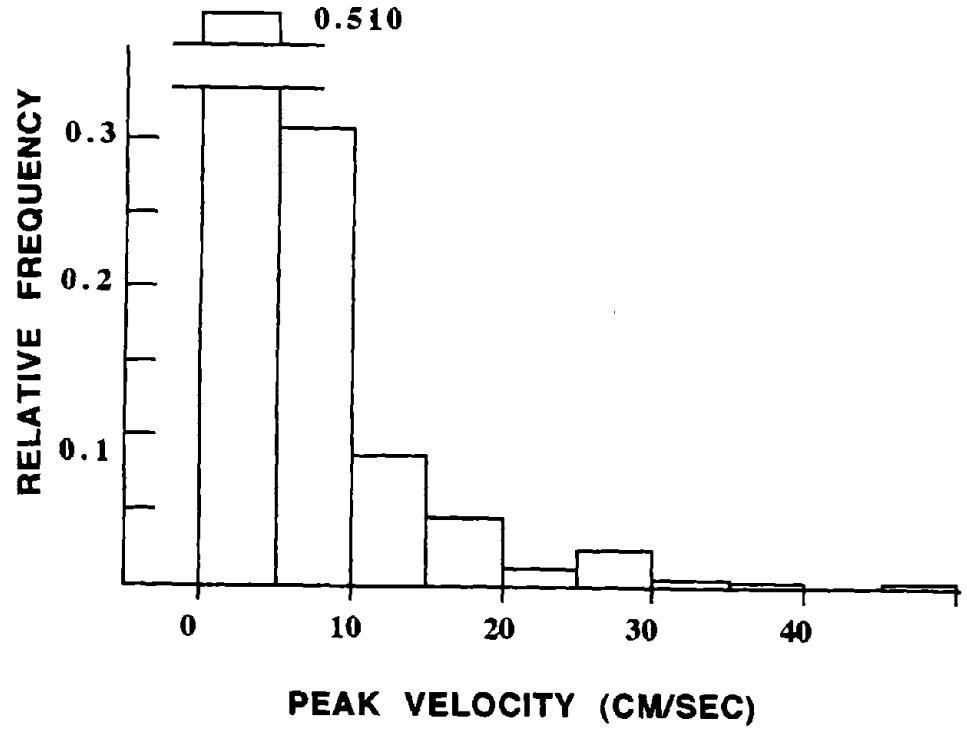

Fig.3-7 Histogram of Peak Horizontal Ground Velocity Used in the Analysis

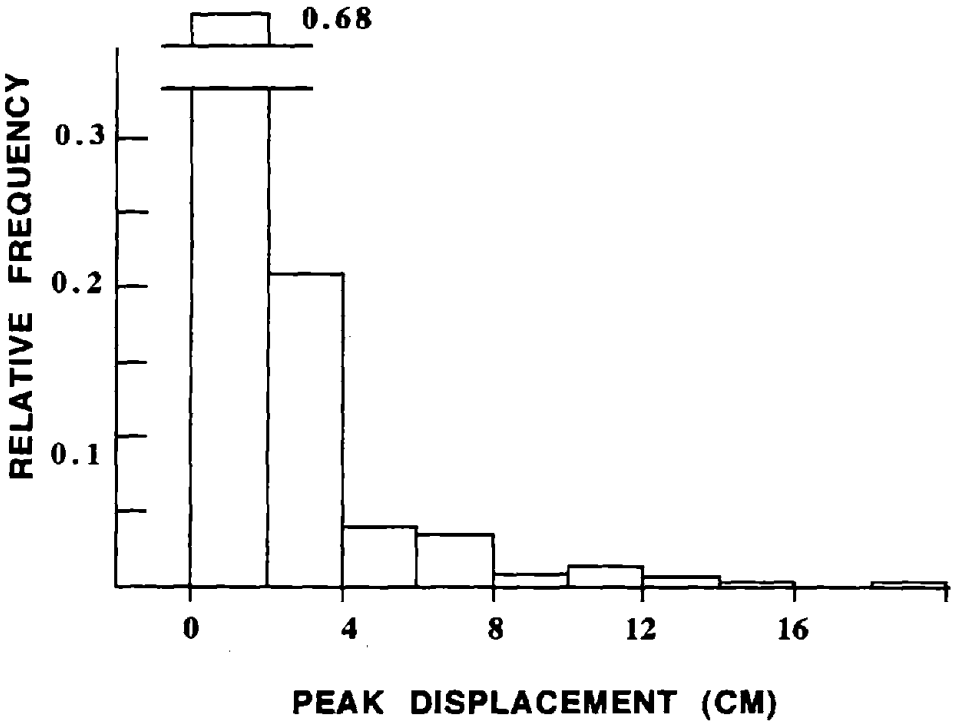

Fig.3-8 Histogram of Peak Horizontal Ground Displacement Used in the Analysis

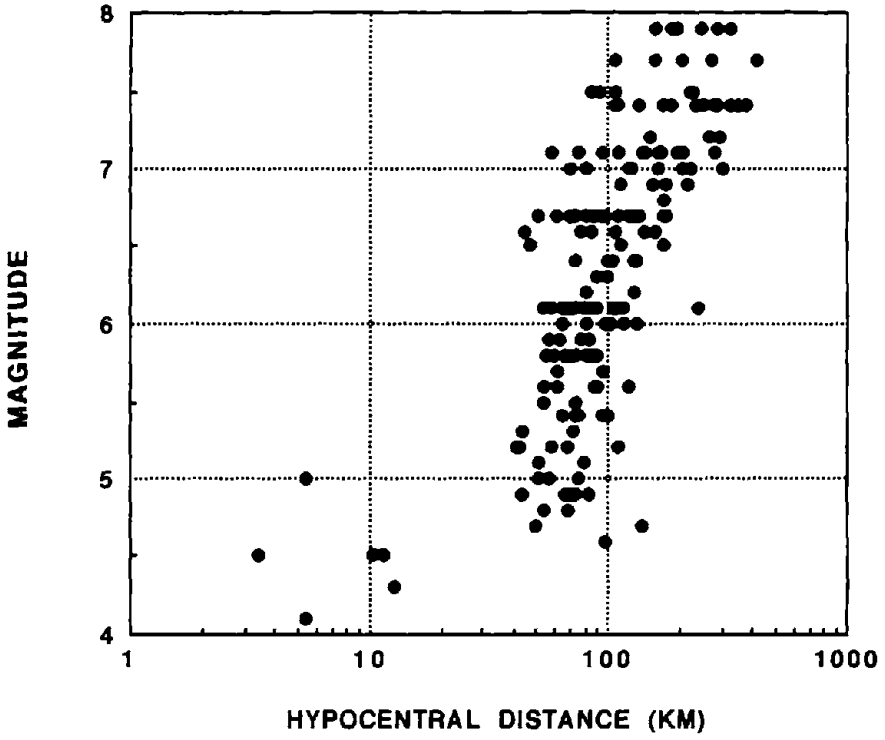

Fig.3-9 Scattergram of Magnitude and Hypocentral Distance in Data

SECTION 4
REGRESSSION ANALYSIS OF THE SEMI-EMPRICAL MODELS

The regression analyses of the semi-empirical models of Eqs.(2.21) through (2.23) were carried out by using the data in Table A-1 with the help of the least-square technique. As mentioned previously, our regression analyses consist of two phases. In the first phase the appropriate values of $\mathbf{r_t}$ are determined using the acceleration model. In the second phase the velocity and displacement models are established using the results for $\mathbf{r_t}$ from the acceleration model. In addition, we need to assign a reference site whose dummy variable $\mathbf{S_j}$ is not given and virtually set to be zero in Eqs.(2.21) through (2.23). Such a reference site, of course, can be picked arbitrarily from any of the observation sites. However our previous studies reveal that it is most desirable to assign a site where there exists outcrop hard enough to satisfy the condition of the seismic bed rock for the other sites. Although the selection of the seismic bed rock might vary according to the dominant frequency content, we initially selected the same reference site for acceleration, velocity and displacement motions on the condition that the definition of the seismic bed rock should be examined based on the resulting amplification factors at each observation site. Herein we choose OFUNATO labelled 12 in Fig. 3-1 as the reference site in accordance with the discussion in Kamiyama and Yanagisawa[9]. The OFUNATO site is situated at a rock outcrop having shear wave velocity in the 1 to 2 km/sec range.

4.1 Regression Analysis for the Acceleration Model

Table 4-I shows the summary of the regression coefficients analyzed for trial values of $\mathbf{r_c}$ in the acceleration model. In Table 4-I, the results of regression coefficients $\mathbf{A_1}$, $\mathbf{A_2}$,---, $\mathbf{A_{N-1}}$ are omitted because the main purpose of the table is to determine the most appropriate values for $\mathbf{b_1}$ and $\mathbf{b_2}$ based on the variations of $\mathbf{r_t}$ in terms of earthquake magnitude. For this reason, the variations of $\mathbf{r_t}$ estimated by Eq.(2.15) are indicated in Table 4-I in stead of the results of $\mathbf{A_i}$. Note that the multiple correlation coefficient **R**, which means the goodness of fit, is largest for $\mathbf{r_c}$ <10 km. Table 4-I also shows that the variation of $\mathbf{r_t}$ depends on $\mathbf{r_c}$ but it becomes relatively stable for $\mathbf{r_c \leq 5.3}$ km. As stated in the preceding section, $\mathbf{r_t}$ is closely related to a characteristic length of the earthquake fault. Hence in addition to the goodness of fit and stability of the $\mathbf{r_t}$ parameter, the choice of $\mathbf{b_1}$ and $\mathbf{b_2}$ is also based on the consistency of $\mathbf{r_t}$ with empirical estimates of fault length. Although the value of $\mathbf{r_t}$ is somewhat arbitrarily related to fault length, it is reasonable to interpret $\mathbf{r_t}$ as nearly equivalent to the radius of the fault which is assumed herein to be circular. The fault area of earthquake has been investigated by many workers. Typically it is related to earthquake magnitude. For instance, Sato[23] derived the following expression.

Table 4-I Regression Coefficients, Multiple Correlation Coefficient, Standard Deviation and r_t for Acceleration Model

	r_c (km)															
	50	40	30	20	10	8.0	6.0	5.8	5.6	5.4	5.3	5.2	5.1	4.8	4.6	4.4
b_1	-1.766	-1.760	-1.555	-1.266	-0.767	-0.608	-0.403	-0.379	-0.354	-0.819	-1.164	-1.150	-1.137	-1.093	-1.063	-1.031
b_2	0.324	0.333	0.333	0.333	0.332	0.332	0.332	0.332	0.332	0.345	0.358	0.358	0.358	0.358	0.358	0.358
c_a	2.126	2.228	2.228	2.228	2.228	2.228	2.283	2.228	2.228	2.637	2.910	2.910	2.910	2.910	2.910	2.910
R	0.845	0.854	0.862	0.876	0.896	0.900	0.905	0.906	0.906	0.894	0.890	0.890	0.890	0.891	0.891	0.891
S	0.228	0.227	0.227	0.227	0.228	0.228	0.228	0.228	0.228	0.243	0.247	0.247	0.247	0.247	0.247	0.247
r_t (km) M=5	41.3	35.1	35.1	35.1	35.1	35.1	35.1	35.1	35.1	19.3	12.8	12.8	12.8	12.8	12.8	12.8
M=6	65.1	56.0	56.0	56.0	56.0	56.0	56.0	56.0	56.0	31.3	21.2	21.2	21.2	21.2	21.2	21.2
M=7	102.6	89.4	89.4	89.4	89.3	89.3	89.3	89.3	89.3	50.8	35.0	34.9	34.9	35.0	35.0	35.0
M=8	161.7	142.8	142.8	142.8	142.5	142.5	142.5	142.5	142.5	82.5	57.9 *	57.8	57.8	57.9	57.9	57.9

b_1, b_2 and c_a=regression coefficients , M= earthquake magnitude
R=multiple correlation coefficient
S= standard deviation

$$r_t = r_c \times 10^{\frac{b_1 + b_2 M}{1.64}}$$

$$S = 10^{M-4.07} \tag{4.1}$$

where S is the area of the fault in square kilometers.

Table 4-II shows the variation of fault radius obtained from Eq.(4.1) assuming a circular fault. A comparison between Table 4-I and Table 4-II indicates that values of $\mathbf{r_c}$ less than or equal to **5.3** km yield the best match between $\mathbf{r_t}$ and empirical estimates of the fault radius by others, even though there is some difference between them. The difference may be due to the possibility that $\mathbf{r_t}$ is related to a characteristic length of a rectangular fault rather than the radius of circular fault. Accordingly, we choose $\mathbf{b_1 = -1.164}$, $\mathbf{b_2 = 0.358}$ **and** $\mathbf{c_a = 2.91}$, which were obtained by setting $\mathbf{r_c = 5.3}$ km, for the acceleration model of Eq.(2.21). The regression coefficients $\mathbf{A_1}$, $\mathbf{A_2}$, ---, $\mathbf{A_{N-1}}$ in Eq.(2.21), which were obtained based on $\mathbf{r_c = 5.3}$, are shown in Table 4-III. In Table 4-III, $\mathbf{A_i}$ **(i=1~N-1)** are given for each observation site except the reference site. Hence the eventual semi-empirical expression for the peak horizontal ground acceleration is

$$a_{max}(i,M,r) = 10^{2.910} 10^{A_i} \qquad (r \le 10^{0.014+0.218M}) \tag{4.2}$$

$$a_{max}(i,M,r) = 10^{2.933+0.358M-1.64\log_{10} r} \times 10^{A_i} \qquad (r > 10^{0.014+0.218M}) \tag{4.3}$$

where $\mathbf{A_i}$ are given in Table 4-III on the condition that $\mathbf{A_i = 0}$ for the reference site.

4.2 Regression Analysis for the Velocity and Displacement Models

The regression coefficients of the velocity and displacement models of Eqs.(2.22) and (2.23) are presented in Table 4-IV, based on $\mathbf{b_1 = -1.164}$ and $\mathbf{b_2 = 0.358}$ from the acceleration model. Hence the semi-empirical expressions for the peak horizontal ground velocity and displacement are

$$v_{max}(i,M,r) = 10^{0.535+0.153M} \times 10^{B_i} \qquad (r \le 10^{0.014+0.218M}) \tag{4.4}$$

$$v_{max}(i,M,r) = 10^{0.558+0.511M-1.64\log_{10} r} \times 10^{B_i} \qquad (r > 10^{0.014+0.218M}) \tag{4.5}$$

$$d_{max}(i,M,r) = 10^{-0.522+0.236M} \times 10^{D_i} \qquad (r \le 10^{0.014+0.218M}) \tag{4.6}$$

Table 4-II Fault Radius Based on the Sato[23] Relation for Fault Area

MAGNITUDE M	RADIUS (KM)
5	1.65
6	5.21
7	16.46
8	52.05

Table 4-III Site Amplification Coefficients for Acceleration Model

NO	SITE NAME	A_i
1	KUSHIRO	0.196
2	CHIYODA	0.127
3	TOKACHI	0.110
4	HOROMAN	-0.202
5	SHIN ISHIKARI	0.396
6	TOMAKOMAI	0.129
7	MURORAN	0.271
8	AOMORI	0.090
9	HACHINOHE	-0.098
10	MAZAKI	-0.092
11	MIYAKO	0.194
12	OFUNATO	---.-----
13	SHIOGAMA	0.193
14	TAIRA	0.046
15	SHINTONE	-0.092
16	KASHIMA JIMU	-0.002
17	KASHIMA PWR	-0.047
18	TONE ESD	-0.139
19	OMIGAWA	-0.104
20	CHIBA	0.021
21	YAMASHITA HEN	-0.123
22	KANNONZAKI	0.129
23	OCHIAI C	-0.768
24	KINOKAWA	-0.771
25	ITAJIMA	0.349
26	HOSOSHIMA	-0.113
27	SOMA	0.239
28	SHINAGAWA	0.032
29	ONAHAMA JI	0.076
30	AKITA	-0.037
31	CHIBA S	-0.032
32	HITACHI NAKA	0.135
33	KASHIMA ZOKAN	0.016

Table 4-IV Regression Coefficients, Site Amplification Coefficients, Multiple Coefficient and Standard Deviation for Velocity and Displacement models

REGRESSION COEFFICIENTS		MAX. VEL	MAX. DIS
α, δ		0.153	0.236
b_1		-1.164	-1.164
b_2		0.358	0.358
c_v , c_d		0.535	-0.522
B_i ,D_i			
1	KUSHIRO	0.431	0.345
2	CHIYODA	0.296	0.294
3	TOKACHI	0.127	0.151
4	HOROMAN	-0.295	-0.302
5	SHIN ISHIKARI	0.748	0.662
6	TOMAKOMAI	0.255	0.241
7	MURORAN	0.313	0.213
8	AOMORI	0.488	0.494
9	HACHINOHE	0.131	0.176
10	MAZAKI	0.039	0.409
11	MIYAKO	0.033	-0.034
12	OFUNATO	--.-----	--.-----
13	SHIOGAMA	0.465	0.161
14	TAIRA	0.310	0.282
15	SHINTONE	0.298	0.204
16	KASHIMA JIMU	0.364	0.239
17	KASHIMA PWR	0.294	0.089
18	TONE ESD	0.346	0.568
19	OMIGAWA	0.357	0.587
20	CHIBA	0.314	0.432
21	YAMASHITA HEN	0.116	0.051
22	KANNONZAKI	0.179	0.067
23	OCHIAI C	-0.534	-0.641
24	KINOKAWA	-0.568	-0.650
25	ITAJIMA	0.356	0.207
26	HOSOSHIMA	0.051	-0.118
27	SOMA	0.110	-0.088
28	SHINAGAWA	0.358	0.136
29	ONAHAMA JI	0.112	0.099
30	AKITA	0.227	0.248
31	CHIBA S	0.342	0.176
32	HITACHI NAKA	0.053	-0.496
33	KASHIMA ZOKAN	0.133	0.050
MULTIPLE CORRELATION COEFFICI.		0.770	0.848
STANDARD DEVIATION		0.264	0.272

$$d_{max}(i,M,r) = 10^{-0.499 + 0.594\ M - 1.64 \log_{10} r} \times 10^{D_i} \qquad (r > 10^{0.014 + 0.218 M}) \tag{4.7}$$

where $\mathbf{B_i}$ and $\mathbf{D_i}$ are given in Table 4-4 on the condition that $\mathbf{B_i = 0}$ or $\mathbf{D_i = 0}$ for the reference site.

Finally, adequacy of the semi-empirical model was checked statistically by inspection of the residuals plots. The residual, which is simply the ratio of the observed to predicted velocities from Eqs.(4.4) and (4.5), were plotted as functions of each independent variable. The residual plots for peak velocity are illustrated in Figs. 4-1 through 4-3. The fact that no particular trend was observed in the residual plots implies that the proposed semi-empirical model is adequate from a statistical point of view.

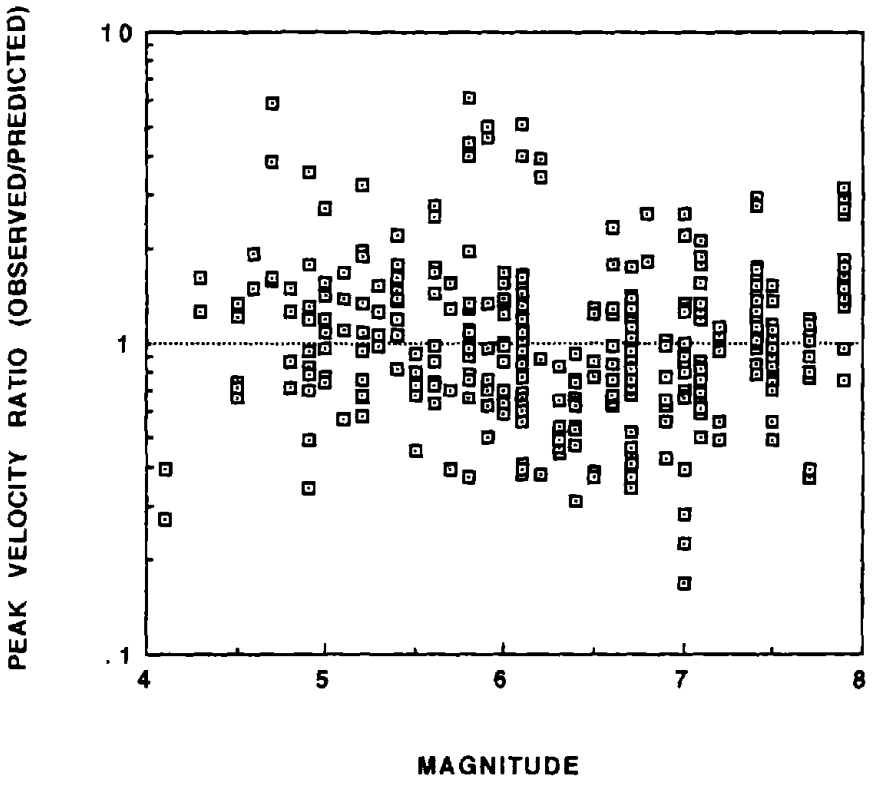

Fig.4-1 Residual Plots of Peak Velocity versus Magnitude

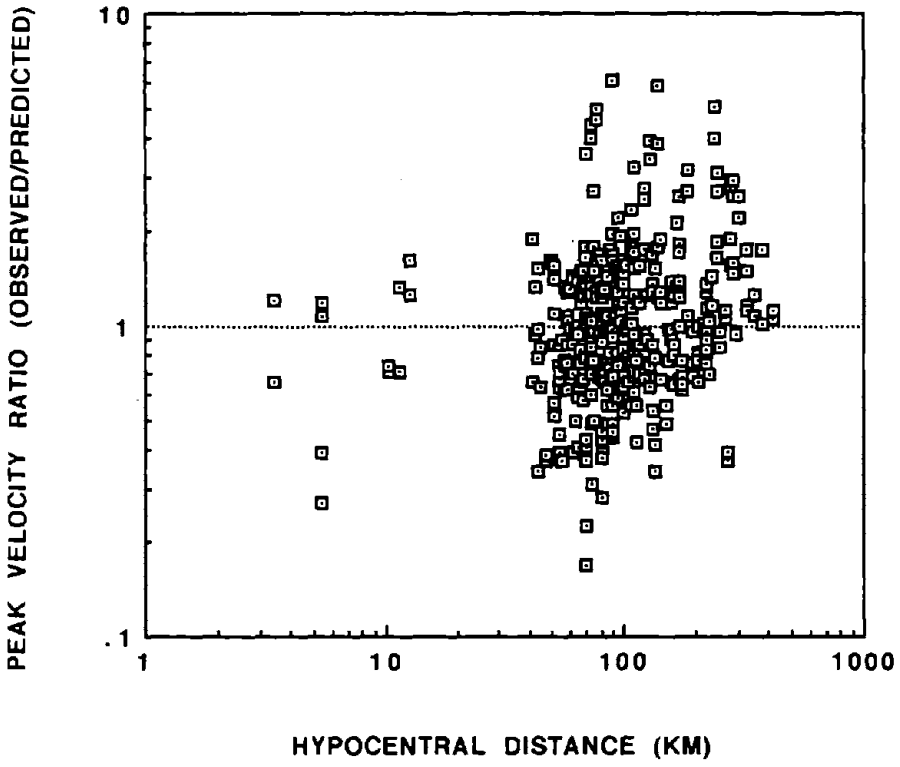

Fig.4-2 Residual Plots of Peak Velocity versus Hypocentral Distance

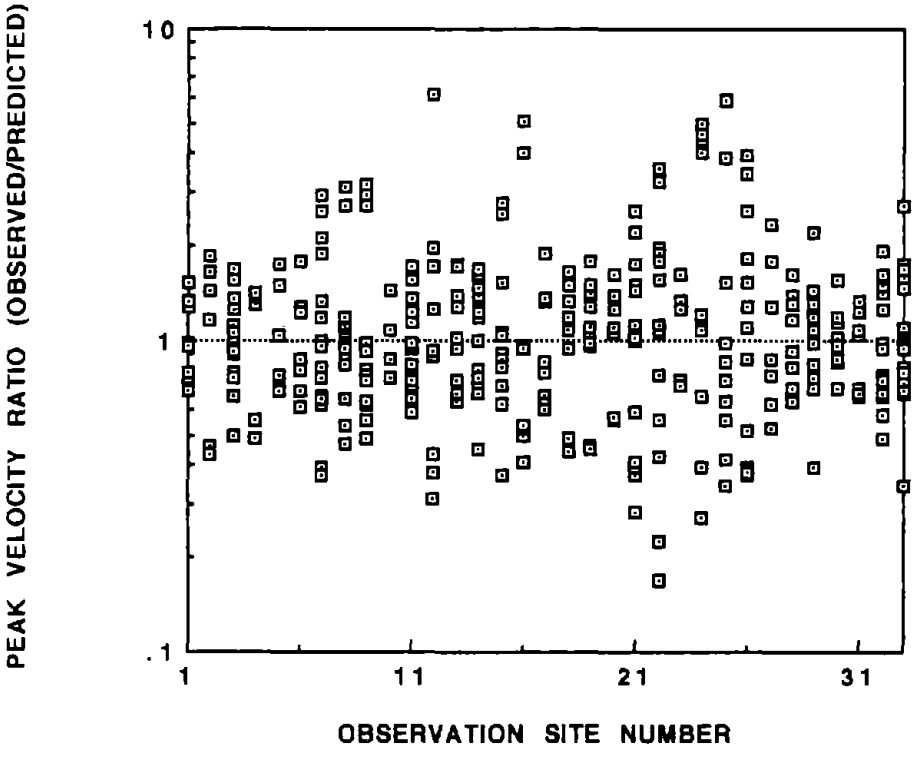

Fig.4-3 Residual Plots of Peak Velocity versus Observation Site Number

SECTION 5
AMPLIFICATION DUE TO LOCAL SITE CONDITIONS

The proposed semi-empirical model provides local soil amplification factors for the peak values at each site. In this section, the amplification factors are discussed in terms of the soil conditions at the sites as well as the frequency content of the motions.

5.1 Amplification Factors for the Peak Acceleration, Velocity and Displacement

As implied in Eq.(4.2) to Eq.(4.7), the amplification factor at each site is given by 10^{A_i}, 10^{B_i} or 10^{D_i} with respect to the reference site which was selected as a candidate to satisfy the condition of the seismic bed rock. Table 5-I lists the amplification factors obtained for the peak acceleration, velocity and displacement at each site along with their mean values and standard deviations. In Table 5-I, the amplification factor at the reference site (OFUNATO) is set to be one by definition. We can see from Table 5-I that the amplification factors vary markedly from site to site probably reflecting the difference in the soil conditions. In addition, the variations of the amplification factors differ depending on the type of motion characteristics: acceleration, velocity and displacement. This significant variation in amplification factors indicates the importance of taking individual site conditions into consideration, as contrasted with the rough classification schemes of soil conditions employed in the past studies. The averages and standard deviations in Table 5-I also reveal that the peak acceleration is less dependent on local site conditions than the peak velocity and displacement. Correlations between the amplification factors for the peak acceleration, velocity and displacement are shown in Figs.5-1 to 5-3. Note that, as shown in Figs.5-1 and 5-2, the amplification factor for peak acceleration is not well correlated with the amplification factors for peak velocity and peak displacement, while Fig.5-3 shows that the amplification factor for peak velocity is fairly well correlated with that for peak displacement. This suggests that there is a difference in the mechanism and frequency content between acceleration motion and the other motions such as velocity and displacement when they are amplified through surface soils.

It is noted in Table 5-I that the two observation sites, OCHIAI C and KINOKAWA give very small amplification factors for the peak acceleration, peak velocity and peak displacement. These amplification factors are considerably smaller than that for the reference site(OFUNATO). The recording conditions of strong motions at these two sites are the most likely reason. Note that almost all the strong-motion records observed at the two sites are lacking in a part of the main-

Table 5-I Amplification Factors for Peak Acceleration, Peak Velocity and Peak Displacement

		AMPLIFICATION FACTORS		
NO	SITE NAME	ACC	VEL	DIS
1	KUSHIRO	1.57	2.70	2.21
2	CHIYODA	1.30	1.98	1.97
3	TOKACHI	1.29	1.34	1.42
4	HOROMAN	0.63	0.51	0.50
5	SHIN ISHIKARI	2.49	5.59	4.67
6	TOMAKOMAI	1.35	1.80	1.74
7	MURORAN	1.86	2.05	1.63
8	AOMORI	1.23	3.08	3.12
9	HACHINOHE	0.80	1.35	1.50
10	MAZAKI	0.81	1.09	2.56
11	MIYAKO	1.56	1.08	0.92
12	OFUNATO	1.00	1.00	1.00
13	SHIOGAMA	1.56	2.91	1.45
14	TAIRA	1.11	2.04	1.91
15	SHINTONE	0.81	1.99	1.60
16	KASHIMA JIMU	1.00	2.31	1.73
17	KASHIMA PWR	0.89	1.97	1.23
18	TONE ESD	0.73	2.27	3.70
19	OMIGAWA	0.79	2.27	3.86
20	CHIBA	1.05	2.06	2.70
21	YAMASHITA HEN	0.76	1.45	1.12
22	KANNONZAKI	1.35	1.51	1.17
23	OCHIAI C	0.17	0.29	0.23
24	KINOKAWA	0.17	0.28	0.22
25	ITAJIMA	2.23	2.27	1.61
26	HOSOSHIMA	0.74	1.12	0.76
27	SOMA	1.73	1.29	0.82
28	SHINAGAWA	1.08	2.28	1.37
29	ONAHAMA JI	1.19	1.31	1.26
30	AKITA	0.92	1.68	1.77
31	CHIBA S	0.93	2.20	1.50
32	HITACHI NAKA	1.36	1.13	0.32
33	KASHIMA ZOKAN	1.03	1.36	1.12
	AVERAGE	1.136	1.805	1.657
	SD	0.497	0.965	1.027

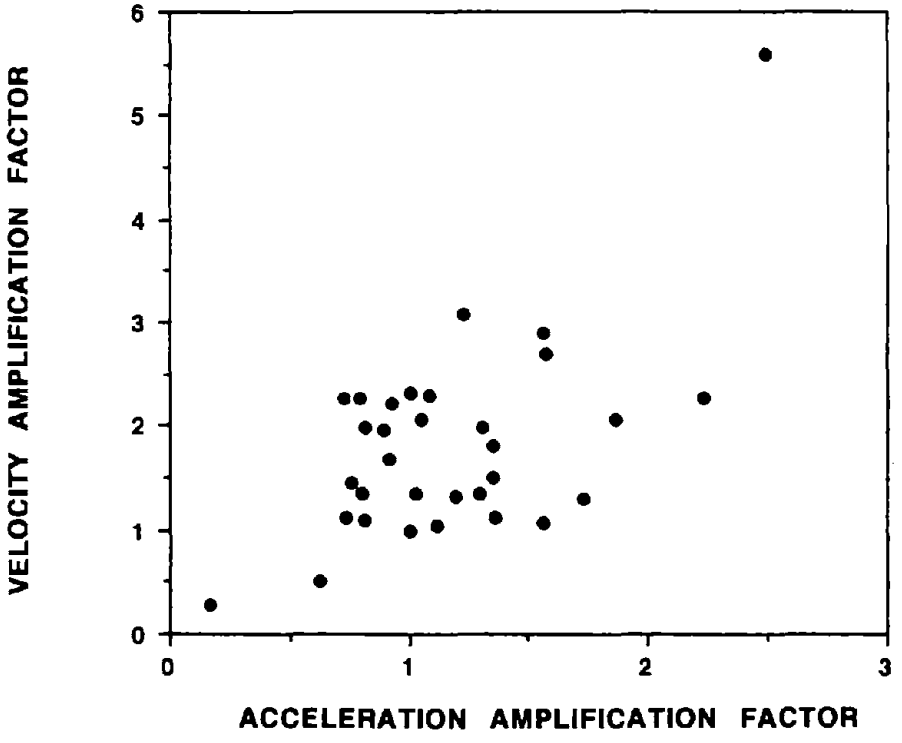

Fig.5-1 Scattergram of Velocity and Acceleration Amplification Factors (Correlation Coefficient =0.635)

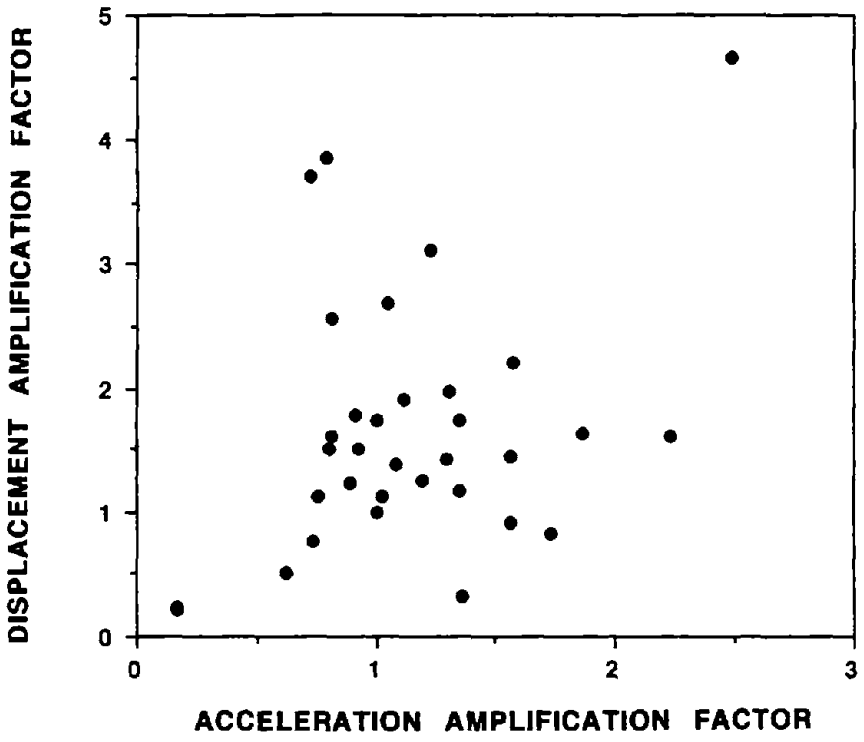

Fig.5-2 Scattergram of Displacement and Acceleration Amplification Factors (Correlation Coefficient=0.329)

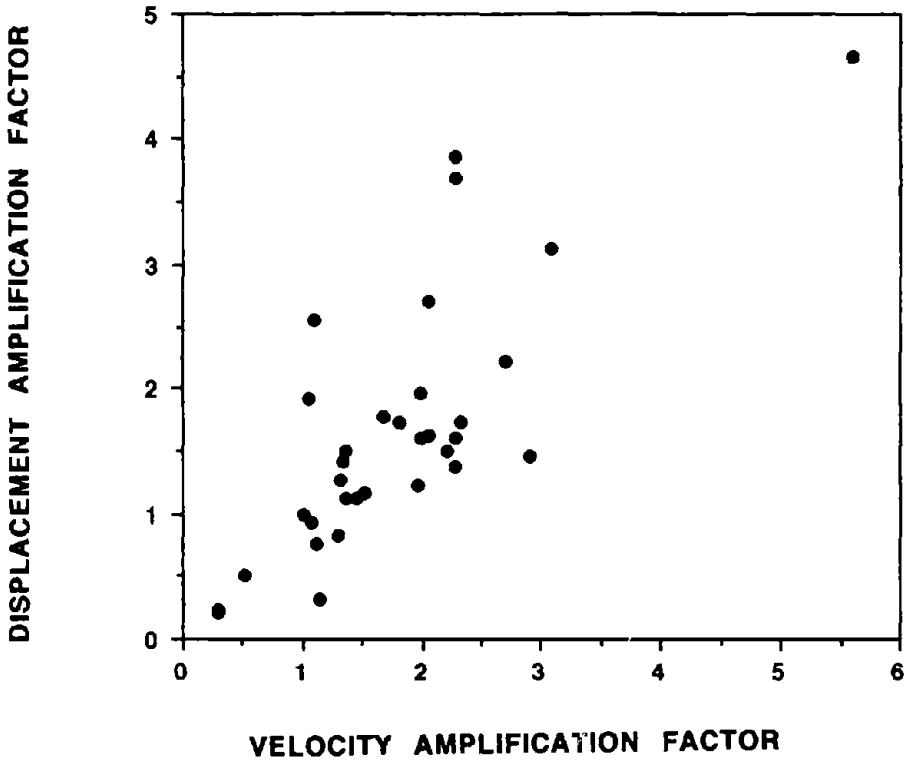

Fig.5-3 Scattergram of Displacement and Velocity Amplification Factors (Correlation Coefficient=0.767)

motions as well as first-motions, resulting from miss triggering of the recording instruments. Incompleteness of the recordings is considered to affect the peak values of acceleration, velocity and displacement at both sites because they were obtained through band-pass filtering as well as the instrument correction. Hence the two sites of OCHIAI C and KINOKAWA are exempted from the discussion of amplification in terms of frequency and local soils which will be described in a later section.

The same reference site was selected for all three motions; acceleration, velocity and displacement. At the same time, OFUNATO was assigned to the reference site as a candidate satisfying the condition of the seismic bed rock for the other sites. However, the difference in the variations of amplification factors for the three motions indicates that the reference site should be selected differently depending on the motion characteristics. In fact, the absolute values of the amplification factors in Table 5-I differ for the peak acceleration, velocity and displacement. Note that, for example, the average amplification factor for the peak acceleration is only slightly larger than 1.0 which is the amplification factor for the reference site, whereas the average amplification factors for the peak velocity and displacement are roughly 1.8 and 1.7 respectively. Since local soil conditions generally amplify the motions incident to the seismic bed rock, the amplification factor is expected to be greater than 1.0 when the reference site is properly selected to satisfy the condition of the seismic bed rock. In the cases of the peak velocity and displacement in Table 5-I, the amplification factors at each site are almost always greater than 1.0, implying a relatively proper selection as seismic bed rock site. The amplification factors for the peak acceleration, on the other hand, show many values less than 1.0. This means that the reference site is improperly selected to satisfy the condition of seismic bed rock for the peak acceleration.

A possible way for obtaining more proper amplification factors is to redo the regression analysis for the peak acceleration by selecting another reference site. However this requires iteration because the selection of the reference site is not the only parameter controlling the amplification factors. Considering that we have obtained meaningful amplification factors as relative values even though they are controversial in the absolute values, we herein renovate the amplification factors in Table 5-I so as to meet the proper condition of amplification. That is, the amplification factors in Table 5-I are multiplied by a value to correspond to the definition of amplification factor with respect to the seismic bed rock. Though the inverse of the least amplification factor in each motion peak in Table 5-I can be a candidate for the multiplier, such simple multiplication gives little reasonable amplification factor because the least amplification factor involves more statistical errors. Herein we make an alternative attempt by renovating the amplification factors in Table 5-I so that the average value minus the one standard error is 1.0. For example, **1/(1.136-0.497)** is

multiplied to the amplification factors in the case of the peak acceleration. This is an attempt to make the amplification factors approach proper values with respect to the seismic bed rock while avoiding the statistical errors. The amplification factors for the peak velocity and peak displacement were also renovated in a similar manner. The final amplification factors for each motion peak are listed in Table 5-II. Note in Table 5-II that the definition of the seismic bed rock differs for peak acceleration, velocity and displacement as a result of the renovations. For example, HOROMAN, OFUNATO and HOROMAN correspond to the seismic bed rock site for the peak acceleration, velocity and displacement respectively because their renovated amplification factors are nearly equal to 1.0. A geological survey shows a rock outcrop at the HOROMAN site as well as OFUNATO. Table 5-II shows that the absolute values for the renovated amplification factors are always greater than 1.0 except at a few sites including OCHIAI C and KINOKAWA. Table 5-II also indicates that the average values of the renovated amplification factors increase proportionally from acceleration to displacement. This is consistent with a theoretical explanation from amplification phenomena through surface soils. That is, the amplification factor for velocity motion is theoretically expected to be greater than that for acceleration motion because velocity motion is generally affected by deeper soil layers with its dominant amplitude components in longer periods than acceleration motion. Similarly the amplification for displacement motion is greater than that for velocity motion.

As a result of the renovations for the amplification factors, the overall semi-empirical expressions of Eqs.(4.2) to (4.7) are modified so that the motion peaks on the seismic bed rock are diminished to offset the increased amplification factors resulting from the renovations. Denoting the renovated amplification factors at the i-th site in Table 5-II as $\mathbf{AMP_i(a)}$, $\mathbf{AMP_i(v)}$ and $\mathbf{AMP_i(d)}$ for the peak acceleration, peak velocity and peak displacement respectively, we rewrite the final semi-empirical expressions as follows:

(peak acceleration)

$$\begin{aligned} a_{max}(i,M,r) &= (1.136 - 0.497) \times 10^{2.910} \times AMP_i(a) && (r \le 10^{0.014+0.218M}) \\ &= 518.9 \times AMP_i(a) && (r \le 10^{0.014+0.218M}) \end{aligned} \tag{5.1}$$

$$a_{max}(i,M,r) = 547.6 \times 10^{0.358M - 1.64\log_{10} r} \times AMP_i(a) \quad (r > 10^{0.014+0.218M}) \tag{5.2}$$

Table 5-II Renovated Amplification Factors for Peak Acceleration, Peak Velocity and Peak Displacement

----------	----------	RENOVATED AMPLIFICATION FACTORS		
NO	SITE NAME	ACC	VEL	DIS
1	KUSHIRO	2.46	3.21	3.51
2	CHIYODA	2.03	2.36	3.13
3	TOKACHI	2.02	1.60	2.25
4	HOROMAN	0.99	0.61	0.79
5	SHIN ISHIKARI	3.90	6.66	7.41
6	TOMAKOMAI	2.11	2.14	2.76
7	MURORAN	2.91	2.44	2.59
8	AOMORI	1.92	3.67	4.95
9	HACHINOHE	1.25	1.61	2.38
10	MAZAKI	1.27	1.30	4.06
11	MIYAKO	2.44	1.29	1.46
12	OFUNATO	1.56	1.19	1.59
13	SHIOGAMA	2.44	3.46	2.30
14	TAIRA	1.74	2.43	3.03
15	SHINTONE	1.27	2.37	2.54
16	KASHIMA JIMU	1.56	2.75	2.75
17	KASHIMA PWR	1.39	2.35	1.95
18	TONE ESD	1.14	2.70	5.87
19	OMIGAWA	1.24	2.70	6.13
20	CHIBA	1.64	2.45	4.29
21	YAMASHITA HEN	1.19	1.73	1.78
22	KANNONZAKI	2.11	1.80	1.86
23	OCHIAI C	0.27	0.35	0.37
24	KINOKAWA	0.27	0.33	0.35
25	ITAJIMA	3.49	2.70	2.56
26	HOSOSHIMA	1.16	1.33	1.21
27	SOMA	2.71	1.54	1.30
28	SHINAGAWA	1.69	2.71	2.17
29	ONAHAMA JI	1.86	1.56	2.00
30	AKITA	1.44	2.00	2.81
31	CHIBA S	1.46	2.62	2.38
32	HITACHI NAKA	2.13	1.35	0.51
33	KASHIMA ZOKAN	1.61	1.62	1.78
----------	AVERAGE	1.778	2.149	2.630
----------	SD	0.778	1.149	1.630

(peak velocity)

$$v_{max}(i,M,r) = (1.805 - 0.965) \times 10^{0.535+0.153M} \times AMP_i(v) \quad (r \le 10^{0.014+0.218M})$$

$$= 2.879 \times 10^{0.153M} \times AMP_i(v) \quad (r \le 10^{0.014+0.218M}) \qquad (5.3)$$

$$v_{max}(i,M,r) = 3.036 \times 10^{0.511M-1.64\log_{10}r} \times AMP_i(v) \quad (r > 10^{0.014+0.218M}) \qquad (5.4)$$

(peak displacement)

$$d_{max}(i,M,r) = (1.657 - 1.027) \times 10^{-0.522+0.236M} \times AMP_i(d) \quad (r \le 10^{0.014+0.218M})$$

$$= 0.189 \times 10^{0.236M} \times AMP_i(d) \quad (r \le 10^{0.014+0.218M}) \qquad (5.5)$$

$$d_{max}(i,M,r) = 0.200 \times 10^{0.594M-1.64\log_{10}r} \times AMP_i(d) \quad (r > 10^{0.014+0.218M}) \qquad (5.6)$$

where $\mathbf{a_{max}}$ is peak acceleration(cm/sec^2), $\mathbf{v_{max}}$ is peak velocity(cm/sec), $\mathbf{d_{max}}$ is peak displacement(cm), **i** is the number for identifying the observation site, **M** is the earthquake magnitude, and **r** is the hypocentral distance(km).

5.2 Relation Between the Amplification Factors and Frequency Content

The above discussion reveals that local site effects for peak acceleration are different than those for peak velocity and displacement. This suggests that the dominant frequency component in acceleration, velocity and displacement motions plays a significant role in determining the amplification factor for peak values. In relation to the frequency content in strong motions, Kamiyama and Yanagisawa[9] derived amplification factors for response spectra using almost same strong-motion records and observation sites as in the present study. These spectral amplifications were presented in a frequency-dependent form. Hence they allow us to examine the frequency effect on the amplification factors for the peak values. Figs.5-4 to 5-8 show spectral amplification factors obtained by Kamiyama and Yanagisawa[9] at sites used in this study. No simple relation exists between the peak value and the spectral characteristics of ground motions

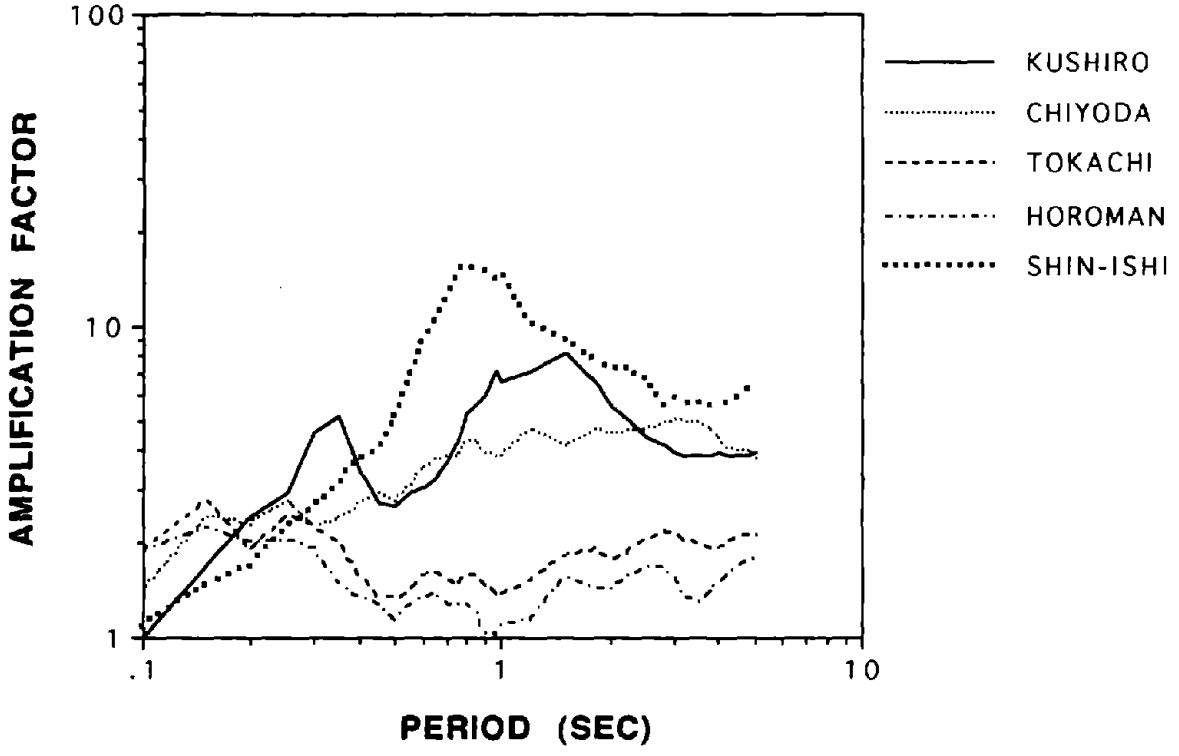

Fig.5-4 Response Spectra Amplification Factors for 5 Sites(Kushiro, Chiyoda, Tokachi, Horoman and Shin Ishikari) in Japan (after Kamiyama and Yanagisawa[9])

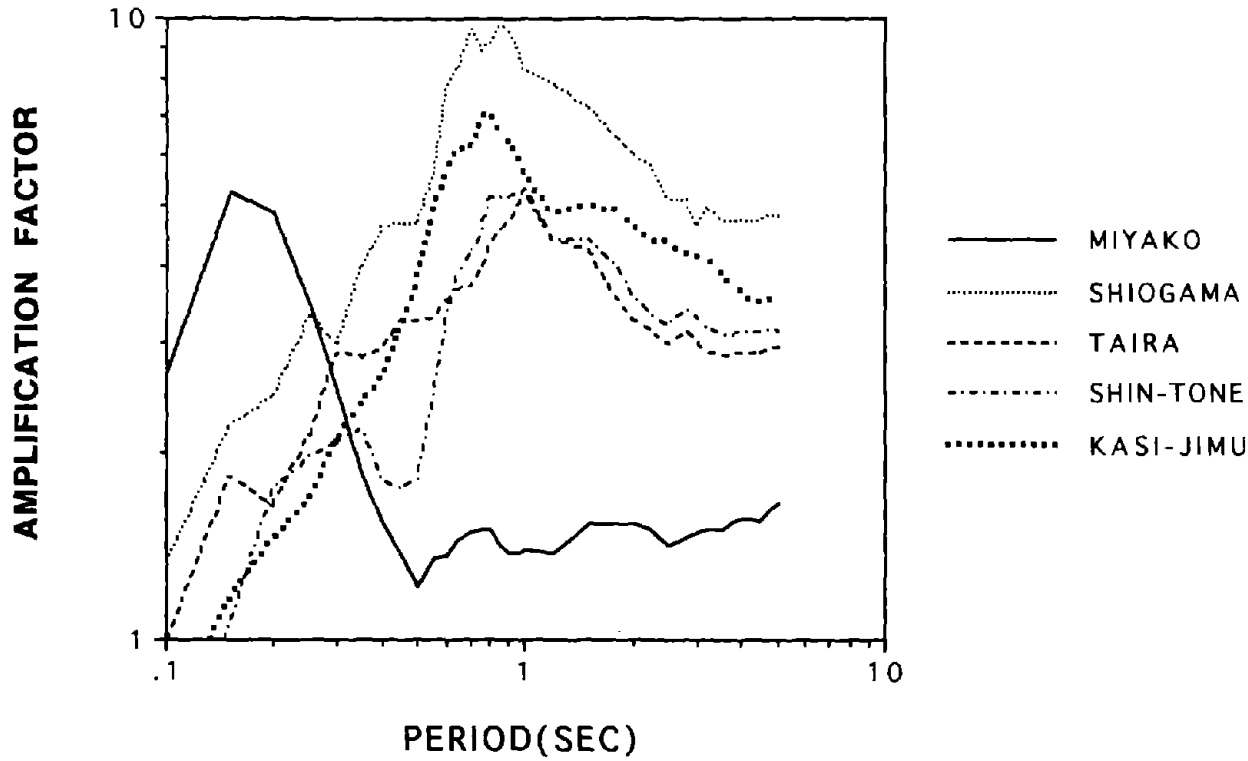

Fig.5-5 Response Spectra Amplification Factors for 5 Sites(Miyako, Shiogama,Taira, Shintone and Kashima Jimu) in Japan (after Kamiyama and Yanagisawa[9])

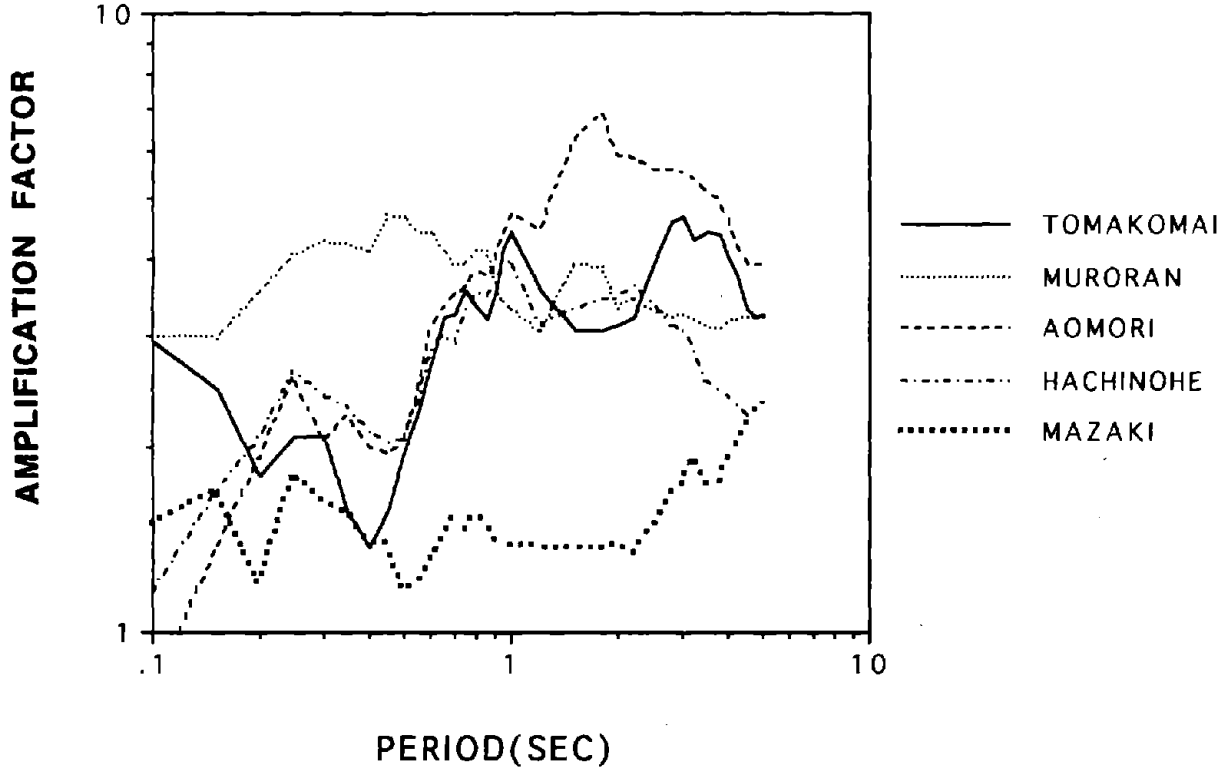

Fig.5-6 Response Spectra Amplification Factors for 5 Sites(Tomakomai, Muroran,Aomori, Hachinohe and Mazaki) in Japan (after Kamiyama and Yanagisawa[9])

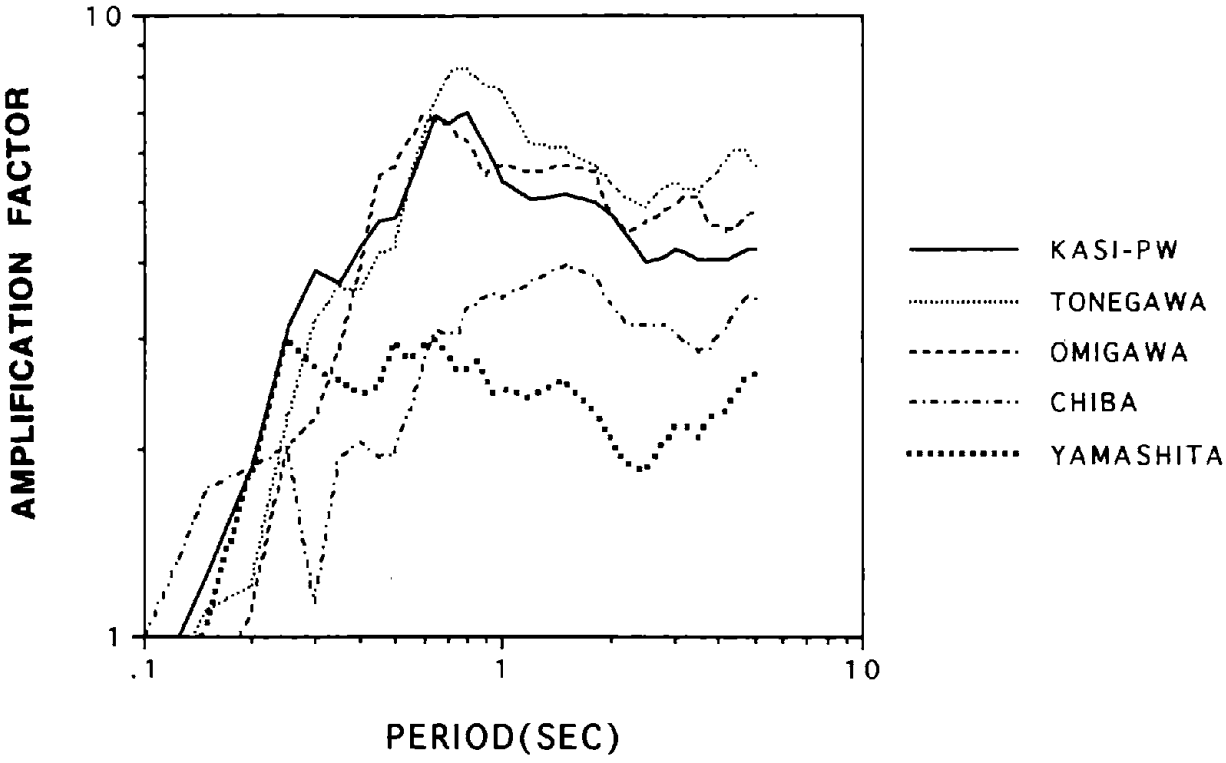

Fig.5-7 Response Spectra Amplification Factors for 5 Sites(Kashima PWR, Tone ESD,Omigawa, Chiba and Yamashita HEN) in Japan (after Kamiyama and Yanagisawa[9])

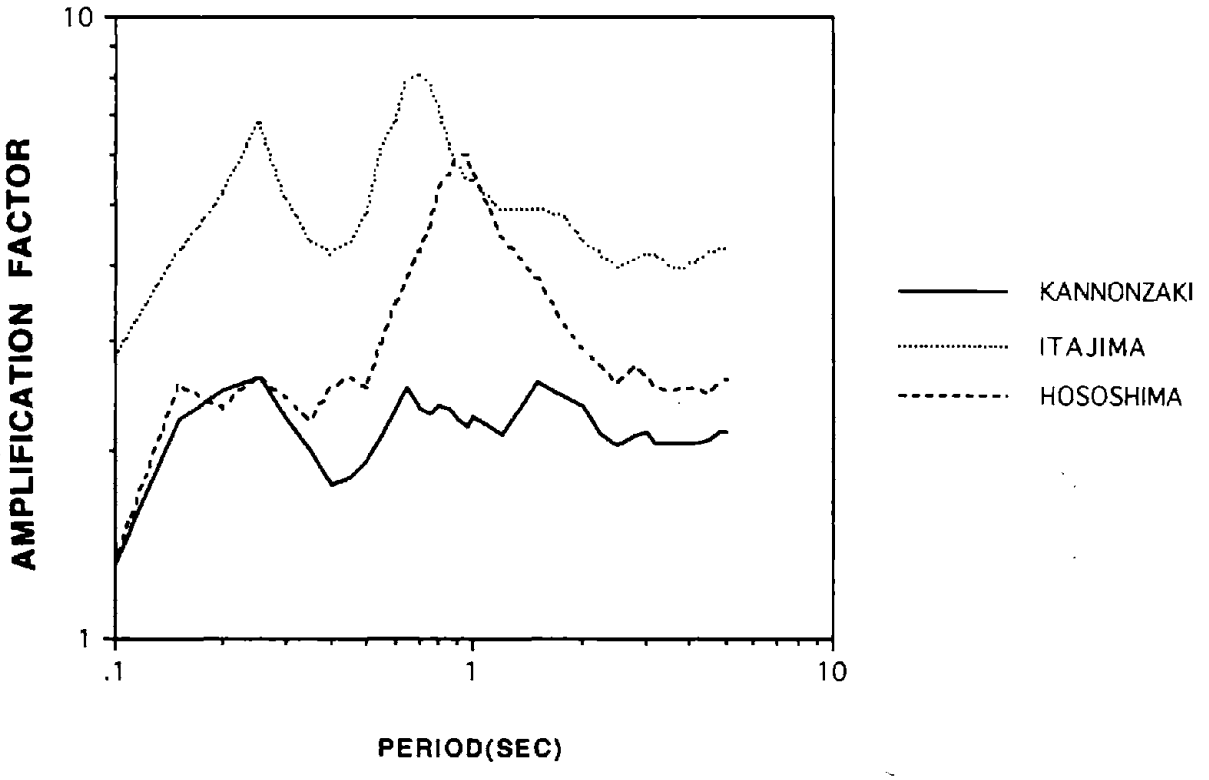

Fig.5-8 Response Spectra Amplification Factors for 3 Sites(Kannonzaki, Itajima and Hososhima) in Japan (after Kamiyama and Yanagisawa[9])

because the peak value results from quite complicated processes. Herein we integrate the amplification spectra in Figs. 5-4 to 5-8 within a period band to investigate how the amplification factors for the peak acceleration, velocity and displacement are associated with their frequency content.

Since short period motions likely control peak acceleration and large period motions likely control peak velocity, band-pass filters were applied to the amplification spectra. The integrated spectral value $\mathbf{SP_i}$ then becomes

$$SP_i = \frac{1}{4.9} \int_{0.1}^{5.0} A_i(T) R(T) dT \qquad (5.7)$$

where $\mathbf{A_i(T)}$ are the period dependent spectral amplifications shown in Figs. 5-4 to 5-8, $\mathbf{R(T)}$ is a high frequency pass filter for peak acceleration and a low frequency pass filter for peak velocity and T is period.

After a number of trials, the high frequency pass filter in Fig.5-9 was chosen for peak acceleration while the low frequency pass filter in Fig.5-10 was chosen for peak velocity. Figs. 5-11 and 5-12 show the correlations between the amplification factors for peak acceleration and peak velocity at some sites in Table 5-II and their corresponding integrated spectral values by Eq.(5.7). The displacement case is omitted herein because of its close correlation with velocity. We can see from Figs.5-9 through 5-12 that the peak acceleration is determined principally by spectral amplifications in periods leass than about 0.3 sec while the peak velocity is determined by periods greater than about 1.0 sec. This means that local soils respond differently to acceleration and velocity motions with a definite period-dependence. It is clear from this result that a site composed of extremely soft soil with high viscosity is expected to show only small peak acceleration in spite of showing a large peak velocity because such a site has spectral amplification with long-period dominance as well as high attenuation in the short period domain. Consider, for example, the SHIN ISHIKATRI site which will be shown later to consist of a deep layer of relatively soft soils. As shown in Fig.5-4, the spectral amplification at this site is large for periods greater than about 1.0 seconds but comparatively small for periods less than 0.3 seconds. As a consequence the amplification factors for the peak velocity and displacement in Table 5-II are about double the peak acceleration amplification factor. Conversely, a site with a thin superficial layer over hard rock tends to exhibit large peak and small peak, respectively, in acceleration and velocity because of the short-period dominance of its spectral amplification. An example is the Miyako site which

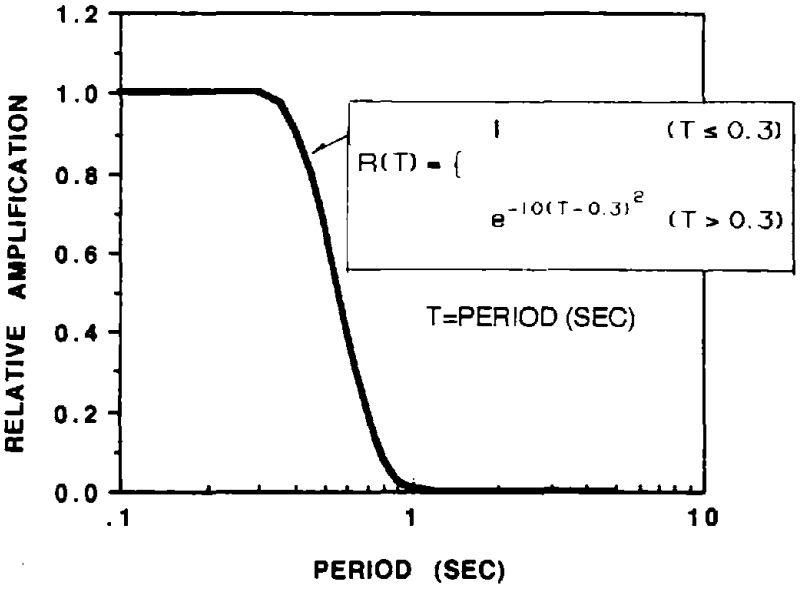

Fig.5-9 High Frequency Pass Filter Applied to Spectra Amplification for Comparison with Peak Acceleration

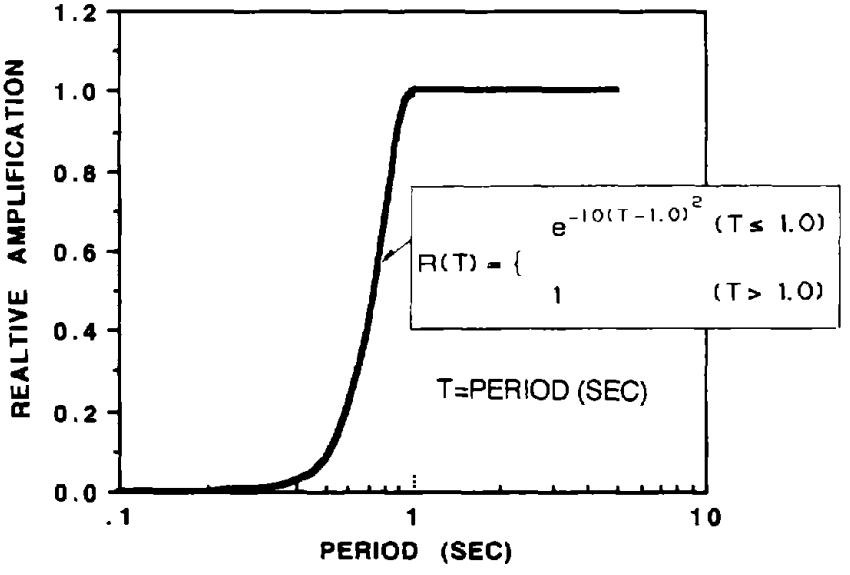

Fig.5-10 Low Frequency Pass Filter Applied to Spectral Amplification for Comparison with Peak Velocity

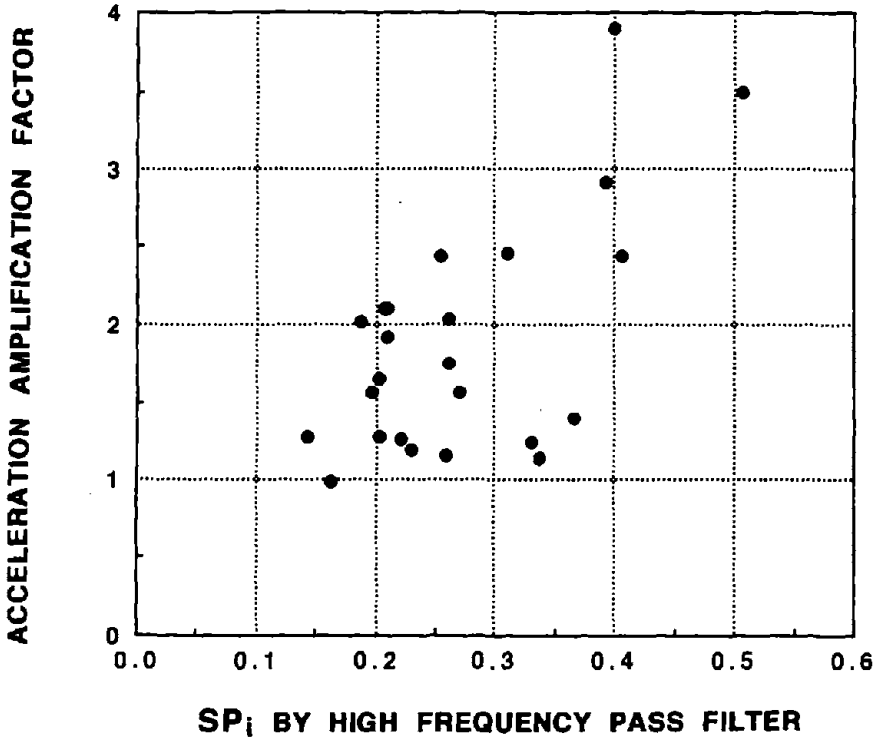

Fig.5-11 Scattergram for Peak Acceleration Amplification Factor and Integrated Spectral Value from Eq.(5.7) Using High Frequency Pass Filter

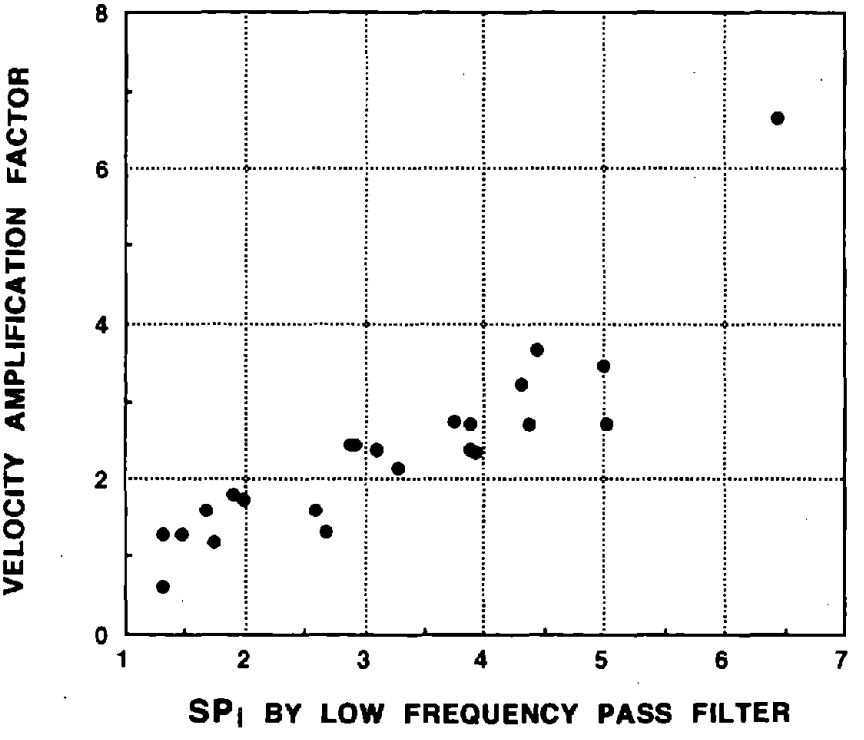

Fig.5-12 Scattergram for Peak Velocity Amplification Factor and Integrated Spectral Value from Eq.(5.7) Using Low Frequency Pass Filter

corresponds to a relatively thin layer over rock. The Miyako site has large spectral amplifications for periods less than 0.3 seconds, as shown in Fig.5-5. The spectral amplification at Miyako is consistent with the small amplification factor for the peak velocity and the relatively large amplification factor for the peak acceleration in Table 5-II.

The above examples suggest that peak velocity can be a candidate parameter more responsible for earthquake damage than peak acceleration which has been regarded as the foremost parameter controlling earthquake damage, because damages were overwhelmingly caused at soft soil sites rather than at firm soil sites in the past earthquakes. In addition, since amplification factors for peak motion are related to different frequency ranges, a two parameter characterization of a site may be appropriate. That is, the seismic hazard for a given site may be given in terms of estimates for both peak acceleration and peak velocity. Peak acceleration would control the design of short period structures while peak velocity would control large period structures.

The difference in the period-dependent amplification between peak acceleration and peak velocity also explains the discrepancy of the reference site noted in the preceding section. The OFUNATO site is not appropriate as a reference site for the peak acceleration while it is justified for peak velocity. Although the OFUNATO site was initially selected as the common reference site because of its outcropping of hard slate, there is a possibility that its surface part has been weathered so as to give a high amplification in short periods. Hence it might fail to offer a proper reference site corresponding to the seismic bed rock for the other sites in the case of the peak acceleration.

5.3 Relation Between the Amplification Factors and the Local Soil Conditions

It is obvious from the foregoing discussion that the peak motion amplification factors are closely related to the corresponding local soil conditions. In order to apply our semi-empirical model to an arbitrary site not included in the present empirical analysis, it is necessary to be able to predict the amplification factors at a site from its local soil conditions. Herein we examine the detailed relation between the empirical amplifications and soil conditions, and propose two methods; one qualitative and the other quantitative for estimating an amplification factor at a new site having soil information.

Soil profiles are available for some of the observation sites in Fig. 3-1. Figs. 5-13(a) to 5-13(q) show the soil profiles at these sites which consist of the soil formation and the standard penetration test results meeting the Japanese Industrial Standard, namely, the N-value. These soil profiles

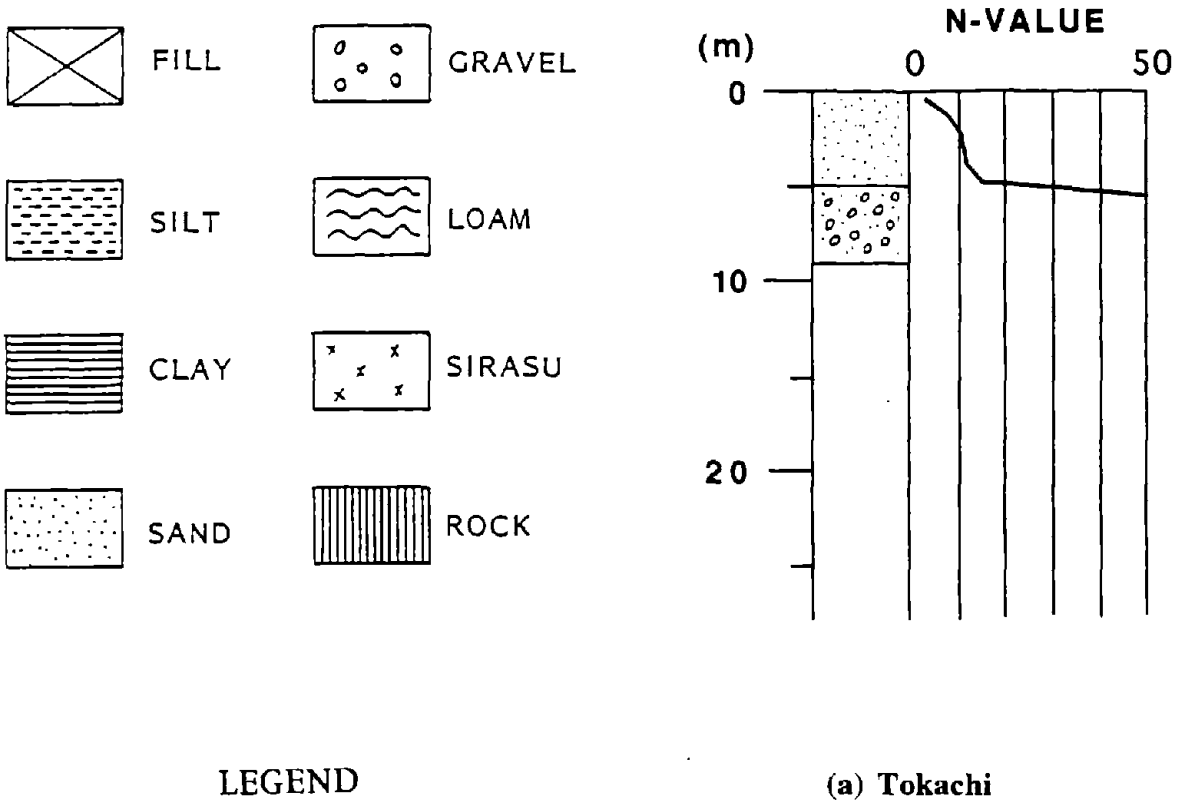

Fig.5-13 Available Soil Profile for Japanese Sites Considered herein

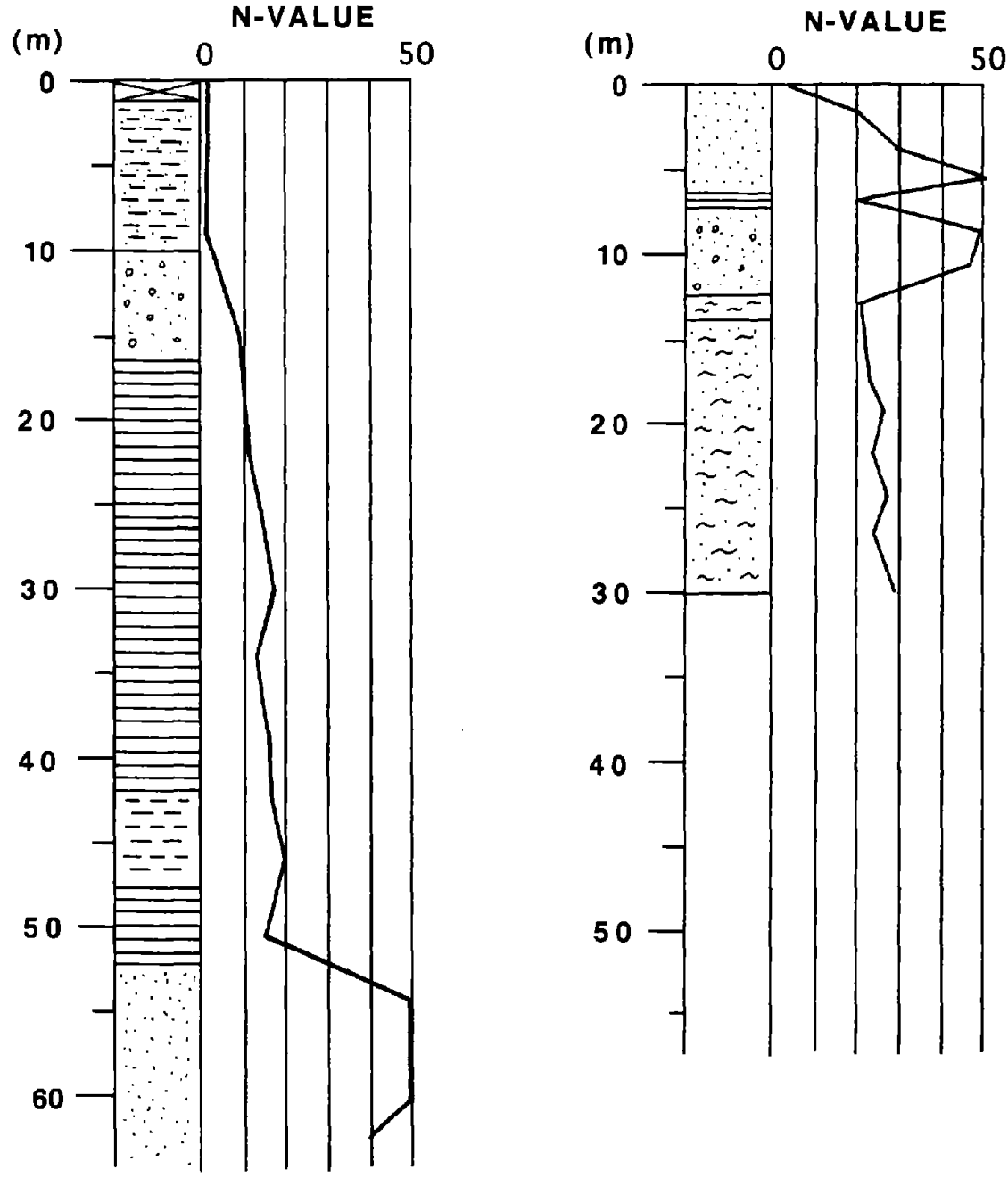

(b) Shin Ishikari

(c) Tomakomai

Fig.5-13 Available Soil Profile for Japanese Sites Considered herein

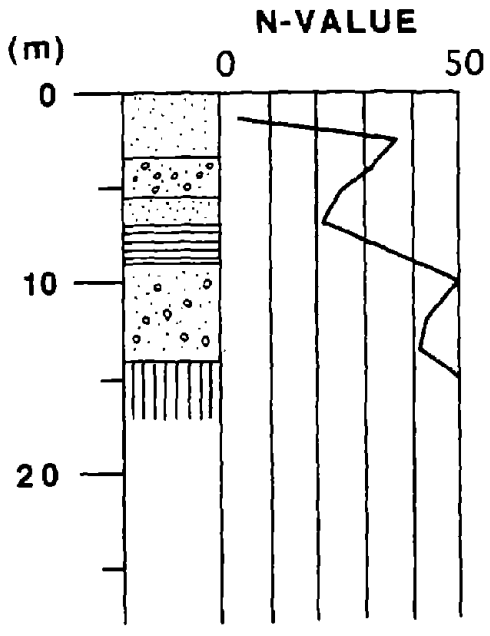

(d) Muroran

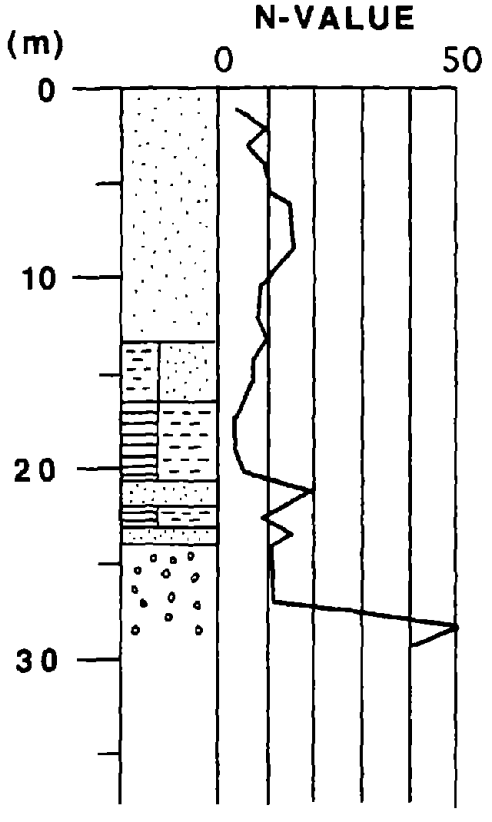

(e) Aomori

Fig.5-13 Available Soil Profile for Japanese Sites Considered herein

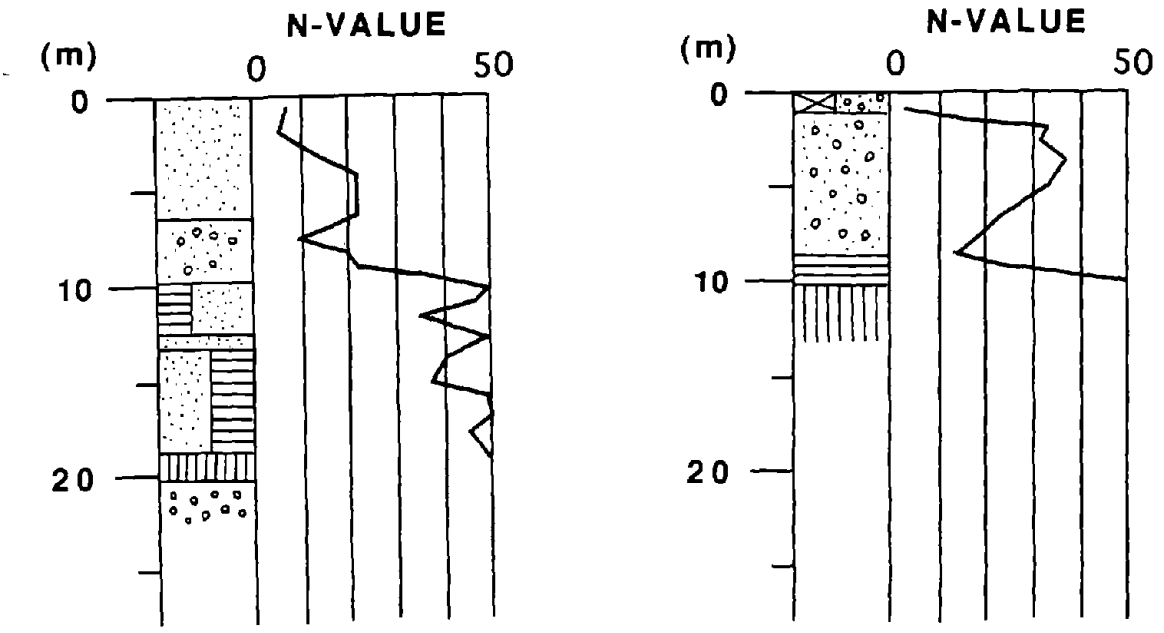

(f) Hachinohe

(g) Miyako

Fig.5-13 Available Soil Profile for Japanese Sites Considered herein

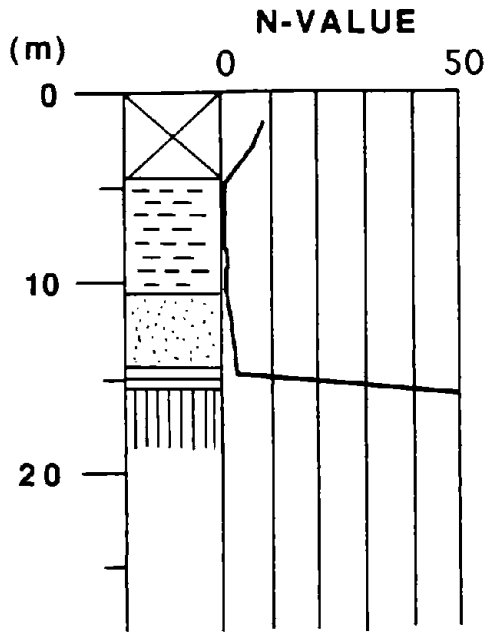

(h) Shiogama

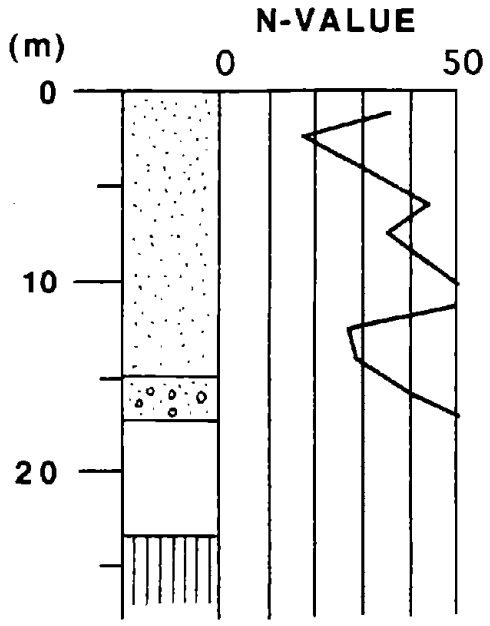

(i) Kashima Jimu

Fig.5-13 Available Soil Profile for Japanese Sites Considered herein

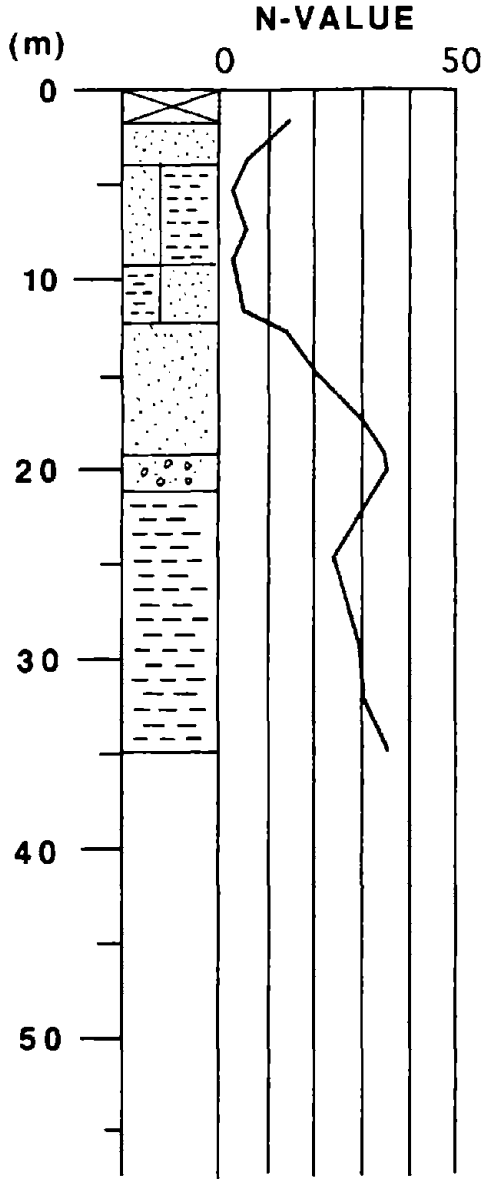

(j) Yamashita Hen

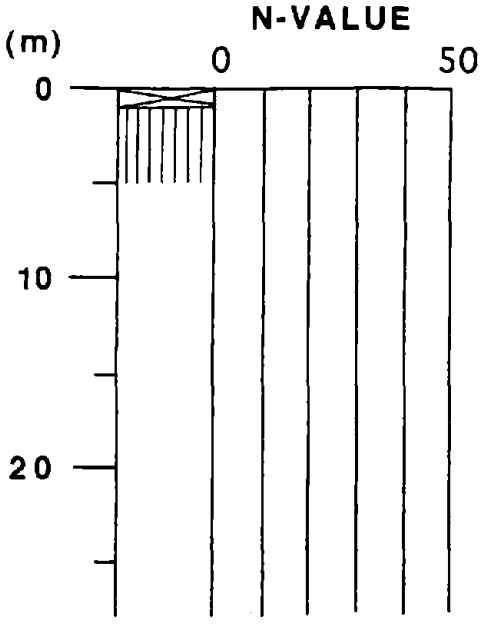

(k) Kannonzaki

Fig.5-13 Available Soil Profile for Japanese Sites Considered herein

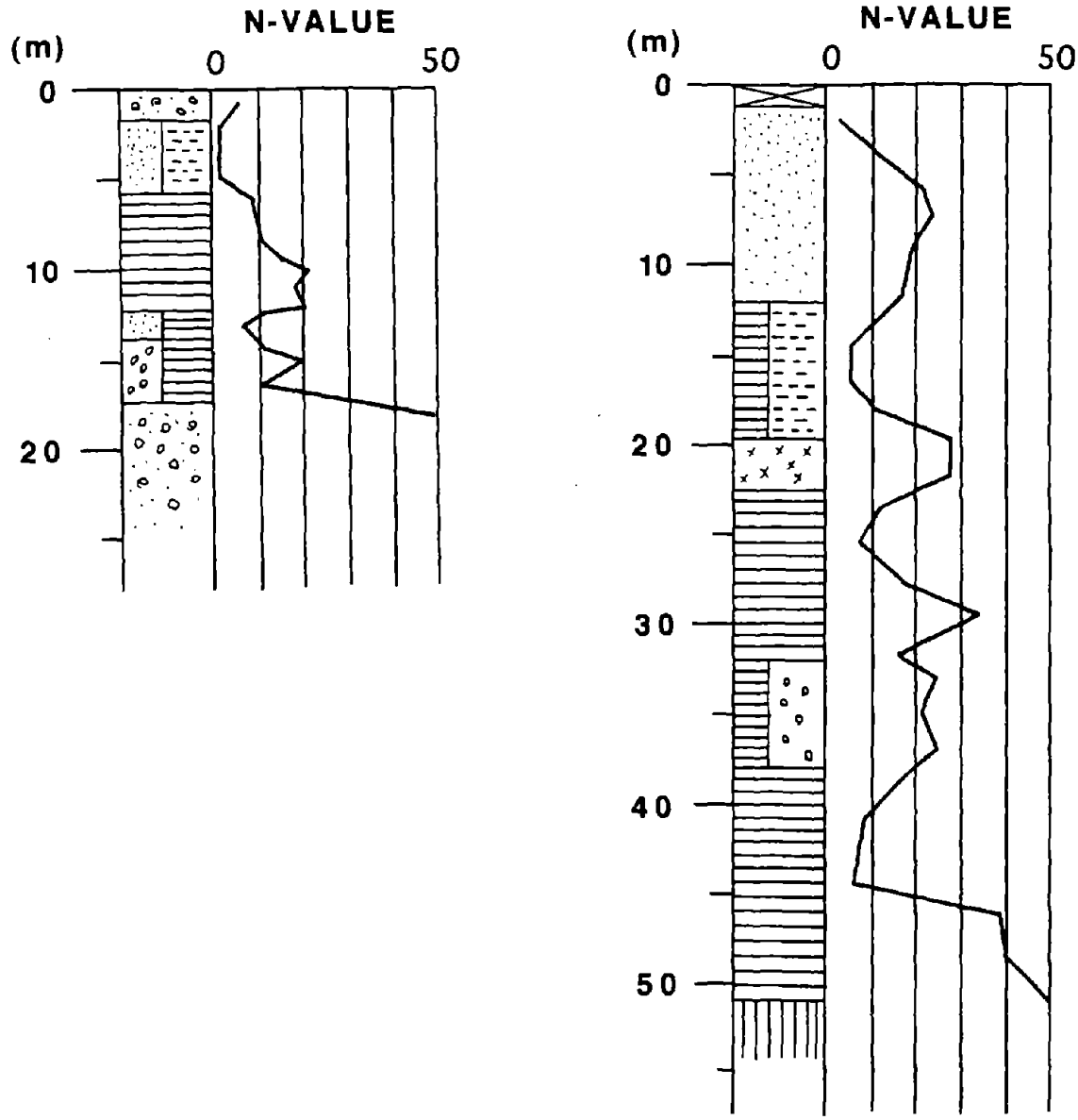

(l) Itajima

(m) Hososhima

Fig.5-13 Available Soil Profile for Japanese Sites Considered herein

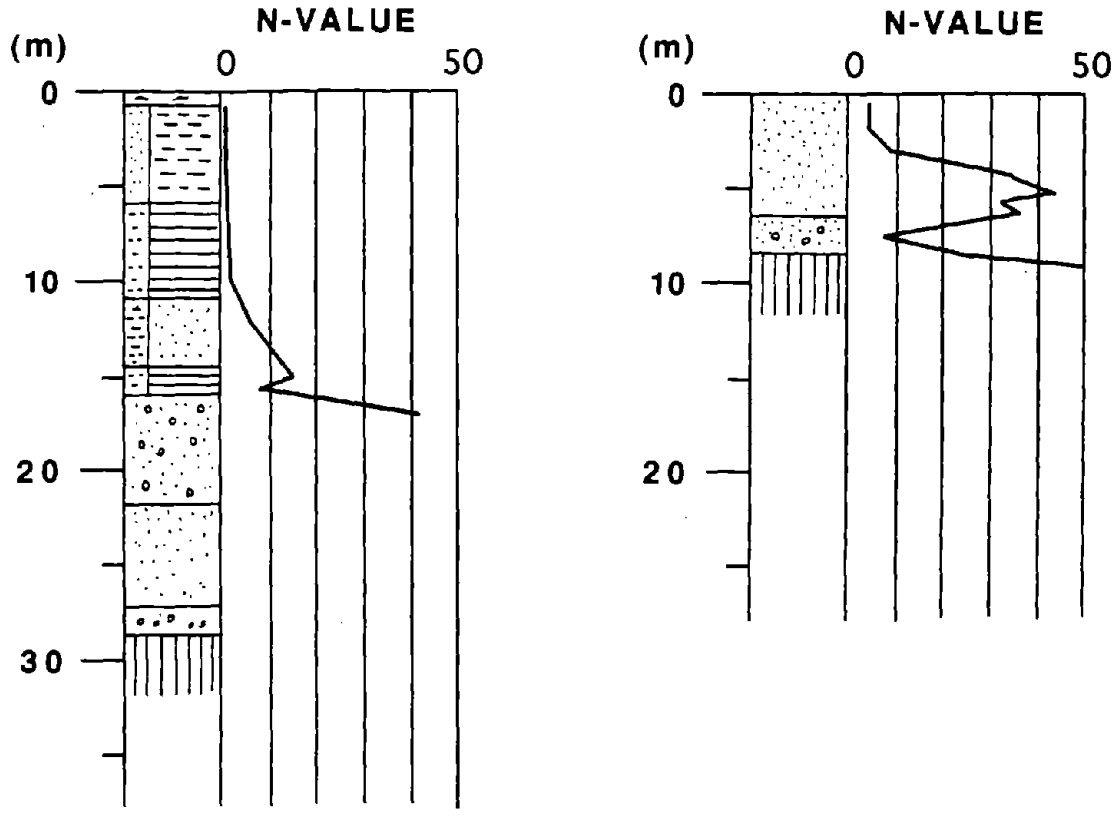

(n) Shinagawa

(o) Onahama Ji

Fig.5-13 Available Soil Profile for Japanese Sites Considered herein

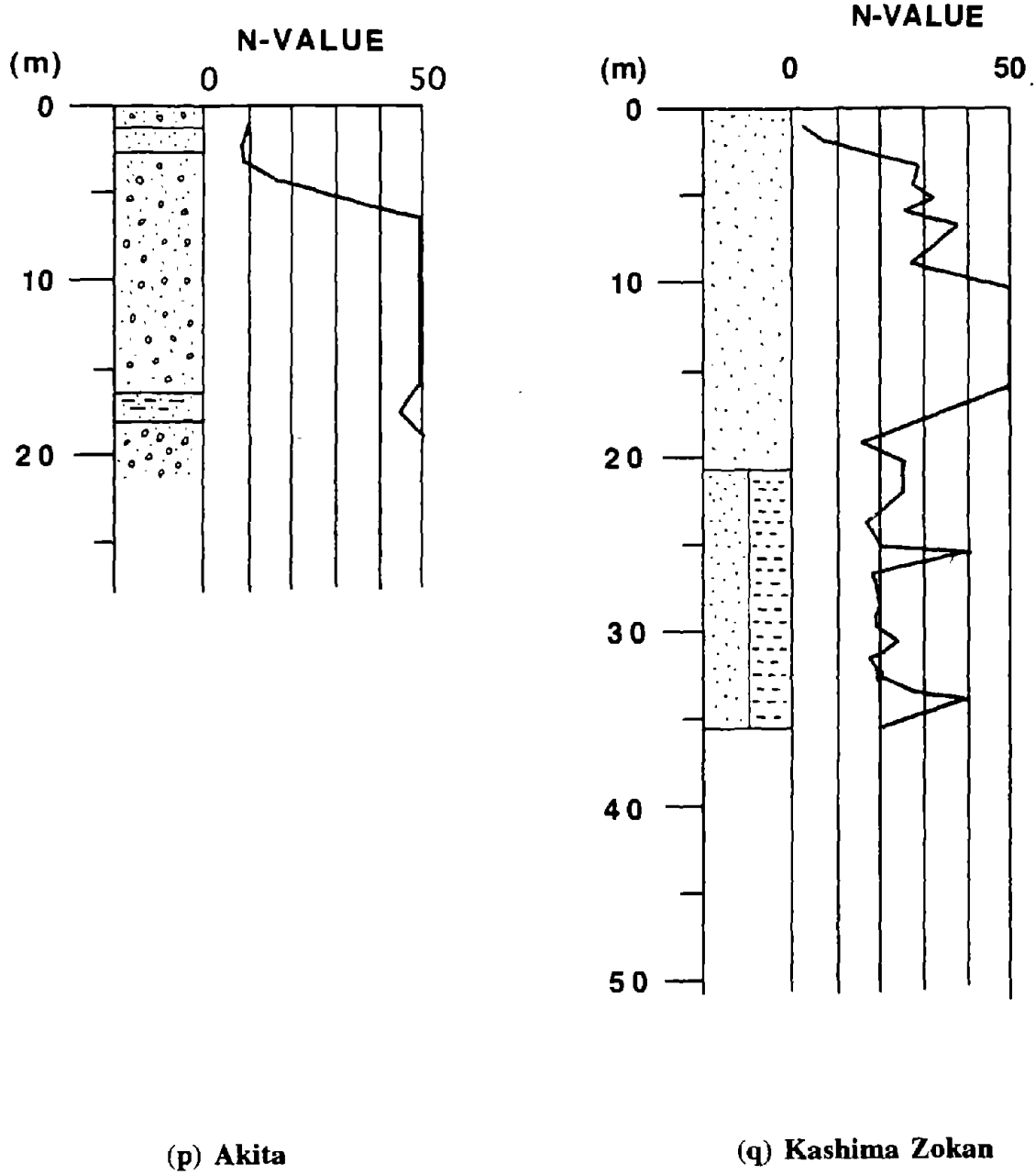

(p) Akita

(q) Kashima Zokan

Fig.5-13 Available Soil Profile for Japanese Sites Considered herein

were obtained primarily from the site data compiled by the Port and Harbor Research Institute, Ministry of Transport of Japan[24].

As illustrated in Figs. 5-13(a) to 5-13(q), each observation site has various types of soil formations as well as soil softness. A close look at both Table 5-II and Figs. 5-13(a) to 5-13(q) indicates that the amplification factors vary depending on the formation and the softness of soils. For example, some soft soil sites like SHIN-ISHIKARI, SHIOGAMA, SHINAGAWA etc. represent large amplification factors for peak velocity and displacement while except for SHIN-ISHIKARI they give relatively small amplifications for acceleration. On the other hand, the stiff soil sites such as TOKACHI, MIYAKO etc. show large amplifications in the peak acceleration while they show extremely small amplifications in the peak velocity and displacement. Such a relation between the amplifications and soil profiles suggests a method for estimating the amplification factor at a new site. That is, given a soil profile at a new site, one can approximately predict an amplification factor at the site by looking for a soil profile in Figs. 5-13 (a) to 5-13(q) most similar to the new site profile and selecting its amplification factor. This method is hereafter called the "qualitative method". Since a variety of soil profiles are compiled in Figs. 5-13(a) to 5-13(q), this method may, despite its simplicity, provide an unexpectedly good way for estimating an amplification factor. For example, both SHINAGAWA(Fig.5-13(n) and SHIOGAMA(Fig.5-13(h) have very soft soils($N<10$) for moderate depth(up to about 15 m). The acceleration and velocity amplification factors for these sites in Table 5-II are somewhat similar (2.44 and 3.46 respectively for SHIOGAMA and 1.69 and 2.71 respectively for SHINAGAWA). That is, both these sites have moderate acceleration amplification but significant velocity amplification. Contrast this with TOKACHI(Fig.5-13(a)) and AKITA(Fig.5-13(p)) which have a thin layer (depth of about 5 m) of moderately soft soils($N\sim10$). Both these sites have low to moderate acceleration amplification factors (2.02 and 1.44 respectively) and somewhat similar velocity amplification factors(1.60 and 2.00 respectively).

The quantitative method for a new site is based upon the concept of the vibration impedance ratio. As described previously, the amplification factors for the peak acceleration, velocity and displacement were obtained with respect to the seismic bed rock at our reference site having S wave velocity of 1 to 2 km/sec range. This strictly means that these amplification factors should be related to soil structures overlaying such seismic bed rock. In general, however, seismic bed rock is laid deep and we have almost no opportunity for finding it in a usual soil profile. In addition, one needs elaborate material information of each layer such as P and S waves velocity, Q values, etc. in order to relate soil conditions to the empirical amplification factors. However such material information is available only at some special sites because of the cost. Hence although vibration

impedance and amplification are directly related to P and S wave velocities, density and Q value(damping), herein we use the N-value variation with depth such as shown in Figs.5-13(a) to 5-13(q) which is the typical information available to a designer and is known to have some relation with the rigidity and density of soils.

Furthermore the quantitative method is restricted to peak velocity amplification factors. This is based on two consideration; first of all Table 5-II indicates that the variation in the peak acceleration amplification factors is relatively small and secondly peak velocity is the parameter of interest for lifeline earthquake engineering studies which is the primary purpose of this study. After a number of trials, the following expression C_{amp} was chosen to represent the impedance characteristics and predominant period of a soil profile.

$$C_{amp} = \mathrm{Max}\left[\frac{\sqrt{N(x_{i+1})}}{\frac{1}{i}\sum_{j=1}^{i}\sqrt{N(x_j)}}\right] \times \frac{x_M}{\frac{1}{M}\sum_{j=1}^{M}\sqrt{N(x_j)}} \qquad (5.8)$$

where $\mathbf{x_j}$ is the depth of the **j-th** N-value, $\mathbf{N(x_j)}$ is the N-value corresponding to the depth of $\mathbf{x_j}$, **i** is the order number of N-value (i=1~L-1), L is the total number of N-values and M is the the order number maximizing the first term on the right-hand side.

In Eq.(5.8), the first term on the right-hand side is the maximum value of the expression within the parenthesis for **i=1** to **i=L-1**, and **M** is the value **i** which maximizes the expression. Eq.(5.8) was derived as a simple approximation based on the concept of the maximum vibrational impedance ratio and the corresponding predominant period. A caluculation of C_{amp} is shown in Appendix B. C_{amp} was estimated for each soil profile in Figs. 5-13(a) to 5-13(q) and is plotted against the corresponding the peak velocity amplification factor $\mathbf{AMP_i}$ **(v)**, in Fig.5-14. Though there is some variance, a positive relation is seen between $\mathbf{c_{amp}}$ and $\mathbf{AMP_i(v)}$. A linear regression expression for $\mathbf{AMP_i(v)}$ as a function of $\mathbf{c_{amp}}$ is

$$AMP_i(v) = 1.25 + 0.112\, C_{amp} \qquad (5.9)$$

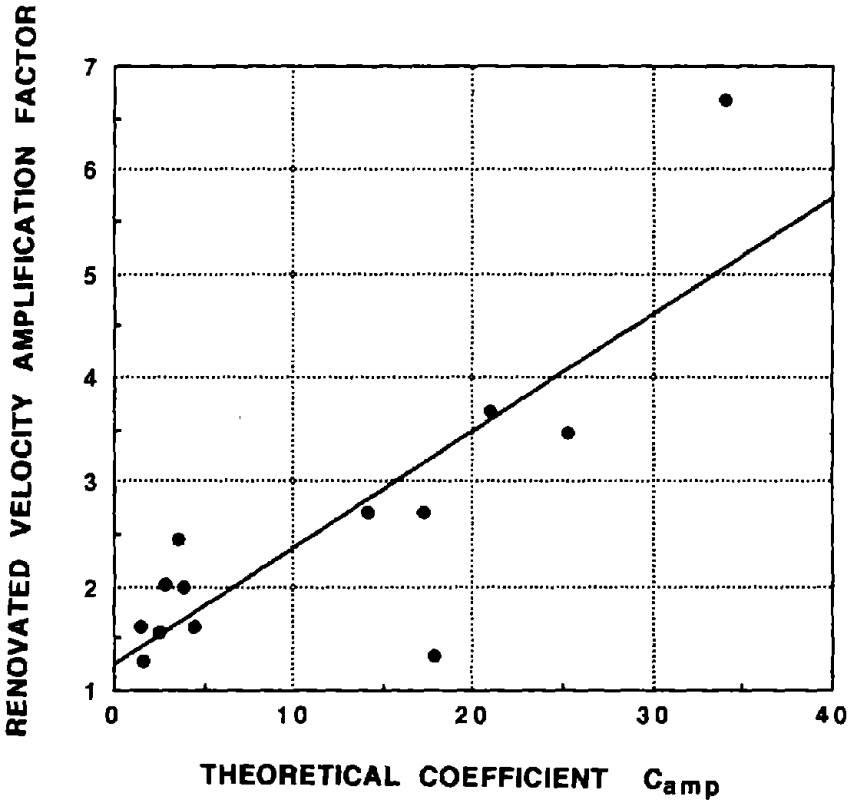

Fig.5-14 Scattergram of Velocity Amplification Factor and Coefficient C_{amp}

Although Eq.(5.8) is simplified and typically would not incorporate information on deep structure down to the seismic bed rock nor Q values, it yields reasonable estimates of the amplification factor for peak velocity. The equation will be applied in a later section.

SECTION 6
ESTIMATES OF THE PEAK ACCELERATION, VELOCITY AND DISPLACEMENT ON SEISMIC BED ROCK

If the local site amplification factors $\mathbf{AMP_i(a)}$, $\mathbf{AMP_i(v)}$ and $\mathbf{AMP_i(d)}$ are set equal to 1.0, Eqs. (5.1) to (5.6) give the peak values on seismic bed rock for acceleration, velocity and displacement. Such bed rock values depend on earthquake magnitude and hypocentral distance but not on local site conditions. As described in the preceding section, the seismic bed rock corresponds to the rock outcrops at HOROMAN, OFUNATO and HOROMAN for peak acceleration, velocity and displacement respectively. Figs. 6-1 to 6-3 show examples of the attenuation with hypocentral distance for the peak acceleration, velocity and displacement on seismic bed rock. In these figures, the attenuation curves are plotted versus earthquake magnitude. We can see from these figures that the peak acceleration in an epicentral area is limited to about **500 gal** irrespective of earthquake magnitude. Conversely the peak velocity and displacement in the epicentral area depend on earthquake magnitude having maxima of about **50 cm/sec** and **15 cm**, respectively, for an earthquake of magnitude of **8.0**. The validity of the peak values of each motion in Figs. 6-1 to 6-3 is confirmed in a later section by a comparison with actually observed peaks during earthquakes in the U.S. and Mexico. In this section we consider a different type of verification.

As is well known, for harmonic motion we have the following relations for the maximum amplitude of acceleration, velocity and displacement motions.

$$v = \frac{a}{2\pi} T_a \tag{6.1}$$

$$d = \frac{v}{2\pi} T_v \tag{6.2}$$

where **a** is the amplitude of acceleration, **v** is the amplitude of velocity, **d** is the amplitude of displacement, $\mathbf{T_a}$ is the period of the acceleration motion and $\mathbf{T_v}$ is the period of the velocity motion.

With respect to a random wave such as earthquake motions, of course, the simple relations in Eqs.(6.1) and (6.2) are not satisfied. However these equations are approximately correct for earthquake motions if we use the predominant period and maximum amplitude of earthquake motions. Given values for the peak acceleration, velocity and displacement, Eqs.(6.1) and (6.2) enable us to estimate predominant periods for acceleration and velocity motions.

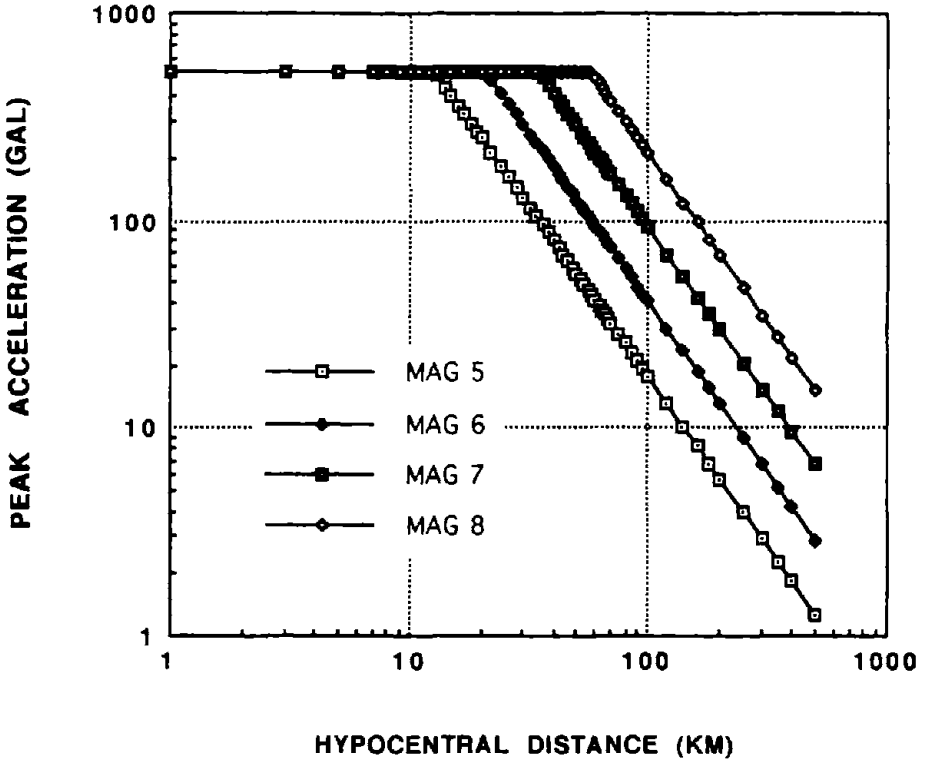

Fig.6-1 Attenuation Relationship for Peak Acceleration on Bed Rock from Proposed Semi-Empirical Model

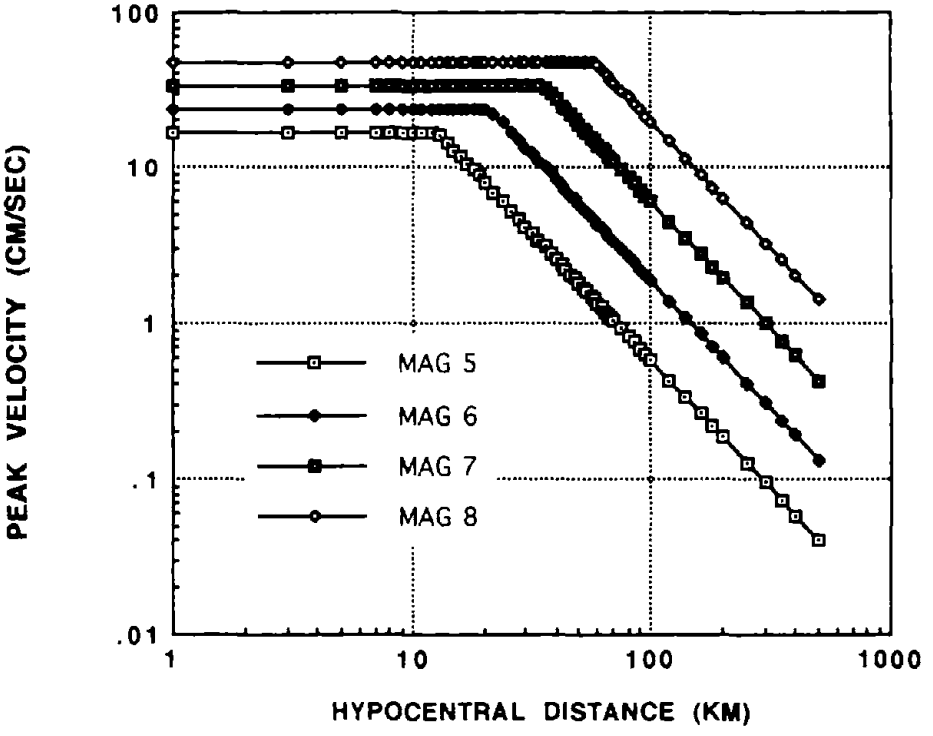

Fig.6-2 Attenuation Relationship for Peak Velocity on Bed Rock from Proposed Semi-Empirical Model

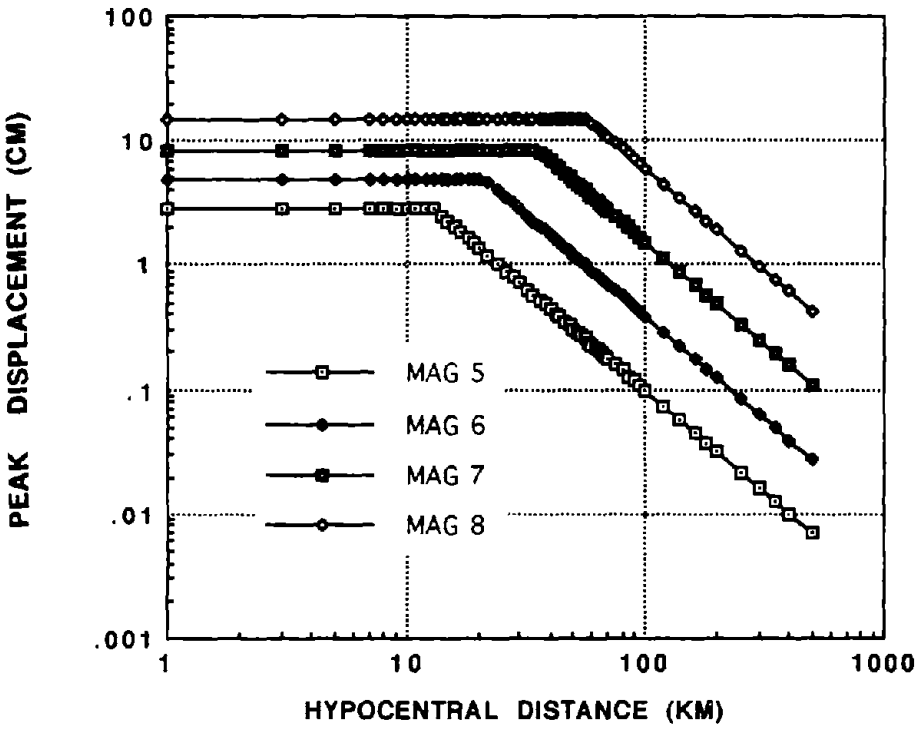

Fig.6-3 Attenuation Relationship for Peak Displacement on Bed Rock from Proposed Semi-Empirical Model

Herein we examined the magnitude-dependence of predominant periods for the acceleration and velocity motions on bed rock. Table 6-I shows the predominant periods of the bed rock acceleration and velocity motions in an epicentral area (the flat area in Figs.6-1 through 6-3) estimated for various earthquake magnitudes using Eqs. (6.1) and (6.2) as well as Figs.6-1 through 6-3. As shown in Table 6-I the predominant periods of the bed rock motions become larger with the increasing earthquake magnitude. The magnitude dependence of predominant period has been noted in other studies. For example Seed et al.[25] graphically presented predominant periods of acceleration motions in an epicentral area resulting from earthquakes in California. The Seed et al. relation is shown in Fig.6-4. A comparison of Table 6-I against the results by Seed et al. indicates that the predominant periods from the model proposed herein are relatively compatible with the Seed et al. results. This provides support for the appropriateness of our semi-empirical model.

Table 6-I Predominant Periods for Bed Rock Acceleration and Velocity from Proposed Semi-Empirical Model

MAGNITUDE M	PREDOMINANT PERIOD(SEC) (ACCELERATION)	PREDOMINANT PERIOD(SEC) (VELOCITY)
5	0.20	1.07
6	0.29	1.30
7	0.41	1.57
8	0.58	1.90

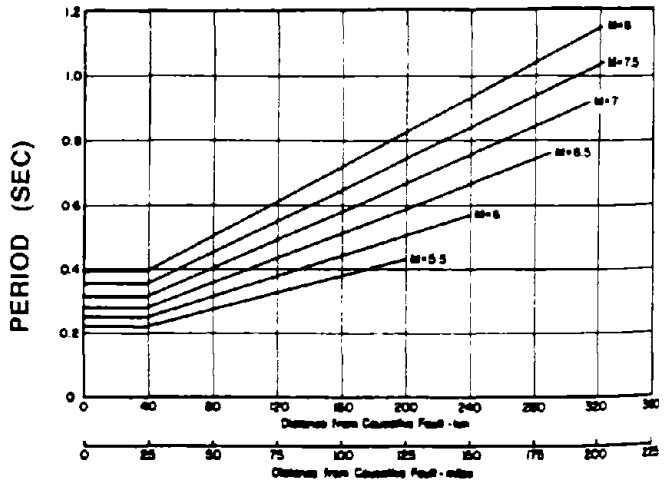

Fig.6-4 Predominant Periods for Acceleration on Rock (after Seed et al.[25])

SECTION 7
COMPARISON WITH OTHER EMPIRICAL RELATIONSHIPS

As mentioned in the introduction, many researchers have developed empirical relations for peak values of strong motions. Herein we compare our proposed semi-empirical model with empirical results by others. We restrict our comparison to peak velocity at rock sites which correspond to the seismic bed rock in our model and correspond to various rocks in the others. We chose peak velocity because the primary focus of our study is lifeline earthquake engineering for which peak velocity is the ground motion parameter of interest. Rock sites are chosen to simplify the comparison by elimination of local soil effects. Trifunac[12], McGuire[26], Joyner and Boore[27], Campbell[28], Sabetta[29], Ohsaki et al.[30], Watabe and Tohdo[31], and Kawashima et al.[32] have developed empirical relationships for peak velocity at rock sites or nearly rock sites. All these empirical expressions for peak velocity are dependent on earthquake magnitude and source-to-site distance. Figs 7-1 and 7-2 show a comparison of the proposed peak velocity attenuation for an earthquake magnitude of 7.0 with these available relations. The first figure shows a comparison with existing relations mainly from the U.S. while the second is for existing relations from Japan. It should be noted that the distance in Figs.7-1 and 7-2 is either epicentral distance, hypocentral distance, or closest distance to fault rupture, depending on what the individual researches choose as the source-to-site distance. That is, the proposed model uses hypocentral distance; Trifunac[12], McGuire[27], Ohsaki et al.[30], Watabe and Tohdo[31] and Kawashima et al.[32] use epicentral distance; and Joyner and Boore[27], Campbell[28] and Sabetta[29] use closest distance to fault rupture.

It is clear in Fig.7-1 that the proposed semi-empirical model yields peak velocities smaller than most of the U.S. empirical models in the near field, while the converse is true for source-to-site distance greater than about 30 km. On the other hand, Fig.7-2 shows that the proposed model predicts larger values than Kawashima et al.[32] at almost all distances. Considering that the data in the present study overlap in part with the more comprehensive data used by Kawashima et al.[32], the comparison in Fig.7-2 shows that the resulting expressions depend greatly on the initial model choice. In other words, both Figs.7-1 and 7-2 show not only the importance of the data set to be analyzed but also the importance of the analysis model. In any case, the validity for each expression in Fig.7-1 and 7-2 should be eventually judged in reference to a comparison against new observation data not included in their analyses. Such a comparison is performed in the following section.

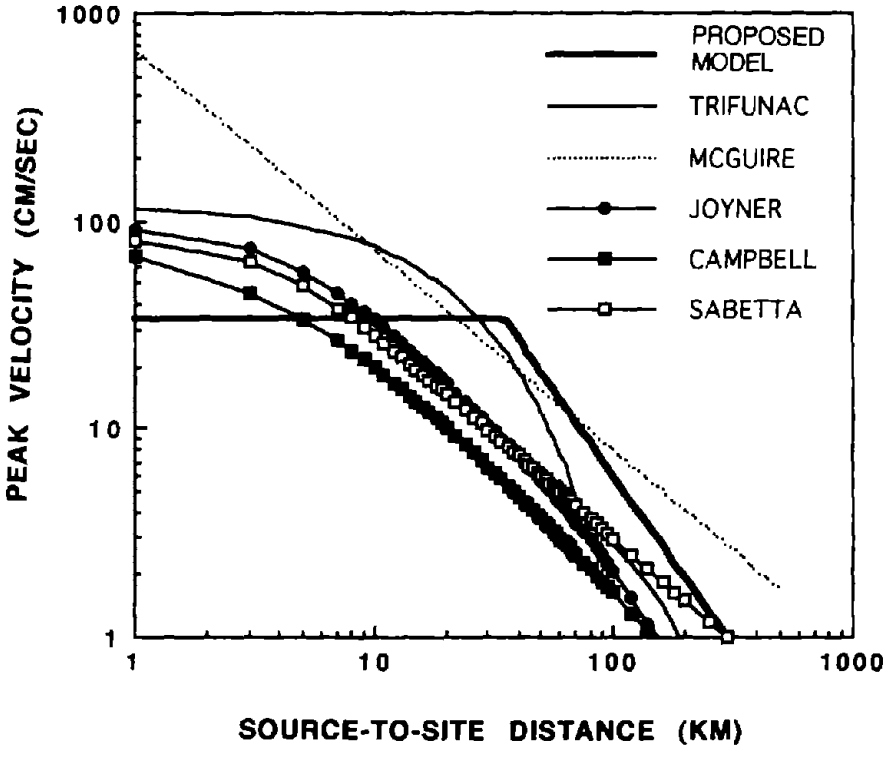

Fig.7-1 Comparison of Proposed Model with Currently Existing Models from the US. and Italy for Magnitude 7.0 Earthquake

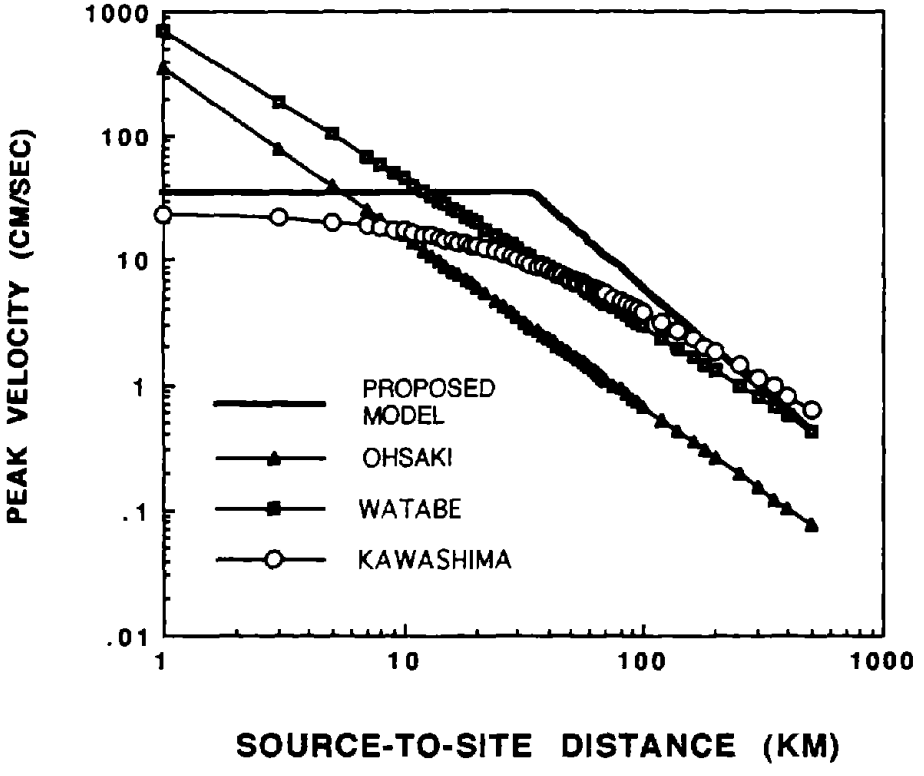

Fig.7-2 Comparison of Proposed Model with Currently Existing Models from Japan for Magnitude 7.0 Earthquake

SECTION 8
COMPARISON BETWEEN THE PROPOSED MODEL AND OSBERVATIONS DURING EARTHQUAKES IN THE U.S. AND MEXICO

The proposed semi-empirical model was developed using only earthquake data observed in Japan. Information from theoretical seismic source models was used to overcome the lack of near field strong-motion data. It is of primary interest, therefore, to investigate how consistent the proposed model is with observed strong-motion data from other countries that are relatively rich in near field data. In addition to confirming the validity of the proposed model, such an investigation is also essential to judge whether or not strong-motion characteristics vary from country to country. In this section, we investigate the validity of the proposed model by comparing its predicted results with the strong-motion data observed during three earthquakes: the 1989 Loma Prieta earthquake in the U.S., the 1985 Michoacan earthquake in Mexico and the 1971 San Fernando earthquake in the U.S. These earthquakes were chosen because they offer strong-motion records from both the near field and far field. Comparing velocity and displacement motions from different countries is complicated by the fact that different filters are used in determining velocity and displacement from original accelerograms. The filter used for the Japanese records was already illustrated in Fig.3-2. It has a flat part between periods of about 0.09 sec and 4.5 sec. Although somewhat different filters are used by different researchers, it seems that the flat portions of the filters are practically the same regardless of country. Herein we use the reported peak acceleration, velocity and displacement from the original text publishing the relevant earthquake data. That is, the effects if any of using filters different from that in Fig.3-2 are neglected. Also we compare exclusively strong motions on rock sites or nearly rock sites because they are less affected by local site conditions.

8.1 1989 Loma Prieta Earthquake

Many useful strong-motion records were obtained at the stations of the California Strong Motion Instrumentation Program (CSMIP) during the 1989 Loma Prieta earthquake. The estimated earthquake location and magnitude are:

Epicenter : 37.037 N, 121.883 W
Depth : 18 km
Magnitude : 7.0 (ML)

The strong-motion data including the geological characteristics of the stations are available in a report from CSMIP[33]. We picked strong-motion data at rock sites from the report and compared

them with the predicted values from the proposed semi-empirical model. Since we consider only rock sites in the comparison, $\mathbf{AMP_i(a)}$, $\mathbf{AMP_i(v)}$ and $\mathbf{AMP_i(d)}$ were set equal to one in Eqs.(5.1) through (5-6). In the comparison, the magnitude scale ML was regarded as identical to the JMA magnitude scale employed in the proposed model.

Figs.8-1 to 8-3 show respectively the comparison between the observed and predicted peak accelerations, peak velocities and peak displacements. In each figure, the error bands of prediction based on the one standard deviation of the regression analysis are plotted in addition to predicted mean values. The standard deviation for the the peak acceleration analysis is shown in Table 4-I(r_c =5.3 km) and those for the peak velocity and displacement are shown in Table 4-IV. Note that there is a good agreement between the observed and predicted values in Figs.8-1 to 8-3, especially for peak velocity of Fig.8-2. Since the proposed model does not use earthquake fault parameters like rupture directivity but uses only simple parameters such as earthquake magnitude and hypocentral distance, some discrepancy between the observed and predicted values is inevitable. However most of the observed peak velocities are distributed within the error band of the prediction.

8.2 1985 Michoacan Earthquake

The 1985 Michoacan earthquake was a large event that caused severe damage in Mexico City and some damage in the epicentral region. The event provided strong motion records in both the near and far fields. Since earthquake engineering design is often based upon such large events, the prediction of strong motions for this type of event is a goal of our semi-empirical model. The location and magnitude of the earthquake are outlined as follows:

Epicenter: 18.14 N, 102.71 W
Depth: 16 km
Magnitude: 8.1 (Ms)

Strong-motion records for this event are contained in a UNAM report[34]. Strong motions obtained at rock sites, especially along the coast of Guerrero during the earthquake are compared with predicted values from the proposed model in Figs.8-4 to 8-6. In this comparison, the earthquake magnitude Ms was treated as equivalent to the JMA magnitude. In contrast to the 1989 Loma Prieta earthquake, Figs.8-4 to 8-6 show that the 1985 Michoacan earthquake motions were somewhat smaller than the predicted values in the near field. However relatively good agreement between the observed and predicted values is notable at intermediate to long distances, giving implicit support for the proposed model.

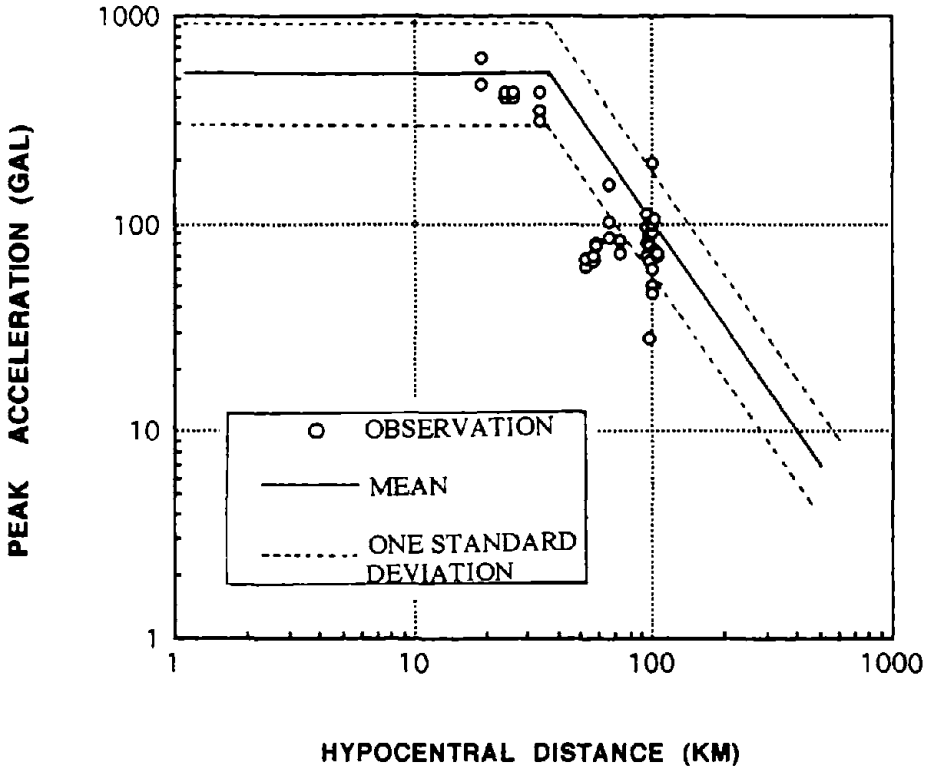

Fig.8-1 Comparison of Peak Acceleration at Rock Sites for the 1989 Loma Prieta Earthquake with Value Predicted by the Proposed Semi-Empirical Model for M=7.0

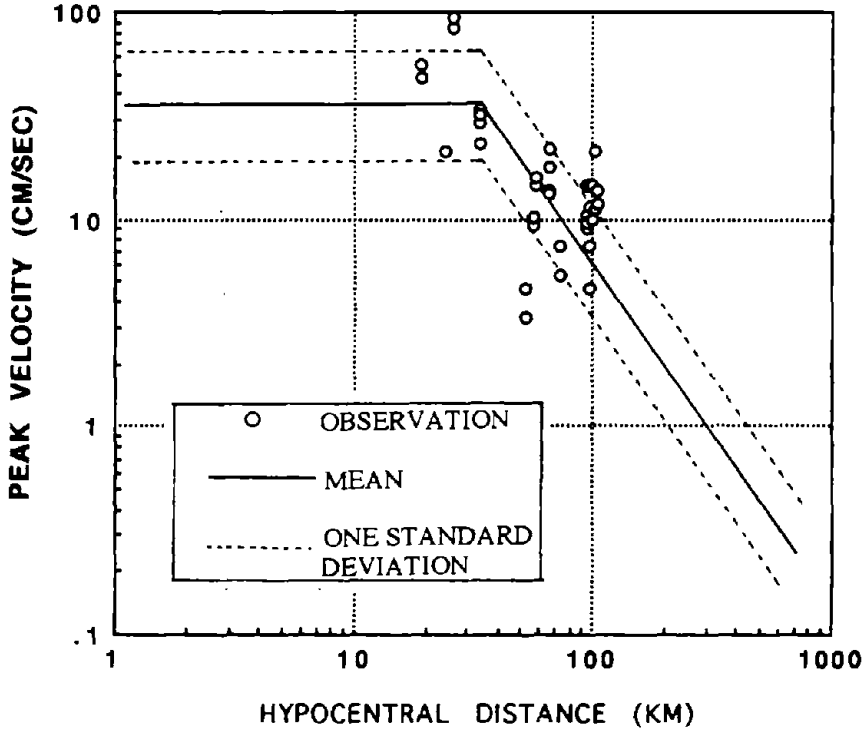

Fig.8-2 Comparison of Peak Velocity at Rock Sites for the 1989 Loma Prieta Earthquake with Value Predicted by the Proposed Semi-Empirical Model for M=7.0

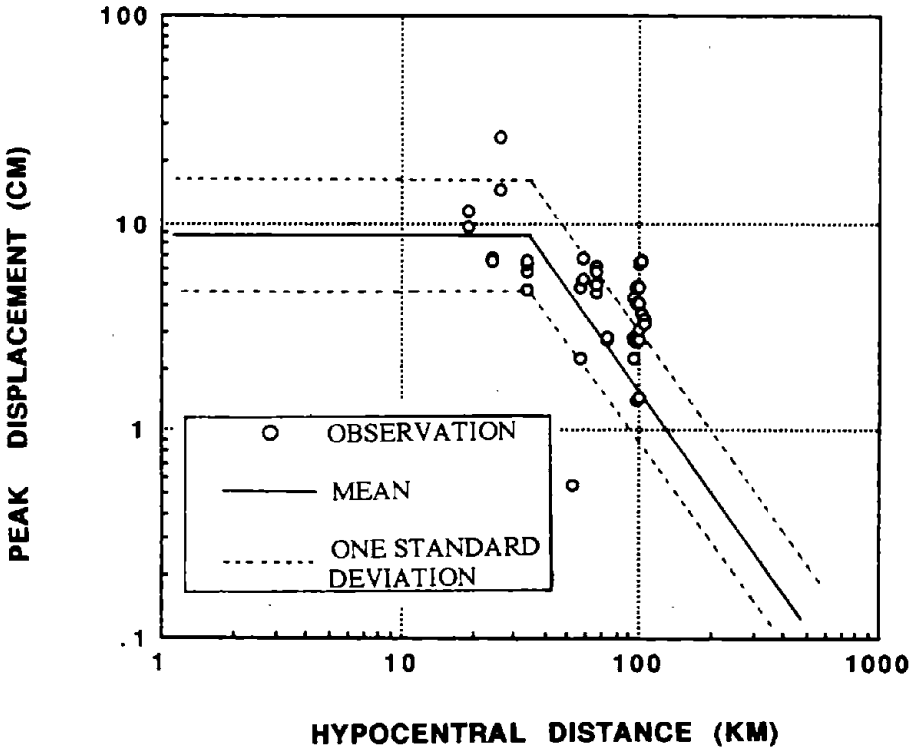

Fig.8-3 Comparison of Peak Displacement at Rock Sites for the 1989 Loma Prieta Earthquake with Value Predicted by the Proposed Semi-Empirical Model for M=7.0

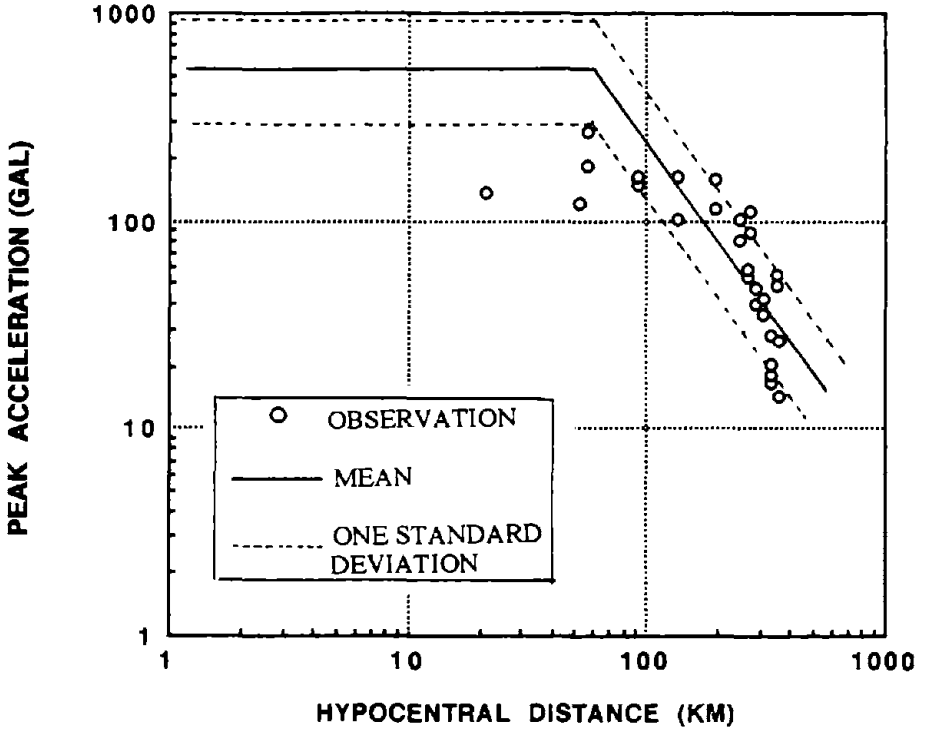

Fig.8-4 Comparison of Peak Acceleration at Rock Sites for the 1985 Michoacan Earthquake with Value Predicted by the Proposed Semi-Empirical Model for M=8.1

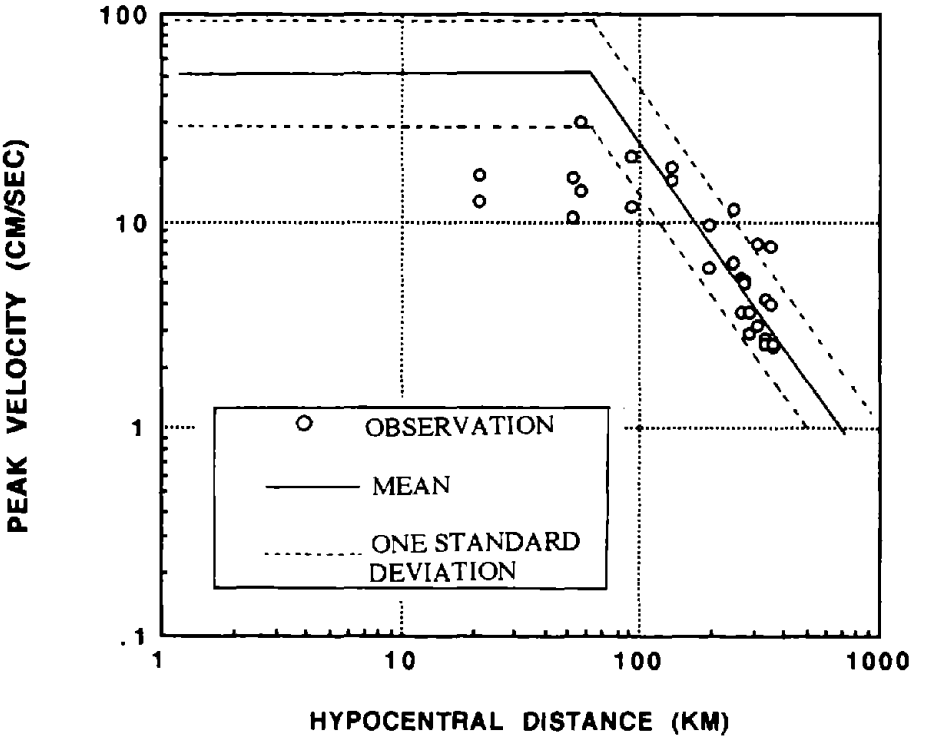

Fig.8-5 Comparison of Peak Velocity at Rock Sites for the 1985 Michoacan Earthquake with Value Predicted by the Proposed Semi-Empirical Model for M=8.1

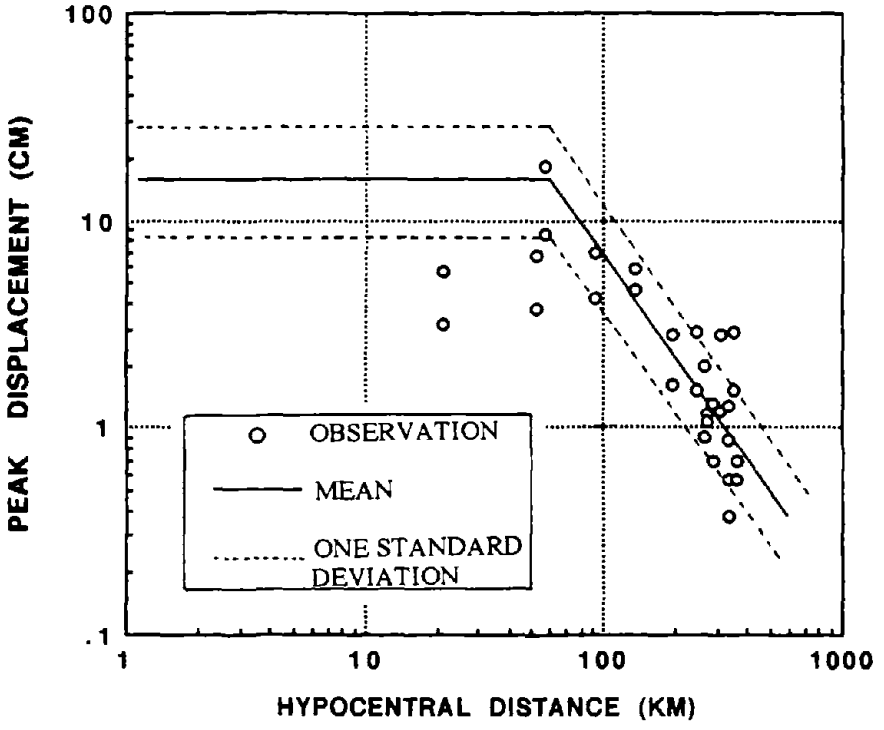

Fig.8-6 **Comparison of Peak Displacement at Rock Sites for the 1985 Michoacan Earthquake with Value Predicted by the Proposed Semi-Empirical Model for M=8.1**

8.3 1971 San Fernando Earthquake

The 1971 San Fernando earthquake was a major source of data for empirical analyses of strong motions by other researchers. This is particularly true for the U.S. empirical expressions discussed in Section 7. Hence a comparison of this earthquake data with the proposed semi-empirical model is meaningful. The strong-motion data and site geological information for this earthquake were taken from a Caltech report[35]. General information for the earthquake is:

Epicenter : 34.40 N, 118.43 W
Depth: 13 km
Magnitude 6.6 (ML)

Taking the Richter magnitude ML as being identical to the JMA magnitude, the peak motion values for the earthquake were estimated by the proposed model using Eqs.(5-1) to (5-6) with $\mathbf{AMP_i = 1.0}$ and compared with the observed peaks at rock sites and nearly rock sites, as shown in Figs. 8-7 to 8-9. It is obvious in Fig.8-7 that the proposed model gives systematically larger acceleration peaks than were observed, whereas a relatively good agreement is found in the cases of velocity and displacement shown in Figs.8-8 and 8-9. It is beyond the scope of this study to explain such differences. However the consistency between the predicted and observed peak velocities lends additional support for our model because we are primarily interested in the prediction of peak velocity.

8.4 Discussion

Among the comparisons shown in Figs.8-1 through 8-9, the observed velocity motions for the three earthquakes match best the predicted values from the proposed semi-empirical model. Except for the observed near field values for the 1985 Michoacan earthquake, the proposed model for peak velocity could serve as a statistical prediction method. This is desirable because the primary goal of this study is to develop an empirical model for estimating peak velocity in connection with the seismic performance of lifelines. In the case of peak acceleration, on the other hand, the observed values for the 1971 San Fernando earthquake are systematically smaller than the predicted values despite relatively good agreement of the predicted values with the observed values for the other earthquakes. However, since the 1971 San Fernando earthquake gives a similar trend in the peak velocity comparison, the systematic difference for the acceleration comparison may be due to the peculiarity of the earthquake. For peak displacement the predicted values for the three earthquakes agree relatively well with the observed values although one may have expected difference due to the different filters used to numerically obtain displacement records. We can see

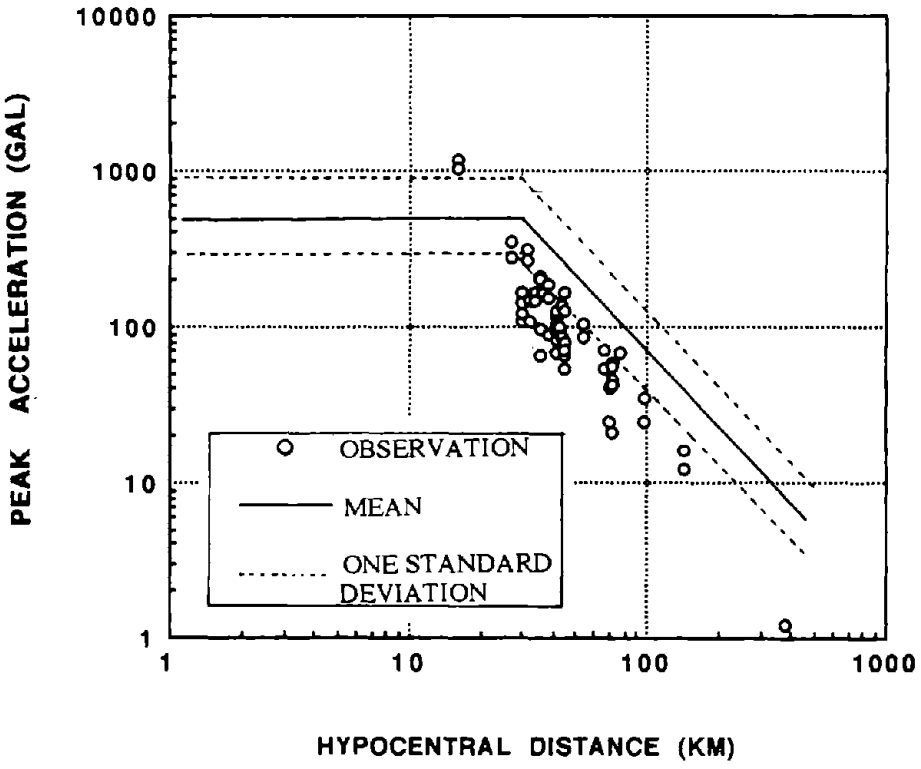

Fig.8-7 Comparison of Peak Acceleration at Rock Sites for the 1971 San Fernando Earthquake with Value Predicted by the Proposed Semi-Empirical Model for M=6.6

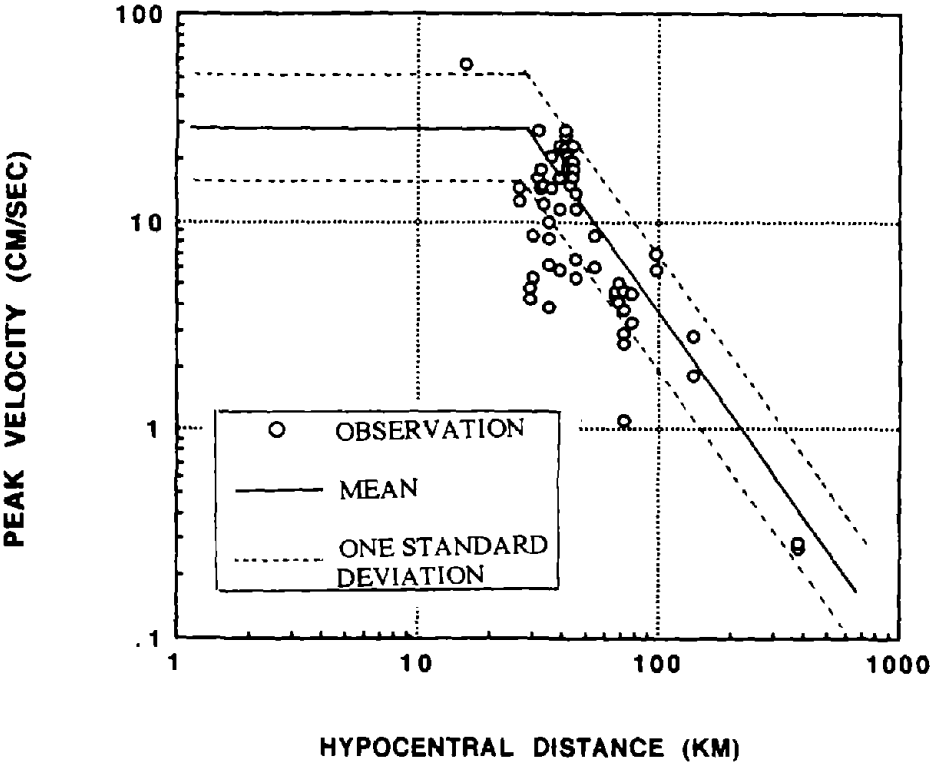

Fig.8-8 Comparison of Peak Velocity at Rock Sites for the 1971 San Fernando Earthquake with Value Predicted by the Proposed Semi-Empirical Model for M=6.6

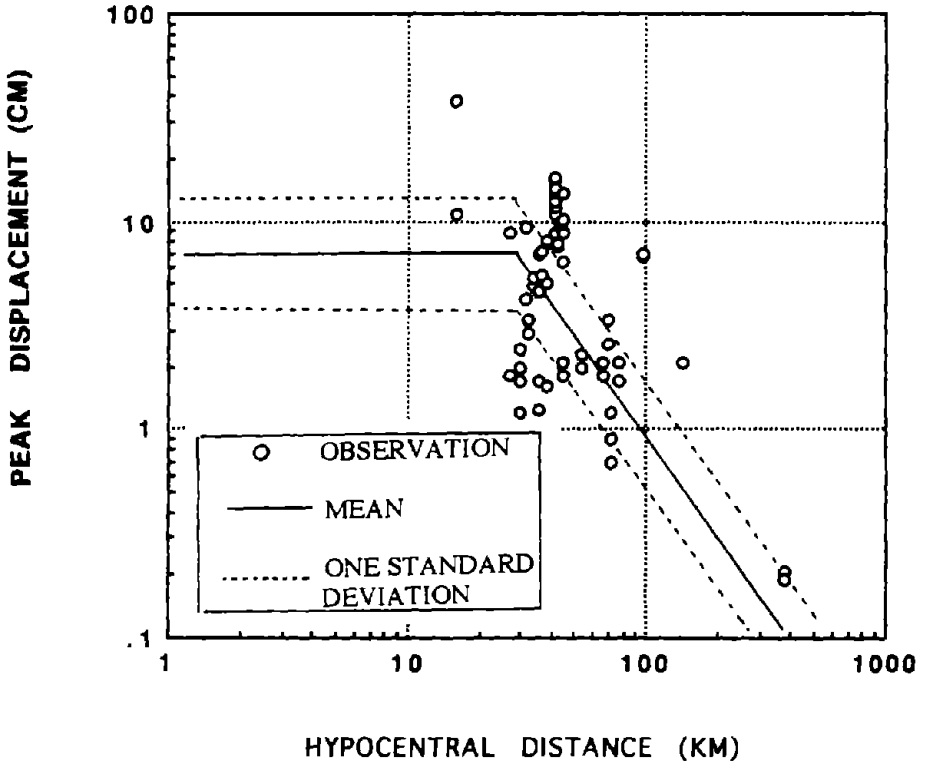

Fig.8-9 Comparison of Peak Displacement at Rock Sites for the 1971 San Fernando Earthquake with Value Predicted by the Proposed Semi-Empirical Model for M=6.6

from the overall comparisons in Figs.8-1 through 8-9 that the present model is applicable to various types of earthquakes. It should be emphasized that the proposed semi-empirical model was based only on earthquake data obtained in Japan. This suggests that earthquakes share a similar attenuation law for strong-motion peaks irrespective of their country of origin.

The observed values in Figs.8-1 through 8-9 were chosen regardless of the detailed material characteristics of rock partly because of a lack of information. On the other hand, the predicted values for the proposed model are estimates for the seismic bed rock which was defined based upon the renovation of the amplification factors. In spite of such variation in the definition of rock the predicted and observed values agree reasonably well. Hence the definition of rock can presumably be flexible for peak value prediction, particularly peak velocity prediction as opposed to spectra and time history predictions.

In this section, we have compared the proposed semi-empirical model, which was based on Japanese data, with earthquakes in the U.S. and Mexico. It is also illustrative to compare the existing U.S. empirical attenuation relations, which were based on U.S. data composed primarily of the 1971 San Fernando data, with the more recent 1989 Loma Prieta and 1985 Michoacan data. Fig.8-10 shows a comparison of the predicted values from Trifunac[12] and McGuire[26] with the observed values for the 1989 Loma Prieta event (M=7.0). Both predicted and observed values are plotted in terms of epicentral distance. We can see from a comparison between Fig.8-2 and Fig.8-10 that Trifunac[12] and McGuire[26] do not give better estimates for the observed values of the Loma Prieta event than the proposed model even though the McGuire estimates are fairly consistent. The predicted values from Joyner and Boore[27], Campbell[28] and Sabetta[29], which use closest distance to fault rupture to characterize source-to-site distance, are compared with the observed values from the Loma Prieta event in Fig.8-11. Note in Fig.8-11 that these three empirical relations underestimate the observed values in the Loma Prieta event. Hence although the existing U.S. empirical attenuation relations are based primarily on U.S. data and in some cases use fairly sophisticated measures for site-to-source distance, they do not provide significantly better estimates for observed peak velocity on rock and in some cases (Fig.8-11) provide significantly worse estimates. A similar comparison for the 1985 Michoacan earthquake (M=8.1) is illustrated in Figs.8-12 and 8-13. Fig.8-12 is a comparison between the observed values for peak velocity at rock sites from the 1985 Michoacan event and the empirical estimates by Trifunac[12] and McGuire[26]. A comparison between Fig.8-5 and Fig.8-12 shows that Trifunac[12] and McGuire[26] give worse estimates than the proposed model for the 1985 Michoacan event. Fig.8-13 compares the observed peak velocities with the empirical estimates from Joyner and Boore[27], Campbell[28] and Sabetta[29] in terms of closest distance to fault

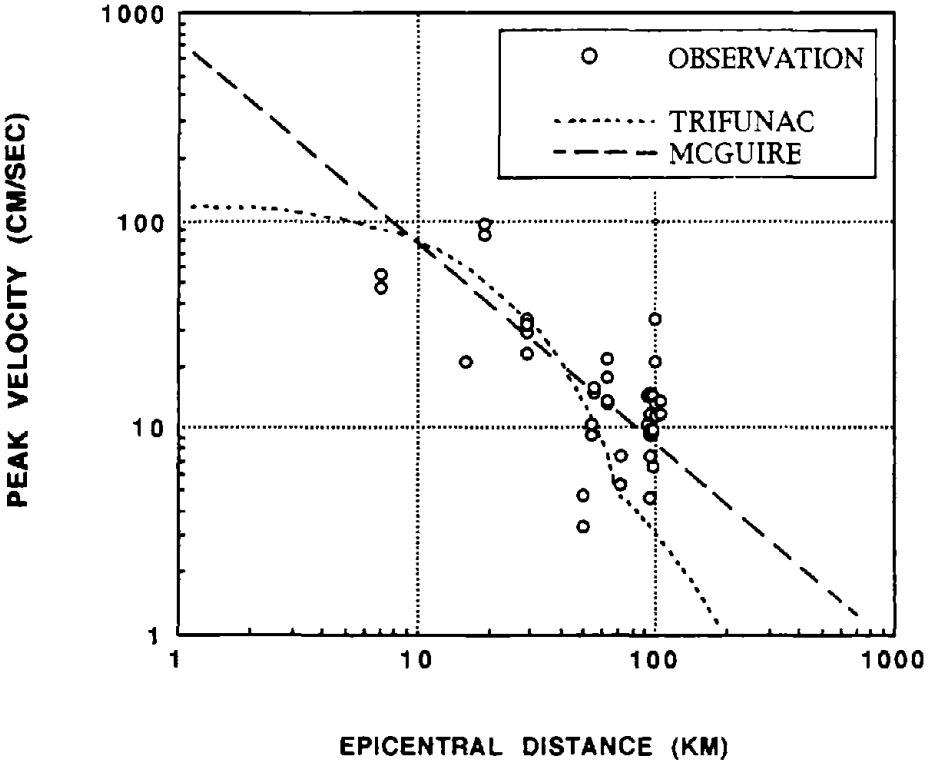

Fig.8-10 Comparison of Observed Peak Velocity at Rock Sites for the 1989 Loma Prieta Earthquake with Empirical Estimates for a Magnitude 7.0 Event by Trifunac and McGuire

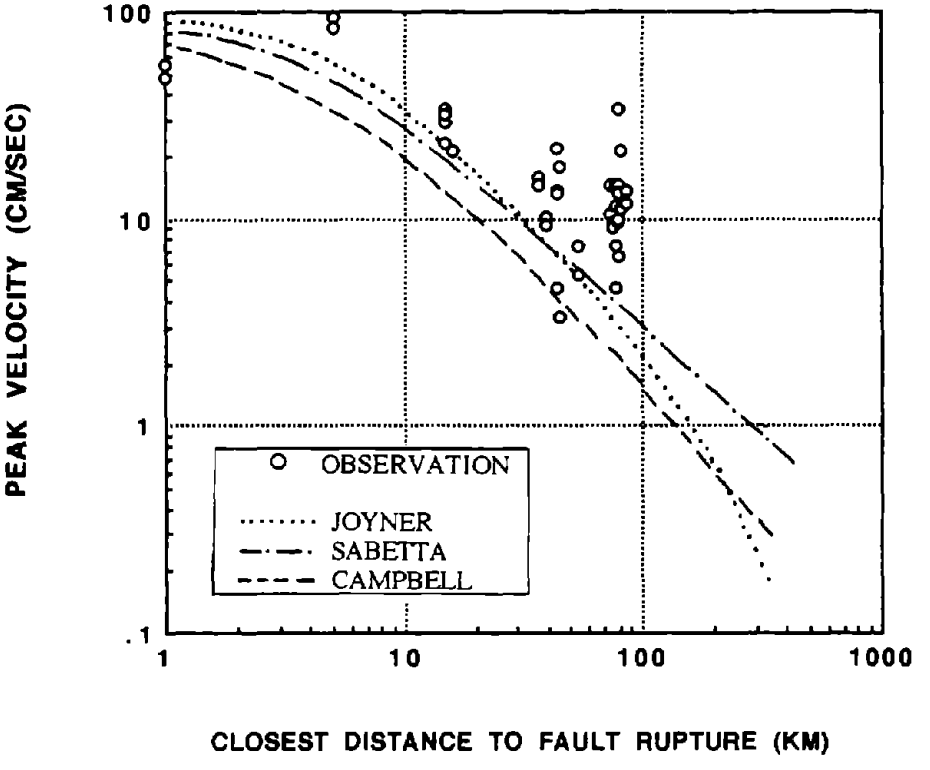

Fig.8-11 Comparison of Observed Peak Velocity at Rock Sites for the 1989 Loma Prieta Earthquake with Empirical Estimates for a Magnitude 7.0 Event by Joyner and Boore, Campbell and Sabetta

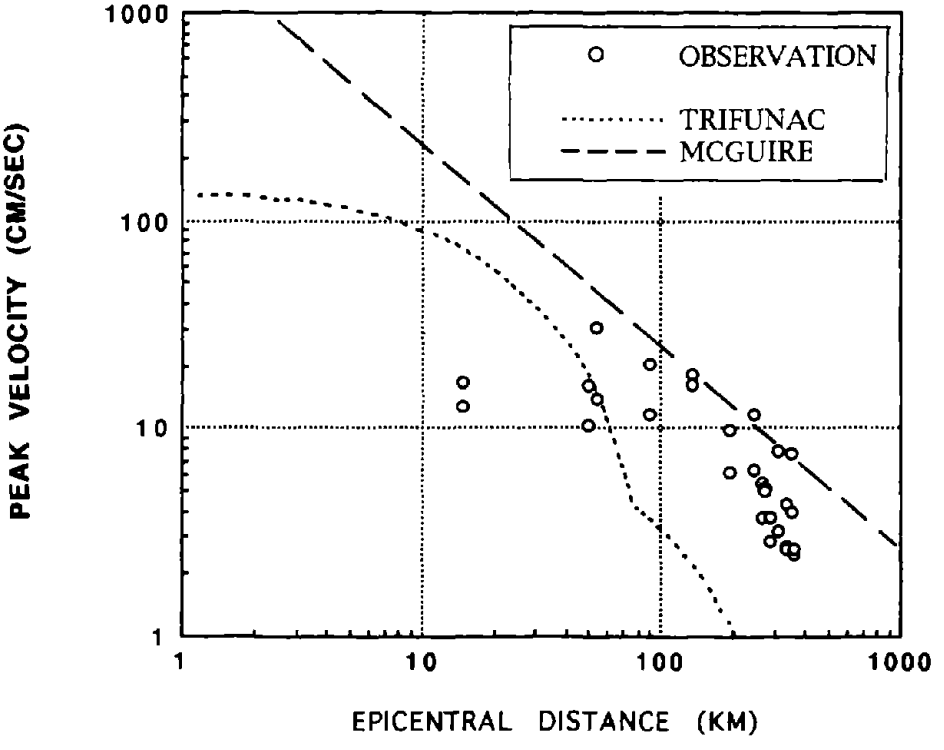

Fig.8-12 Comparison of Observed Peak Velocity at Rock Sites for the 1985 Michoacan Earthquake with Empirical Estimates for a Magnitude 8.1 Event by Trifunac and McGuire

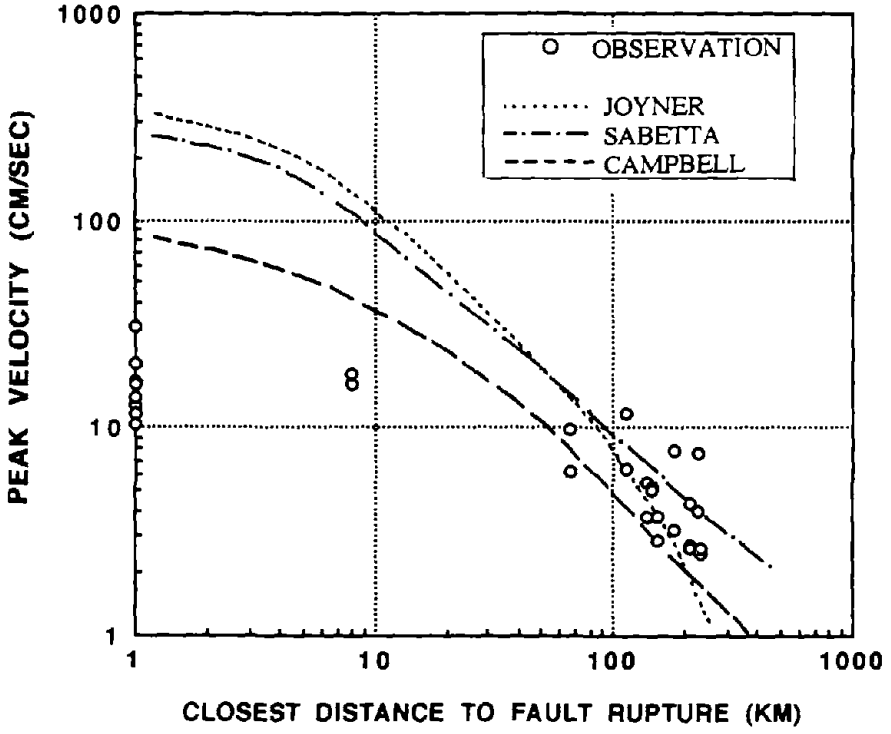

Fig.8-13 Comparison of Observed Peak Velocity at Rock Sites for the1985 Michoacan Earthquake with Empirical Estimates for a Magnitude 8.1 Event by Joyner and Boore, Campbell and Sabetta

rupture. In this figure, the observed values in the fault area are plotted with distance=1 km. Note that the predicted values are good for distance greater than about 80 km but significantly overestimate the observed values at short distances. Hence it is concluded from these comparisons that the existing U.S. empirical relations do not provide more reasonable estimates of peak velocity than the proposed model.

As shown above, the proposed semi-empirical model appears superior to presently existing empirical relations. However there is disparity between the observed and predicted values for the model. The disparity is attributable to several reasons including incompleteness of the model and the peculiarities of each earthquake. Some of the incompleteness result from the simplification of the proposed model being developed for engineering application. In particular, the proposed model does not consider the faulting process at the seismic source which affects peak values of strong motions. Regarding the peculiarities of each earthquake, characteristic scatter of observed peak values is often discussed based on the polarization of the azimuth from seismic focus to observation sites. Such polarization is associated with the rupture directivity of faulting. This suggests that the effects of rupture directivity can explain some of the scatter of observed values about the semi-empirical model. For example, Fig.8-14 shows the observed values of peak velocity at rock sites during the 1989 Loma Prieta earthquake for the sites south and north of the epicenter. Note that the sites situated south of the epicenter generally have smaller peak values than those north, implying that a characteristic rupture directivity of the earthquake influences peak values at each observation site. The effects of rupture directivity are easy to grasp if the rupture is assumed to progress in a uniform manner as illustrated in Fig.8-15. Assuming a unilaterally uniform rupture directivity, Hirasawa and Stauder[36] has shown that amplitude coefficient is given as a function of the azimuth angle ψ by

$$\frac{1}{1-\frac{v}{\beta}\cos\psi} \tag{8.1}$$

where v is the rupture propagation velocity and β is the shear wave velocity.
Eq. (8.1) explains the well-known phenomenon that the amplitudes of motions are larger at sites located in the direction of the rupture progress.

Now assuming that the case of $\psi = \frac{\pi}{2}$ in Eq.(8.1) is equivalent to the mean value estimated by the proposed semi-empirical model as well as assuming $\frac{v}{\beta} = 0.8$, we obtained expected scatters on the basis of the directivity effect. Such upper and lower bounds for predicted value are drawn

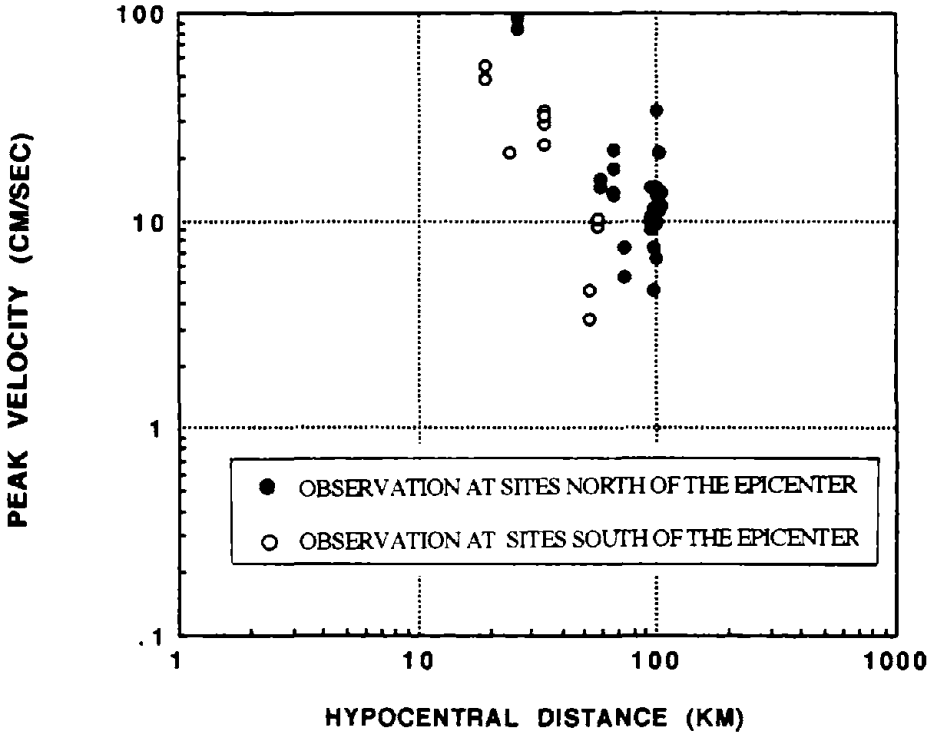

Fig.8-14 Peak Velocity at Rock Sites North and South of the Epicenter, Loma Prieta 1989

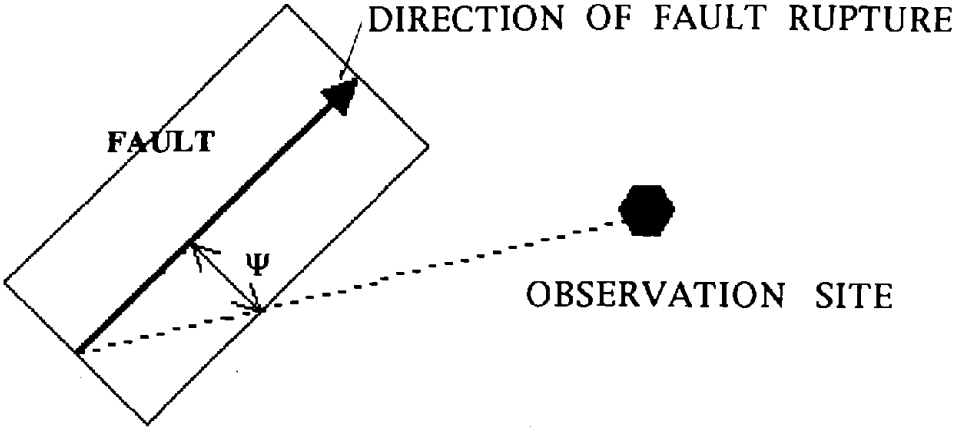

Fig.8-15 Sketch showing Azimuth Angle for an Arbitrary Observation Site with Respect to the Direction of Fault Rupture

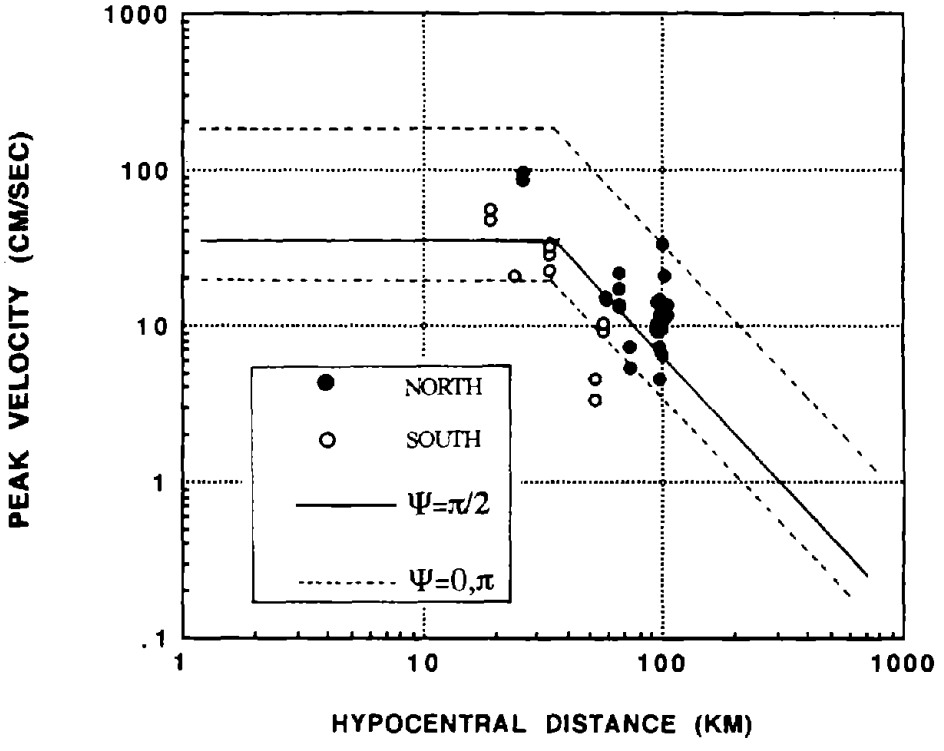

Fig.8-16 Peak Velocity at Rock Sites for the Loma Prieta Event with Scatter Bands Based upon Rupture Directivity in Fig.8-15

in Fig.8-16 together with the mean prediction value. This figure shows that the scatter of observed values about the predicted value from the proposed model, at least for the case of peak rock velocity from the 1989 Loma Prieta event, is explained by fault rupture directivity effects. However fault rupture directivity is not included in the proposed model because it is not known a priori.

As mentioned in **Section 2**, we derived our semi-empirical model of strong-motion peaks based on the assumption that peak acceleration in a fault zone is independent of earthquake magnitude. The validity of this assumption can be judged by a comparison between the predicted and observed values. However the comparisons shown in Figs.8-1, 8-4 and 8-7 are not enough to judge the validity because observed data within the fault zones are few. We need more strong-motion records observed on rock sites in a fault zone having different size to finally judge our assumption.

SECTION 9
ESTIMATION OF SOIL STRAIN

We have obtained relatively good agreement between the observed peak values of motions and the predicted values from the proposed model. The best agreement was found for peak velocity. This motivates us to apply it to the estimation of soil strain which is associated with peak velocity. In this section, a simplified method for estimating soil strain is presented together with comparisons between predicted and observed values.

9.1 Simplified Method for Estimating Soil Strain

Soil strains induced during earthquakes have been known to play a pivotal role not only in controlling non-linear behavior of ground motions including liquefaction of sandy soils but also in determining the seismic performance of buried pipelines. Despite such importance, there have been relatively few observations of soil strain because of the technical difficulties involved. Hence it is almost impossible at present to derive an empirical expression for soil strain using the technique described previously for strong-motion peaks. However, since strain is theoretically proportional to the corresponding particle velocity, it is possible to indirectly estimate maximum soil strain using our semi-empirical model for peak velocity. According to wave theory for one dimensional propagation, the maximum horizontal soil strain ε_{max} , in the direction of propagation, is given by

$$\varepsilon_{max} = \frac{v_{max}}{C} \tag{9.1}$$

where v_{max} is the peak particle velocity, and C is the apparent propagation velocity of the wave with respect to the ground surface .

The term v_{max} in Eq. (9.1), needless to say, can be calculated for a site if the soil profile is known, using our semi-empirical model. We now consider methods to approximate the apparent propagation velocity **C.**

The apparent propagation velocity C is a function of the wave type. In the case of body waves, the apparent velocity is a function of angle of incidence and material properties of the surface soils. O'Rourke et al.[37] studied the apparent horizontal propagation velocity of S-wave using theoretical analysis as well as observed values in the U.S.and Japan. They concluded that it falls in the range of **2.0** to **5.0** km/sec with an average of about **3.5** km/sec. Since they studied a

number of different sites, the average velocity of **3.5** km/sec would be acceptable as a first-approximation. Herein we employ the value of **3.5** km/sec as the apparent propagation velocity of body waves with respect to the ground surface.

For the case of surface waves, Rayleigh wave(R-wave) induces soil strain alternating between tension and compression in the direction of propagation. For R-waves, the propagation velocity is a function of frequency. This relation is quantified by a dispersion curve for the phase or propagation velocity. For typical soil profiles with shear wave velocity increasing with depth, the propagation velocity is an increasing function of period. For example, Fig.9-1 shows an approximate dispersion curve developed by O'Rourke et al.[38] for the fundamental R-wave for a uniform soil layer over a half space. For long period motion $hf/c_L \leq 0.25$, the phase velocity is somewhat less than the shear wave velocity of the half space, while for short period motion $hf/c_L \geq 0.5$, the phase velocity is equal to the shear wave velocity of the surface layer, $\mathbf{C_L}$. Note however that the R-wave phase velocity corresponding to the natural frequency of the soil layer in shear $f = C_L/4h$ is $\mathbf{0.875C_H}$, that is, it is controlled by the shear wave velocity of the half space. For sites subject to both body and surface waves, we assume herein that the peak particle velocity $\mathbf{v_{max}}$ occurs during the later arriving R-wave portion of the record. We further assume that the predominant frequency of the R-wave portion matches the natural frequency of soil layer in shear. That is, for sites subject to surface waves

$$\varepsilon_{max} = \frac{v_{max}}{0.875 \cdot C_H} \tag{9.2}$$

where $\mathbf{v_{max}}$ is the peak particle velocity from Eq.(5.3) or Eq.(5.4)) and $\mathbf{C_H}$ is the shear wave velocity of the seismic bed rock which underlies the site. Based upon the reference site and the seismic bed rock for peak velocity in section 5.1, we choose 2.0 km/sec as a representative value for $\mathbf{C_H}$.

The above considerations gives us a simplified way to estimate the maximum longitudinal or normal strain separately for body waves and surface waves. The next problem is to identify which wave type is likely to be most prominent in a given record. This complicated phenomenon has been studied by several workers. In general a large earthquake with a shallow focal depth is more likely to generate surface waves. Since the detailed consideration about this problem is beyond the scope of this report and our target is to develop a simplified method for estimating the maximum soil strain, the discussion is herein confined to an assumption of surface wave generation suggested by Nakamura[39]. Nakamura[39] investigated the existence of surface waves in

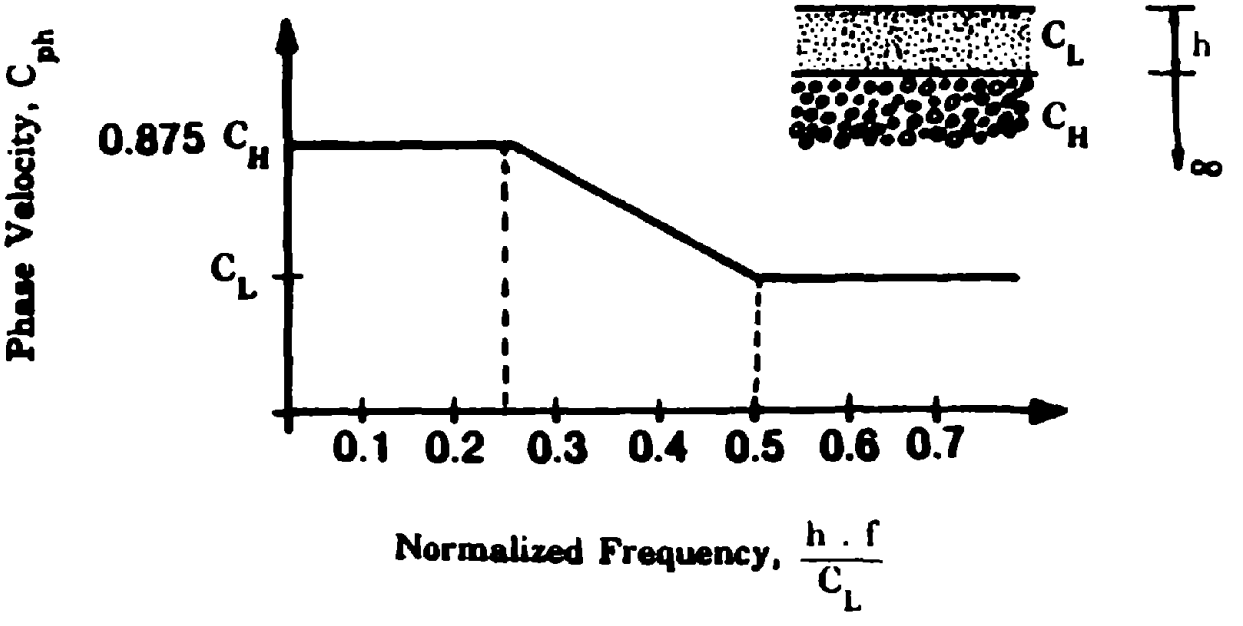

Fig.9-1 Approximate Dispersion Curve for Fundamental R-wave for Uniform Soil Layer over a Half Space(after O'Rourke et al.[38])

records obtained during a total of 29 earthquakes by the use of non-stationary spectra analysis. A table in that work identifies the generation of surface waves as being dependent on earthquake magnitude and an apparent angle defined by focal depth and epicentral distance. From the Nakamura table, we herein establish the following conditions for generation of surface waves:

$$M > 6.0 \quad \text{and} \quad \frac{\Delta}{D} > 1.5,$$

$$6.0 \geq M > 5.0 \quad \text{and} \quad \frac{\Delta}{D} > 6.0$$

where **M** is the earthquake magnitude, Δ is the epicentral distance and **D** is the focal depth. It should be noted that the above standard for surface wave generation is an approximation. Hence our simplified method for estimating the maximum soil strain can be summarized as follows;
For sites subject to surface waves, that is $M > 6.0$ and $\Delta/D > 1.5$, or $6.0 \geq M > 5.0$ and $\Delta/D > 6.0$

$$\varepsilon_{max} = \frac{v_{max}}{1.75 \times 10^5} \tag{9.3}$$

while for all other sites, body waves control and

$$\varepsilon_{max} = \frac{v_{max}}{3.5 \times 10^5} \tag{9.4}$$

where $\mathbf{v_{max}}$ is the peak particle velocity in cm/sec given by Eq.(5.3) or Eq.(5.4).

Eqs.(9.3) and (9.4) make it possible to estimate the maximum strain at a site provided that earthquake magnitude, epicentral distance, focal depth and hypocentral distance are known as well as the surface profile. For example, Fig.9-2 is a plot of the attenuation of estimated maximum strain at a rock site, for which $\mathbf{AMP_i(v)}$ is taken as **1.0** in Eq.(5.3) or Eq.(5.4), subject to surface waves.

9.2 Comparison of Estimated Soil Strain with Observed Values

In this section, the estimated strains given by Eq.(9.3) or Eq.(9.4) are compared with strains observed at representative sites to check the validity of the simplified method.
The Kubota Corp. in Japan has been observing soil strains as well as the behavior of pipelines during earthquakes at two separate sites in Aomori Prefecture, namely Kansen and Shimonaga.

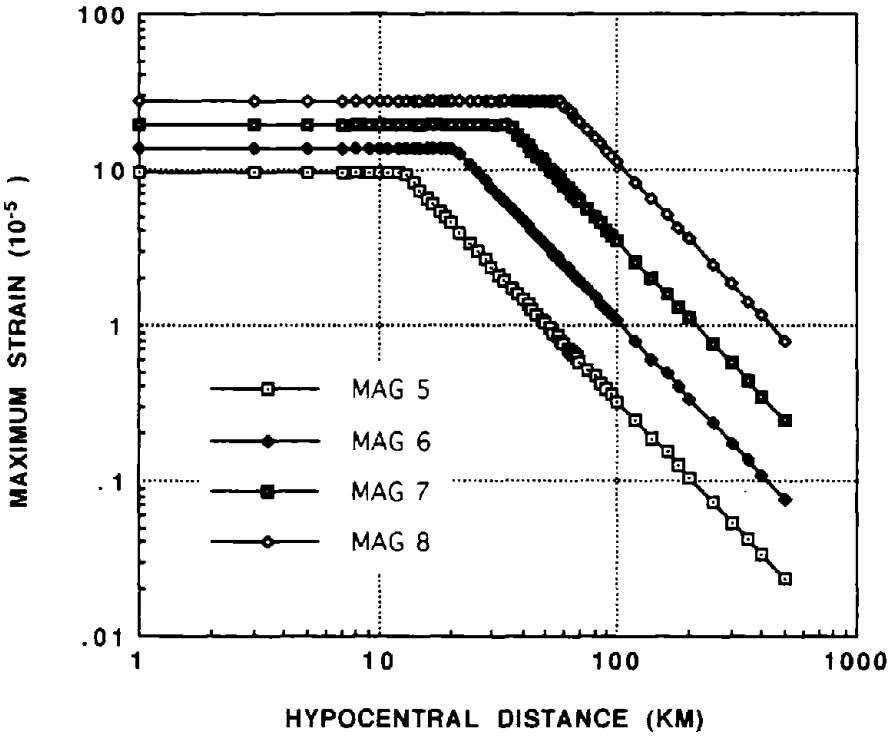

Fig.9-2 Attenuation for Estimated Maximum Soil Strain at Rock Site Subject to Surface Waves

The details of these observation systems including soil profiles at both sites are available in Iwamoto et al.[40]. Figs 9-3 and 9-4 each show the soil logs at the Kansen and Shimonaga sites. Although the observations at both sites have been carried out since 1975 giving useful data relevant to seismic performance of buried pipelines, the maximum soil strains observed until 1983 are compared with estimated normal strains from Eq.(9.3) or Eq.(9.4).

In order to estimate the maximum soil strain based on Eq.(9.3) or Eq.(9.4), one needs the amplification coefficient $\mathbf{AMP_i(v)}$ applicable to both the Kansen and Shimonaga sites. We offered two methods: the "qualitative method" and "quantitative method" for the estimate of $\mathbf{AMP_i(v)}$ at a site not included in our statistical analysis. According to the qualitative method, the value of $\mathbf{AMP_i(v)}$ at the Kansen site is expected to be about **2.70** since the Kansen soil profile in Fig.9-3 is most similar to the Itajima site in Fig. 5-13(l). On the other hand, the estimated $\mathbf{AMP_i(v)}$ by the quantitative method which consists of Eq.(5.8) and Eq.(5.9) is **2.18** because the value of $\mathbf{C_{amp}}$ is **8.30** by Eq.(5.8). The calculation of C_{amp} for the Kansen site is shown in Appendix B. This example shows that the qualitative method gives fairly accurate amplification factor, although it is simple. Since the quantitative method is expected to yield the more accurate value, we use **2.18** as the amplification factor for the Kansen site. Similarly, the quantitative method resulted in $\mathbf{AMP_i(v)}$ **=5.28** at the Shimonaga site via $\mathbf{C_{amp}=35.9}$. Having obtained the amplification factors $\mathbf{AMP_i(v)}$ at both sites, it is possible to predict the maximum soil strains expected at both sites knowning the earthquake magnitude, epicentral distance, focal depth and hypocentral distance. The predicted maximum soil strains at the Kansen and Shimonaga sites are plotted, respectively, in Figs.9-5 and 9-6 and compared with observed maximum normal or longitudinal soil strains. In both figures, data points with an open circle are estimated values using Eq.(9.3) (surface wave source) while the closed circle indicates values from Eq.(9.4) (only body wave source). Fig.9-5 and 9-6 show that the predicted values coincide relatively well with the observed values. Comparisons similar to Figs.9-5 and 9-6 between the predicted and observed maximum strains are shown in Figs. 9-7 and 9-8 for two other observation sites. These are University of Tokyo, Chiba site[41] and Chubu Electrical Power Corp., Chubu site[42]. The observed strain at the Chiba site was obtained by observing pipe strain[41] and herein we assume that the pipe strain represents soil strain. Again Figs.9-7 and 9-8 show that the comparison between predicted and observed strains is relatively good.

9.3 Discussion of Simplified Method for Soil Strain

As shown in Figs.9-5 through 9-8, on average the simplified method predicts well the observed maximum normal or longitudinal soil strains. However there is some scatter between observed

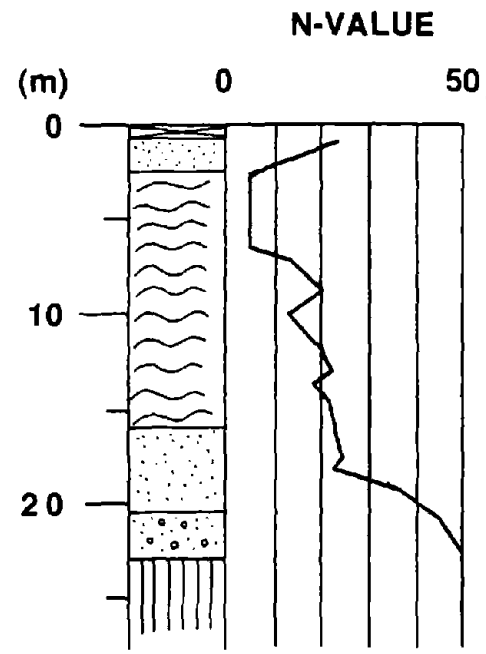

Fig.9-3 Soil Profile for the Kansen Site
(Kubota Corp. Soil Strain Installation)

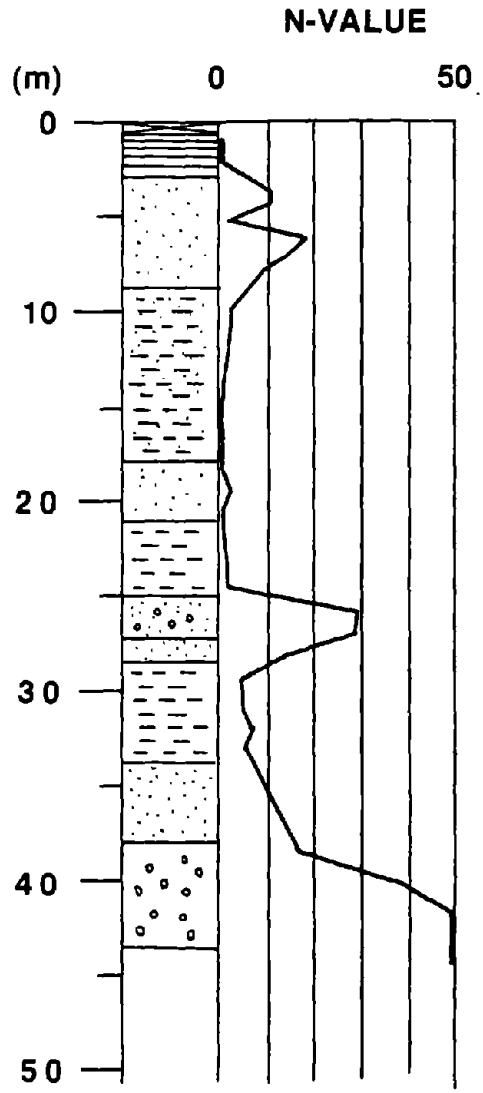

Fig.9-4 Soil Profile for the Shimonaga Site (Kubota Corp. Soil Strain Installation)

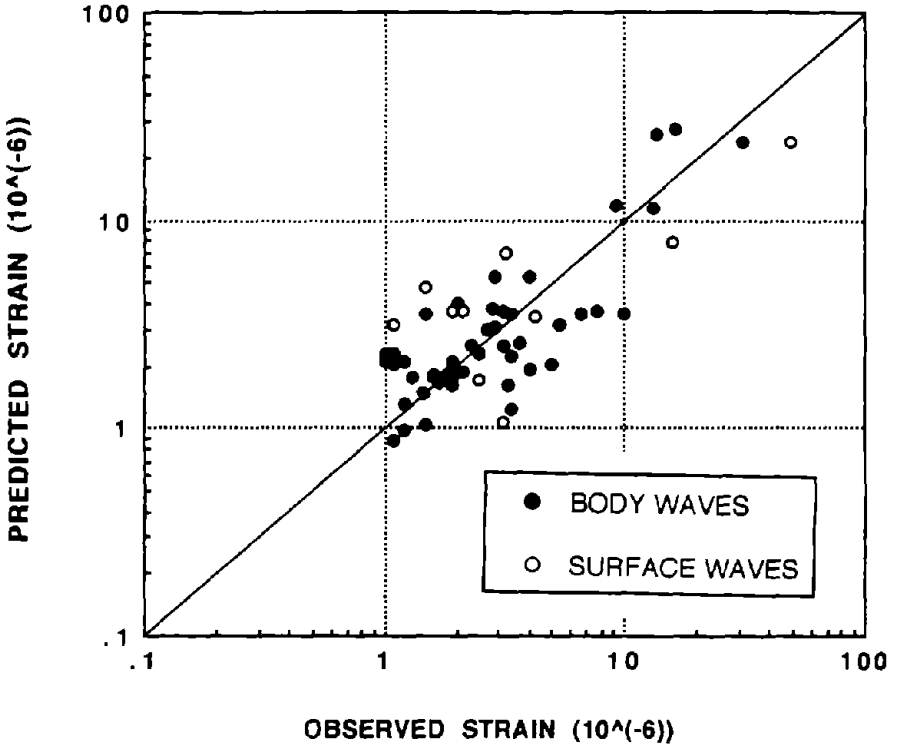

Fig.9-5 **Comparison Between Observed Soil Strain at the Kubota Corp. Kansen Site and Predicted Values from Eqs.(9.3) or (9.4)**

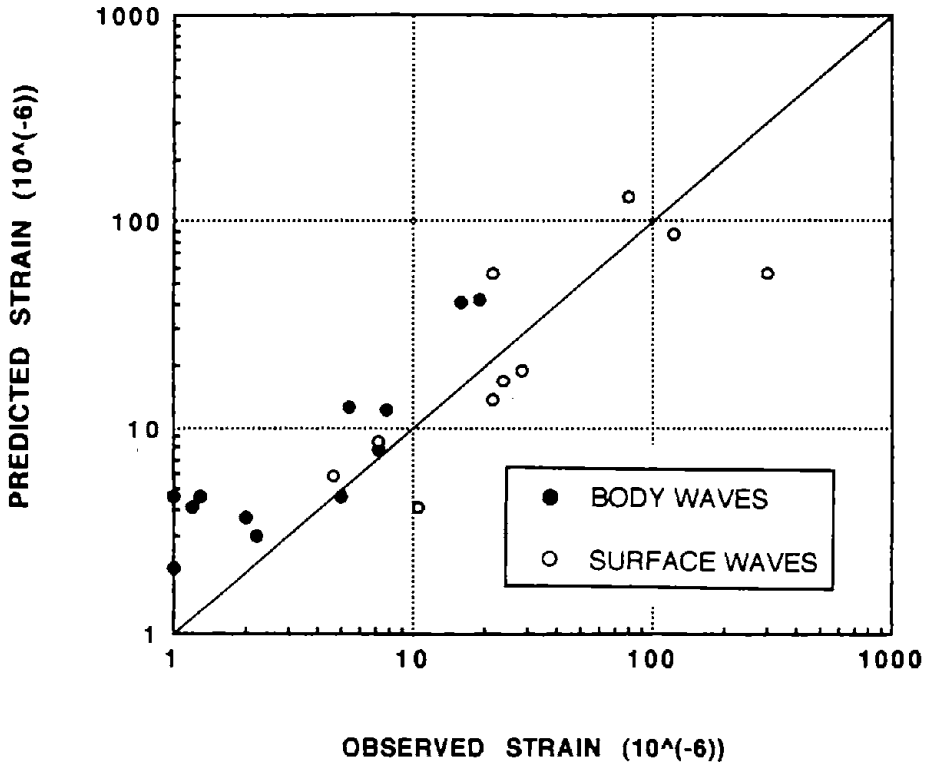

Fig.9-6 **Comparison Between Observed Soil Strain at the Kubota Corp. Shimonaga Site and Predicted Values from Eqs.(9.3) or (9.4)**

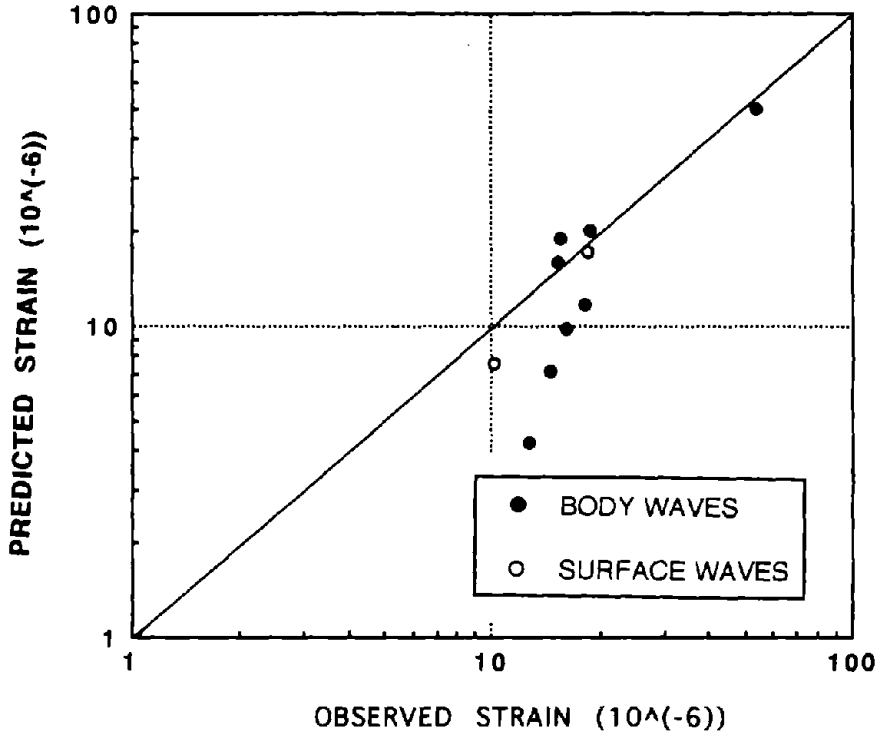

Fig.9-7 Comparison Between Observed Soil Strain at the Univ. of Tokyo Chiba Site and Predicted Values from Eqs.(9.3) or (9.4)

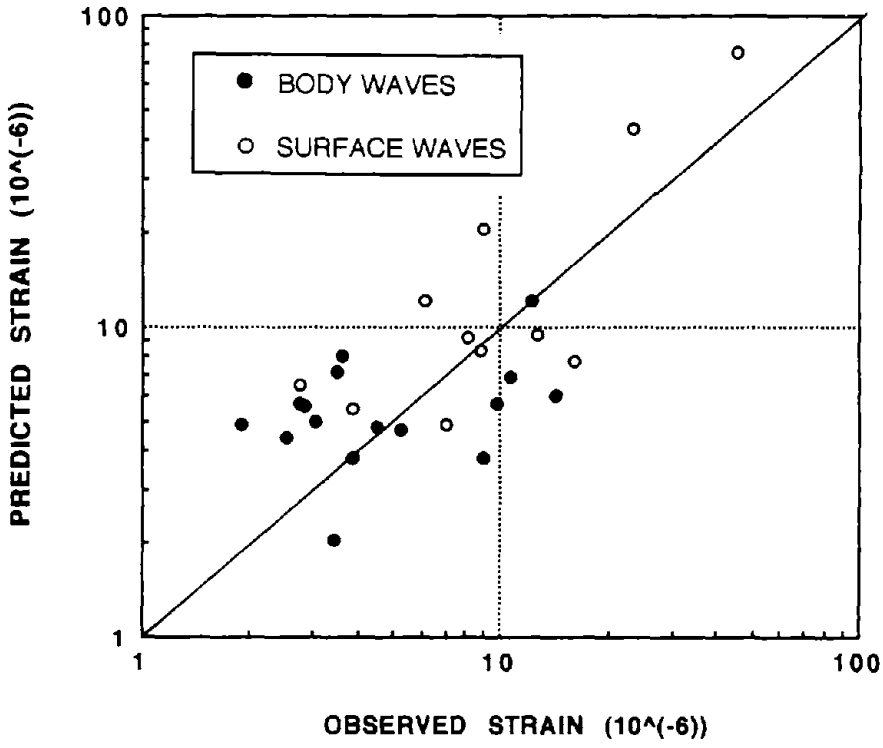

Fig.9-8 Comparison Between Observed Soil Strain at the Chubu Electric Power Corp.Chubu Site and Predicted Values from Eqs.(9.3) or (9.4)

and predicted values. Some of this scatter is attributed to errors in estimated values for the peak particle velocity, $\mathbf{v_{max}}$, as shown for example in Fig.4-3. Another source for error is inaccuracy in the measured soil strain. For example the measured strain would be less than the maximum soil strain at a site if the measuring device was not parallel to the direction of wave propagation. This is a possible explanation for points above the 1 to 1 match line in Figs.9-5 through 9-8. Finally for sites where surface waves are likely, we assume that the peak velocity, $\mathbf{v_{max}}$, occurs during the later surface wave portion of the record. In addition we assume that predominant period of that peak motion corresponds to the natural frequency of soil layer in shear. It is of course possible that the peak velocity, $\mathbf{v_{max}}$, may occur during the body wave portion of the record. It is also possible that the predominant frequency of surface waves is somewhat higher than $\mathbf{0.25C_L/h}$ and R-wave phase velocity in Fig.9-1 would hence be less than $\mathbf{0.875C_H}$. However if both these happen together, the soil strain which is a quotient might remain relatively unchanged from that given by Eq.(9.3).

SECTION 10
SUMMARY AND CONCLUSIONS

This report dealt with a semi-empirical model for estimating the peak values of strong motions with emphasis on the peak velocity which is needed for lifeline earthquake engineering studies. In the derivation of the model, theoretical information about seismic sources was combined with a statistical analysis of strong-motion data from Japan. The concept of dummy variables was used to obtain amplification factors due to individual local site conditions in the statistical analysis. An attenuation law for the peak acceleration, peak velocity and peak displacement on a rock was also obtained in terms of earthquake magnitude and hypocentral distance. The resulting amplification factors for peak velocity due to local site conditions were examined in connection with spectral amplification and soil profile, providing a method to predict the amplification factor at a new site. In addition, the resulting attenuation law for peak values on a rock was successfully compared with strong-motion data observed during three representative earthquakes in the U.S. and Mexico. Attenuation laws for strong motions by other researchers were also compared against the proposed model. Finally, a simplified method for estimating soil strain was developed. The main conclusions from this study are summarized as follows:

(1) Purely empirical models for prediction of strong-motion parameters suffer due to the fact that there usually is a correlation between the supposed independent variables in the strong-motion data. It is possible to overcome this difficulty as done herein by employing a standard attenuation coefficient empirically derived from extensive earthquake data collected by JMA.

(2) Amplification factor due to local site effects depends on the individual observation sites in contrast to the rough classification system commonly used by other researches. We developed a method for obtaining amplification factors at each observation site with the help of dummy variables. Results indicated that amplification factors vary remarkably from site to site and also depend on motion characteristics of interest, i.e.: acceleration, velocity and displacement.

(3) From a comparison against the amplification spectra, it was concluded that acceleration amplification is exclusively determined by period components less than about 0.3 sec while velocity's amplification is closely related to period components greater than about 1.0 sec. These amplification factors are also intimately related to the soil profile. In this study, we proposed two methods for predicting amplification factors, the "qualitative method" and "quantitative method." In the former method the amplification factor is estimated by a visual comparison of soil profiles. In the latter method the amplification factor is calculated from the distribution of N-values in the soil profiles.

(4) Besides the amplification factors due to local site effects, we obtained a set of attenuation laws for peak values on the seismic bed rock using the proposed model. The seismic bed rock was defined based on the selection of reference site for the regression analysis and then a reconsideration based upon the resulting amplification factors. For example, the seismic bed rock for peak velocity corresponds to the rock outcrop at OFUNATO whose shear wave velocity is about **2000** m/sec. The attenuation laws for seismic bed rock are expressed in terms of earthquake magnitude and hypocentral distance. The expressions for attenuation including the amplification factors $\mathbf{AMP_i}$ are given in Eqs.(5.1) to (5.6).

(5) On the assumption that earthquake strong motions are analogous to simple harmonic motion, we obtained a rough estimate of the predominant periods of acceleration and velocity motions expected at a rock site. The resultant predominant periods, which are summarized in Table 6-I, indicated a tendency of longer periods with increasing earthquake magnitude. Also the resulting predominant periods compared favorably with observations by Seed et al.

(6) The peaks of strong motions at a rock site predicted by the proposed model were compared with the observed values from the 1989 Loma Prieta earthquake, the 1985 Michoacan earthquake and 1971 San Fernando earthquake. It was shown that the proposed model predicts relatively well the observed data. In particular, we found a good agreement between the predicted and observed values in the comparisons of peak velocity which is a primary goal of this study. Since the proposed model was based solely on Japanese strong-motion data, this suggests that strong-motion peaks have a common attenuation law irrespective of country of origin. Empirical models developed by other researchers, though established using the strong-motion data in the U.S., were also compared with the proposed semi-empirical model. The comaprison showed that these existing empirical relarions do not provide better estimates to the observed data than the proposed semi-empirical model.

(7) Based upon the proposed semi-empirical model for peak velocity, a simplified method for estimating maximum normal or longitudinal soil strain was developed herein. A comparison of predicted strains with observed values showed that the simplified method is reasonably accurate.

Finally it is pointed out that the basic logic used in this report could be used to estimate not only peaks of strong motions but also other parameters related to earthquakes.

In this report, some simplified procedures were adopted based on practical considerations. For instance, the derivation of the amplification factors for a soil profile was performed using only typically available N-value data for soil, and deep layers down to real bed rock were not considered. Using more detailed soil and rock information, more accurate amplification factor

could be obtained. Furthermore, non-linear material characteristics of soft soils were not dealt with in this report. These problems are open questions for possible further study.

SECTION 11
REFERENCES

1. Okamoto, S., Introduction to Earthquake Engineering, University of Tokyo Press, 1984, pp.65-96

2. Barenberg, M. E., Correlation of Pipeline Damage with Ground Motions, Journal of Geotechnical Engineering, Vol.114, No.6, 1988, pp.706-711

3. Aki, K., Seismological Synthesis of Strong Ground Motion, Proc. 9th World Conf. on Earthq. Eng., Vol.3, 1988, pp.9-17

4. Luco, J.E., On Strong Ground Motion Estimated Based on Models of the Radiated Spectrum, Bull. Seism. Soc. Am., Vol.75, No.3, 1985, pp.641-649

5. Joyner, W.B. and Boore, D. M., Measurement, Characterization and Prediction of Strong Ground Motion, in Earthquake Engineering and Soil Dynamics, Vol.2(Ed. J.L. Von Thun), ASCE, 1988, pp.103-155

6. Campbell, K.W., Strong Motion Attenuation Relations: Ten-Year Perspective, Earthquake Spectra, Vol.1, No.4, 1985, pp.759-804

7. Campbell, K.W., Near-Source Attenuation of Peak Horizontal Acceleration, Bull. Seism. Soc. Am., Vol.71, 1981, pp.2039-2070

8. Fukushima, Y. and Tanaka, T., A New Attenuation Relation for Peak Horizontal Acceleration of Strong Earthquake Ground Motion in Japan, Bull. Seism. Soc. Am., Vol.80, No.4, 1990, pp.757-783

9. Kamiyama, M. and Yanagisawa, E., A Statistical Model for Estimating Response Spectra of Strong Earthquake Ground Motions With Emphasis on Local Soil Conditions, Soils and Foundations, Vol.26, No.2, 1986, pp.16-32

10. Draper, N. R. and Smith, H., Applied Regression Analysis, New York, John Wiley And Sans Inc., 1966

11. Joyner, W.B. and Boore, D.M., Peak Horizontal Acceleration and Velocity from Strong-Motion Records Including Records from the 1979 Imperial Valley, California, Earthquake, Bull. Seism. Soc. Am., Vol.71, 1981, pp.2011-2038

12. Trifunac, M.D., Preliminary Analysis of the Peaks of Strong Earthquake Ground Motion - Dependence of Peaks on Earthquake Magnitude, Epicentral Distance, and Recording Site Conditions, Bull. Seism. Soc. Am., Vol.66, 1976, pp.189-219

13. Richter, C.F., Elementary Seismology, Freeman, San Francisco, 1958

14. Kanbayashi, Y. and Ichikawa, M., A Method for Determining Magnitude of Shallow Earthquakes Occurring in and around Japan, Quarter Journal Seismology, Vol.41, 1977, pp.57-61(in Japanese)

15. Aki, K., Asperities, Barriers, Characteristic Earthquakes and Strong Motion Prediction, Journal Geophys. Res., Vol.89, No.B7, 1984, pp.5867-5872

16. Papageorgiou A.S. and Aki, K., A Specific Barrier Model for the Quantitative Description of Inhomogeneous Faulting and the Prediction of Strong Ground Motion, Part 1 and Part 2, Bull. Seism. Soc. Am., Vol.73, 1983, pp.693-722, pp.953-978

17. Ida, Y. The Maximum Acceleration of Seismic Ground Motion, Bull. Seism. Soc. Am., Vol.63, 1973, pp.959-968

18. Chin B.H and Aki, K., Simultaneous Study of the source , Path, and Site Effects on Strong Ground Motion During the 1989 Loma Prieta Earthquake: A Preliminary Result on Pervasive Nonlinear Site Effects, Bull. Seism. Soc. Am., Vol.81, No.5, 1991, pp.1859-1884

19. Kamiyama, M. and Matsukawa, T., An Empirical Scaling of Strong-Motion Spectra with Application to Estimate of Source Spectra, Structural Eng. and Earthq. Eng.(Proc. of Japan Soc. Civil Eng.), Vol.7, No.2, 1990, pp.331-342

20. Tsuchida, H. et al., Annual Report on Strong-Motion Earthquake Records in Japan Ports 1968-199, Technical Notes of the Port and Harbor Research Institute, No.98-No.649, The Port and Harbor Research Institute, Ministry of Transport, 1969-1990

21. Iwasaki, T. et al., Strong-Motion Acceleration Records from Public Works in Japan No.1-No.8, Technical Notes of the Public Works Research Institute, Vol.32-38, The Public Works Research Institute, Ministry of Construction, 1978-1983

22. Iai, S., Kurata, E. and Tsuchida, H., Digitization and Correction of Strong-Motion Accelerograms, Technical Note of the Port and Harbor Research Institute, No.286, 1978, pp.5-56(in Japanese)

23. Sato, R., Theoretical Basis on Relationship Between Focal Parameters and Earthquake Magnitude, Journal Phys. Earth, Vol.27, 1979, pp.353-372

24. Tsuchida, H. et al., Site Characteristics of Strong-Motion Earthquake Stations in Ports and Harbors in Japan (Part 1, 2 and 3), Technical Note of the Port and Harbor Research Institute, No.34, 107, 156, 1967-1973

25. Seed, H.B., Idriss, I.M. and Kiefer, F.W., Characteristics of Rock Motions During Earthquakes, Journal of Soil Mechanics and Foundations, ASCE, 1969 Septm, pp.1199-1218

26. McGuire, R.K., Seismic Ground Motion Parameter Relations, Journal Geotech. Eng. Div., ASCE, Vol.104, 1978, pp.481-490

27. Joyner, W.B. and Boore, D.M., Prediction of Earthquake Response Spectra, U.S. Geological Survey, Open-File Report 82-977, 1982, pp. 1-16

28. Campbell, K.W., Predicting Strong Ground Motion in Utah, in Evaluation of Regional and Urban Earthquake Hazards and Risks in Utah, 1988

29. Sabetta, F. and Pugliese A., Attenuation of Peak Horizontal Acceleration and Velocity from Italian Strong-Motion Records, Bull. Seism. Soc. Am., Vol.77, 1987, pp.1491-1513

30. Ohsaki, Y., Sawada, Y., Hayashi, T. Omura, H. and Kumagai, C., Spectral Characteristics of Hard Rock Motions, Proc. 7th World Conf. on Earthq. Eng., Vol.1, 1980, pp.231-238

31. Watabe, M. and Tohodo, M., Research on the Design Earthquake Ground Motions, Transaction of Architechture Institute of Japan, No.303, 1981, pp.41-51(in Japanese)

32. Kawashima, K., Aizawa, K. and Takahashi, K., Attenuation of Peak Ground Motion and Absolute Acceleration Response Spectra, Proc. 8th World Conf. on Earthq. Eng., Vol.2, 1984, pp.257-264

33. Shakal, A. et al., CSMIP, Strong-Motion Records from the Santa Cruz Mountains(Loma Prieta), California Earthquake of 17 October 1989, Report OSMS 89-06, 1989

34. UNAM, Institute of Engineering(II), Catalogo de Acelerograms por Fechas, Internal Report, 1991

35. California Institute of Technology, Earthquake Engineering Research Laboratory, Strong Motion Earthquake Accelerograms, Corrected Accelerograms and Integrated Ground Velocities and Displacements, Vol.2, Parts A-Y, 1971-1975

36 Hirasawa, T. and Stauder W., On the Seismic Body Waves from a Finite Moving Source, Bull. Seism. Soc. Am., Vol.55, 1965, pp.237-262

37. O'Rourke, M.J., Bloom, M. and Dobry, R., Apparent Propagation Velocity of Body Waves, International Journal of Earthquake Engineering and Structural Dynamics, Vol.10, 1982, pp.283-294

38 O'Rourke, M.J., Castro, G. and Hossain, I., Horizontal Soil Strain due to Seismic Waves, Journal of Geotechnical Engineering, Vol.110, No.9, 1984, pp.1173-1187

39 Nakamura, S., Prediction of the Characteristics of Surface Wave Considering Irregularity of Stratum and Application to Design, Doctoral Thesis, Tohoku University, 1989

40. Iwamoto, T. Yamamura, Y. and Miyamoto, H., Observation on Behaviors of Buried Pipelines and Ground Strain During Earthquakes, Proc. 9th World Conf. on Earthq. Eng., Vol.7, 1988, pp.35-41

41. Sato, N., Katayama, T. Nakamura, M., Iwamoto, T. and Ohbo, N., Observation of Seismic Ground Motion and Buried Pipe strain in a Very Dense Seismometer Array, Proc. 9th world Conf. on Earthq. Eng., Vol.7, 1988, pp.29-34

42. Ieda, R., Tsuchiyama, S., Nakamura, S. Yoshida, N. and Tsujino, S., Effect of Earthquake Motion on the Dynamic Behavior of Underground Transmission Line, Proc. 3rd International Conference on Soil Dynamics and Earthquake Engineering, 1987, pp.295-309

APPENDIX A

Table A-I List of Strong-Motion Records Used in This Study

357 strong motion records obtained at 33 observation sites

Observation site list

NO	SITE NAME
1	KUSHIRO
2	CHIYODA
3	TOKACHI
4	HOROMAN
5	SHIN ISHIKARI
6	TOMAKOMAI
7	MURORAN
8	AOMORI
9	HACHINOHE
10	MAZAKI
11	MIYAKO
12	OFUNATO (Reference site: hard slate)
13	SHIOGAMA
14	TAIRA
15	SHINTONE
16	KASHIMA JIMU
17	KASHIMA PWR
18	TONE ESD
19	OMIGAWA
20	CHIBA
21	YAMASHITA HEN
22	KANNONZAKI
23	OCHIAI
24	KINOKAWA
25	ITAJIMA
26	HOSOSHIMA
27	SOMA
28	SHINAGAWA
29	ONAHAMA JI
30	AKITA
31	CHIBA S
32	HITACHI NAKA
33	KASHIMA ZOKAN

Table A-I List of Strong-Motion Records Used in This Study (Cont'd)

NO	SITE	M	D (KM)	R_e (KM)	r (KM)	A_{max} (cm/sec^2)	V_{max} (cm/sec)	D_{max} (cm)
1	1	7.0	60.0	209.0	217.4	98.700	7.040	1.770
2	1	7.0	60.0	209.0	217.4	79.900	7.210	1.790
3	1	5.8	60.0	61.0	85.6	155.100	5.960	2.900
4	1	5.8	60.0	61.0	85.6	87.100	5.890	0.720
5	1	7.1	26.0	191.0	193.3	77.100	5.140	2.720
6	1	7.1	26.0	191.0	193.3	56.800	5.620	1.690
7	1	7.4	40.0	128.0	134.1	224.600	29.270	6.300
8	1	7.4	40.0	128.0	134.1	125.400	15.220	2.860
9	7	7.9	0.0	285.8	285.8	252.300	22.090	8.580
10	7	7.9	0.0	285.8	285.8	240.000	19.790	6.720
11	7	7.5	40.0	216.0	219.7	191.600	6.950	1.280
12	7	7.5	40.0	216.0	219.7	123.700	5.550	3.050
13	7	6.9	80.0	170.0	174.6	70.400	3.290	0.880
14	7	6.9	80.0	170.0	174.6	47.800	3.430	1.820
15	7	7.1	130.0	103.0	165.9	155.400	15.550	3.560
16	7	7.1	130.0	103.0	165.9	237.800	9.670	1.490
17	8	7.9	0.0	244.0	244.0	319.500	45.980	18.690
18	8	7.9	0.0	244.0	244.0	200.000	39.710	13.790
19	8	7.5	40.0	219.0	222.6	82.600	9.060	2.620
20	8	7.5	40.0	219.0	222.6	106.000	9.670	2.520
21	8	6.4	80.0	103.0	130.4	70.600	3.780	1.090
22	8	6.4	80.0	103.0	130.4	86.900	3.310	0.670
23	8	7.2	0.0	293.0	293.7	22.000	4.530	1.730
24	8	7.2	0.0	293.0	293.7	29.400	4.580	1.670
25	8	6.9	80.0	212.0	215.7	32.400	5.480	2.170
26	8	6.9	80.0	212.0	215.7	35.700	5.630	2.900
27	9	7.2	0.0	150.0	151.3	46.800	3.460	0.910
28	9	7.2	0.0	150.0	151.3	41.600	3.020	1.920
29	9	6.9	80.0	150.0	155.2	42.100	4.080	1.510
30	9	6.9	80.0	150.0	155.2	30.600	3.270	2.000
31	9	6.6	40.0	75.0	85.0	71.200	5.960	2.010
32	9	6.6	40.0	75.0	85.0	62.800	4.910	1.590
33	9	7.9	0.0	185.0	185.0	327.300	27.580	10.780
34	9	7.9	0.0	185.0	185.0	209.500	32.280	12.180
35	9	6.4	80.0	59.0	99.4	93.100	4.420	1.320
36	9	6.4	80.0	59.0	99.4	88.400	3.100	1.020
37	9	5.6	40.0	49.5	53.4	116.300	3.890	1.010
38	9	5.6	40.0	49.5	53.4	107.600	3.300	0.910
39	9	7.4	40.0	273.0	275.9	75.300	8.160	1.780
40	9	7.4	40.0	273.0	275.9	73.200	8.660	2.010
41	11	7.9	0.0	191.0	191.0	179.000	7.440	3.120
42	11	7.9	0.0	191.0	191.0	196.100	5.910	1.610
43	11	7.5	40.0	214.0	217.7	161.100	5.350	1.310
44	11	7.5	40.0	214.0	217.7	138.300	4.500	1.170
45	11	6.3	30.0	94.0	98.7	87.400	2.930	0.620

M=Magnitude, D=Depth, R_e=Epicentral distance, r=Hypocentral distance
A_{max} =Peak acceleration, V_{max} =Peak velocity, D_{max} =Peak displacement

Table A-I List of Strong-Motion Records Used in This Study (Cont'd)

NO	SITE	M	D (KM)	R_e (KM)	r (KM)	A_{max} (cm/sec^2)	V_{max} (cm/sec)	D_{max} (cm)
46	11	6.3	30.0	94.0	98.7	153.300	2.260	1.330
47	11	6.0	30.0	96.0	100.6	118.400	3.710	1.080
48	11	6.0	30.0	96.0	100.6	76.800	2.340	1.280
49	11	6.7	50.0	99.0	110.9	130.300	3.280	0.770
50	11	6.7	50.0	99.0	110.9	98.300	4.360	1.500
51	11	7.4	40.0	166.0	170.8	246.900	8.970	1.930
52	11	7.4	40.0	166.0	170.8	175.000	7.070	1.180
53	13	6.4	50.0	117.0	127.2	58.600	4.430	0.690
54	13	6.4	50.0	117.0	127.2	64.000	5.140	0.670
55	13	6.7	50.0	110.0	120.8	223.600	10.040	1.140
56	13	6.7	50.0	110.0	120.8	163.900	19.010	3.410
57	13	7.4	40.0	100.0	107.7	335.300	29.800	6.220
58	13	7.4	40.0	100.0	107.7	299.400	50.630	12.250
59	12	6.2	40.0	70.2	80.8	51.300	1.500	0.600
60	12	6.2	40.0	70.2	80.8	167.900	3.500	4.200
61	12	6.4	50.0	54.0	73.6	69.200	1.800	0.800
62	12	6.4	50.0	54.0	73.6	138.000	5.400	0.900
63	12	6.7	50.0	49.0	70.0	130.700	3.900	1.000
64	12	5.8	70.0	57.0	90.3	62.000	4.100	0.500
65	12	5.8	70.0	57.0	90.3	144.200	12.600	4.700
66	12	7.4	40.0	103.0	110.5	222.900	12.200	2.700
67	12	7.4	40.0	103.0	110.5	273.300	16.800	3.800
68	21	7.0	70.0	288.5	296.9	81.400	4.500	1.400
69	21	7.0	70.0	288.5	296.9	60.500	3.900	1.300
70	21	7.0	0.0	80.0	80.0	63.100	4.200	3.000
71	21	7.0	0.0	80.0	80.0	55.200	5.900	4.600
72	21	6.7	10.0	69.0	69.0	94.300	5.000	1.500
73	21	6.7	10.0	69.0	69.0	76.200	5.500	1.600
74	21	6.1	80.0	48.0	84.9	86.000	7.100	1.000
75	21	6.1	80.0	48.0	84.9	71.000	6.800	1.500
76	26	7.5	30.0	86.0	91.1	325.800	18.600	7.800
77	26	7.5	30.0	86.0	91.1	365.000	25.800	6.100
78	26	6.5	10.0	46.0	47.1	103.800	5.900	1.200
79	26	6.5	10.0	46.0	47.1	139.500	5.700	1.000
80	26	6.7	10.0	50.5	51.5	171.300	8.700	1.800
81	26	6.7	10.0	50.5	51.5	152.500	14.500	2.400
82	26	6.1	10.0	53.1	54.0	72.400	2.900	1.100
83	26	6.1	10.0	53.1	54.0	74.800	3.000	1.300
84	26	6.2	120.0	47.5	129.1	83.300	7.000	1.100
85	26	6.2	120.0	47.5	129.1	88.500	8.100	1.500
86	5	7.9	0.0	323.0	323.0	185.700	25.600	7.200
87	5	7.9	0.0	323.0	323.0	169.900	29.500	14.500
88	5	7.5	40.0	224.0	227.5	97.400	13.300	3.600
89	5	7.5	40.0	224.0	227.5	172.100	19.600	4.300
90	5	6.7	50.0	166.6	173.9	73.100	7.800	2.000
91	5	6.7	50.0	166.6	173.9	82.300	8.900	2.700
92	2	7.9	0.0	243.0	243.0	86.000	15.800	5.600

M=Magnitude, D=Depth, R_e=Epicentral distance, r=Hypocentral distance
A_{max} =Peak acceleration, V_{max} =Peak velocity, D_{max} =Peak displacement

Table A-I List of Strong-Motion Records Used in This Study (Cont'd)

NO	SITE	M	D (KM)	R_e (KM)	r (KM)	A_{max} (cm/sec^2)	V_{max} (cm/sec)	D_{max} (cm)
93	2	7.9	0.0	243.0	243.0	110.400	17.900	7.600
94	2	6.7	50.0	62.7	80.2	139.600	6.500	2.300
95	2	6.7	50.0	62.7	80.2	120.900	6.200	2.300
96	2	7.4	40.0	228.7	232.2	108.700	6.700	2.300
97	2	7.4	40.0	228.7	232.2	93.400	8.300	2.400
98	4	7.9	0.0	156.4	156.4	133.100	7.100	3.200
99	4	7.9	0.0	156.4	156.4	107.900	6.600	2.200
100	4	7.5	40.0	74.7	84.7	104.600	4.200	2.300
101	4	7.5	40.0	74.7	84.7	97.400	4.800	2.100
102	4	6.7	50.0	35.4	61.3	246.500	8.200	1.700
103	4	6.7	50.0	35.4	61.3	191.800	8.200	2.100
104	14	5.4	50.0	85.1	98.7	60.600	3.100	1.300
105	14	5.4	50.0	85.1	98.7	57.600	3.700	1.300
106	14	5.1	50.0	59.7	77.9	65.300	3.300	0.800
107	14	5.1	50.0	59.7	77.9	74.800	4.000	0.900
108	14	5.5	40.0	60.7	72.7	58.900	3.100	0.800
109	14	5.5	40.0	60.7	72.7	48.300	3.400	2.100
110	14	5.5	50.0	20.2	53.9	90.000	4.700	1.100
111	14	5.5	50.0	20.2	53.9	85.200	3.100	0.500
112	14	7.4	40.0	165.6	170.4	97.700	12.000	2.400
113	14	7.4	40.0	165.6	170.4	104.300	9.800	2.100
114	17	5.2	40.0	9.4	41.1	67.600	4.800	0.800
115	17	5.2	40.0	9.4	41.1	257.300	13.800	1.000
116	17	5.9	50.0	26.8	56.7	105.400	13.100	2.800
117	17	5.9	50.0	26.8	56.7	96.200	6.100	1.200
118	17	5.8	60.0	33.2	68.6	103.300	8.600	1.400
119	17	5.8	60.0	33.2	68.6	92.900	5.100	0.900
120	17	6.1	60.0	41.4	72.9	90.600	7.000	2.000
121	17	6.1	60.0	41.4	72.9	71.700	5.000	1.100
122	17	6.1	40.0	55.4	68.3	176.000	12.600	1.500
123	17	6.1	40.0	55.4	68.3	174.200	12.300	1.800
124	20	5.1	50.0	11.0	51.2	83.400	2.700	1.200
125	20	5.1	50.0	11.0	51.2	92.900	5.200	3.100
126	20	6.1	50.0	74.4	89.6	94.900	10.000	2.800
127	20	6.1	50.0	74.4	89.6	57.600	3.400	1.700
128	20	5.3	70.0	12.9	71.2	87.500	3.700	0.600
129	20	5.3	70.0	12.9	71.2	71.300	4.400	1.300
130	20	5.4	60.0	20.6	63.4	94.100	6.600	1.500
131	15	6.1	50.0	29.4	58.0	84.100	7.600	1.400
132	15	6.1	50.0	29.4	58.0	89.700	12.500	3.100
133	15	5.6	100.0	71.3	122.8	49.600	5.000	1.200
134	15	5.6	100.0	71.3	122.8	81.300	5.400	0.900
135	15	5.8	50.0	23.6	55.3	130.800	8.400	1.500
136	15	5.8	50.0	23.6	55.3	86.600	3.400	0.800
137	22	5.2	100.0	46.6	110.3	57.600	2.200	0.300
138	22	5.2	100.0	46.6	110.3	60.300	3.600	0.500
139	22	7.1	70.0	266.4	275.4	85.200	4.400	1.100

M=Magnitude, D=Depth, R_e=Epicentral distance, r=Hypocentral distance
A_{max} =Peak acceleration, V_{max} =Peak velocity, D_{max} =Peak displacement

Table A-I List of Strong-Motion Records Used in This Study (Cont'd)

NO	SITE	M	D (KM)	R_e (KM)	r (KM)	A_{max} (cm/sec^2)	V_{max} (cm/sec)	D_{max} (cm)
140	22	7.1	70.0	266.4	275.4	62.600	3.600	0.800
141	22	7.2	50.0	256.7	261.5	67.000	3.000	1.600
142	22	7.2	50.0	256.7	261.5	54.500	3.200	1.400
143	22	4.9	60.0	33.9	68.9	259.500	6.000	0.500
144	22	4.9	60.0	33.9	68.9	176.500	3.000	0.700
145	22	6.9	10.0	113.7	114.1	62.100	4.300	1.400
146	22	6.9	10.0	113.7	114.1	46.200	3.300	0.900
147	22	7.0	0.0	69.8	69.8	140.900	4.400	1.100
148	22	7.0	0.0	69.8	69.8	88.200	3.300	1.100
149	23	4.5	0.0	11.4	11.4	97.900	2.800	0.500
150	23	4.5	0.0	11.4	11.4	102.300	5.200	0.800
151	23	4.5	0.0	10.3	10.3	76.400	3.300	0.900
152	23	4.5	0.0	10.3	10.3	76.400	3.400	0.700
153	23	4.3	10.0	7.7	12.6	115.800	4.200	0.500
154	23	4.3	10.0	7.7	12.6	197.000	3.300	0.300
155	24	5.0	0.0	5.5	5.5	96.200	6.100	1.100
156	24	5.0	0.0	5.5	5.5	138.300	6.600	2.000
157	24	5.9	60.0	46.3	75.8	63.000	4.300	0.700
158	24	5.9	60.0	46.3	75.8	59.500	4.000	0.900
159	24	5.8	60.0	41.6	73.0	81.300	3.600	0.700
160	24	5.8	60.0	41.6	73.0	45.700	3.300	0.600
161	24	4.1	0.0	8.9	5.4	90.900	1.100	0.200
162	24	4.1	0.0	8.9	5.4	73.700	1.600	0.700
163	10	5.6	40.0	45.9	60.9	107.300	4.960	3.300
164	10	5.6	40.0	45.9	60.9	92.400	2.960	1.350
165	10	6.7	50.0	115.0	125.4	25.900	2.910	2.020
166	10	7.4	40.0	180.5	184.9	102.100	4.890	5.150
167	19	6.1	60.0	39.8	72.0	108.400	9.460	5.270
168	19	6.1	60.0	39.8	72.0	133.900	13.770	6.440
169	19	6.3	40.0	81.2	90.5	35.100	3.800	1.940
170	19	6.3	40.0	81.2	90.5	36.700	3.860	2.250
171	19	5.8	50.0	65.1	82.1	49.100	7.060	2.840
172	19	5.8	50.0	65.1	82.1	29.000	5.220	2.220
173	19	6.1	40.0	57.6	70.1	112.500	11.120	7.160
174	19	6.1	40.0	57.6	70.1	111.600	10.300	6.690
175	19	5.4	60.0	44.9	74.9	134.200	7.210	2.350
176	19	5.4	60.0	44.9	74.9	85.800	6.030	1.500
177	18	5.2	40.0	12.8	42.0	103.900	10.800	4.040
178	18	5.2	40.0	12.8	42.0	109.700	7.710	5.540
179	18	6.1	60.0	35.3	69.6	101.800	16.930	6.810
180	18	6.1	60.0	35.3	69.6	85.800	11.110	5.260
181	18	6.3	40.0	80.3	89.7	42.700	3.760	1.890
182	18	6.3	40.0	80.3	89.7	49.100	4.170	1.900
183	18	6.1	40.0	52.9	66.3	120.800	13.150	5.340
184	18	6.1	40.0	52.9	66.3	155.600	16.640	6.270
185	3	7.1	130.0	95.0	161.0	92.800	6.300	2.500
186	3	7.1	130.0	95.0	161.0	121.500	6.300	1.900

M=Magnitude, D=Depth, R_e=Epicentral distance, r=Hypocentral distance
A_{max} =Peak acceleration, V_{max} =Peak velocity, D_{max} =Peak displacement

Table A-I List of Strong-Motion Records Used in This Study (Cont'd)

NO	SITE	M	D (KM)	R_e (KM)	r (KM)	A_{max} (cm/sec^2)	V_{max} (cm/sec)	D_{max} (cm)
187	3	5.5	70.0	17.0	72.0	84.400	2.600	0.800
188	3	5.5	70.0	17.0	72.0	63.300	2.200	1.100
189	3	7.1	40.0	64.0	75.5	164.000	8.500	3.300
190	3	7.1	40.0	64.0	75.5	259.600	13.400	1.400
191	7	7.1	40.0	137.0	142.7	172.600	11.100	2.100
192	7	7.1	40.0	137.0	142.7	183.100	17.400	2.400
193	16	5.9	40.0	48.0	62.5	49.900	4.900	1.300
194	16	5.9	40.0	48.0	62.5	82.800	9.500	2.200
195	16	6.1	60.0	50.0	64.0	48.900	4.900	1.600
196	16	6.1	60.0	50.0	64.0	116.300	11.200	1.800
197	16	6.3	40.0	90.0	98.5	75.500	3.900	0.700
198	16	6.3	40.0	90.0	98.5	54.300	4.000	1.100
199	16	6.1	40.0	55.0	234.9	72.500	7.200	1.100
200	16	6.1	40.0	55.0	234.9	92.100	5.700	0.900
201	6	7.1	40.0	102.0	109.6	89.800	7.700	3.200
202	6	7.1	40.0	102.0	109.6	93.200	8.700	4.800
203	6	6.5	130.0	22.4	169.7	101.600	3.900	1.000
204	6	6.5	130.0	22.4	169.7	98.500	3.700	1.600
205	15	4.8	50.0	20.2	53.9	67.500	2.600	0.600
206	15	4.8	50.0	20.2	53.9	51.600	2.100	0.400
207	15	5.4	80.0	41.0	72.7	64.900	3.900	0.600
208	15	5.4	80.0	41.0	72.7	41.900	3.000	0.900
209	15	6.1	80.0	83.7	109.1	40.100	6.600	1.300
210	15	6.1	80.0	83.7	109.1	24.200	3.500	0.700
211	14	5.9	70.0	45.1	83.3	54.800	4.100	0.700
212	14	5.9	70.0	45.1	83.3	76.600	3.800	0.600
213	14	5.4	90.0	41.7	99.2	49.600	2.700	0.600
214	14	5.4	90.0	41.7	99.2	83.300	3.300	0.800
215	22	6.1	80.0	49.0	85.4	65.500	3.800	0.800
216	22	6.1	80.0	49.0	85.4	109.500	5.300	0.700
217	24	4.5	0.0	3.4	3.4	127.200	3.100	0.400
218	24	4.5	0.0	3.4	3.4	148.500	5.700	0.500
219	25	7.5	30.0	103.0	107.3	201.300	14.400	3.240
220	25	7.5	30.0	103.0	107.3	213.200	19.560	3.990
221	25	6.6	40.0	18.7	44.2	699.100	33.020	9.300
222	25	6.6	40.0	18.7	44.2	810.600	24.650	4.340
223	25	5.3	40.0	18.3	44.0	213.800	8.250	1.930
224	25	5.3	40.0	18.3	44.0	298.600	12.930	2.310
225	25	6.7	10.0	135.4	135.8	141.000	2.890	0.310
226	25	6.7	10.0	135.4	135.8	126.800	2.350	0.630
227	25	4.7	10.0	137.5	137.9	125.500	3.790	0.750
228	25	4.7	10.0	137.5	137.9	78.100	2.470	0.500
229	28	6.1	70.0	41.0	81.2	140.000	12.900	1.260
230	28	6.1	70.0	41.0	81.2	102.000	10.500	1.480
231	28	4.9	78.0	28.0	82.9	29.500	2.470	0.640
232	28	4.9	78.0	28.0	82.9	33.100	1.330	0.420
233	28	6.1	78.0	46.0	90.6	73.500	4.610	0.840

M=Magnitude, D=Depth, R_e=Epicentral distance, r=Hypocentral distance
A_{max} =Peak acceleration, V_{max} =Peak velocity, D_{max} =Peak displacement

Table A-I List of Strong-Motion Records Used in This Study (Cont'd)

NO	SITE	M	D (KM)	R_e (KM)	r (KM)	A_{max} (cm/sec^2)	V_{max} (cm/sec)	D_{max} (cm)
234	28	6.1	78.0	46.0	90.6	68.700	6.160	0.870
235	28	6.7	58.0	73.0	93.2	122.900	14.940	2.160
236	28	6.7	58.0	73.0	93.2	109.200	10.530	1.660
237	28	6.0	96.0	11.0	96.6	190.200	7.480	0.840
238	28	6.0	96.0	11.0	96.6	65.100	3.410	0.650
239	27	6.4	52.0	84.0	98.8	107.800	2.910	0.720
240	27	6.4	52.0	84.0	98.8	78.000	2.430	0.460
241	27	6.7	35.0	127.0	131.7	123.800	3.610	0.590
242	27	6.7	35.0	127.0	131.7	145.300	5.370	1.000
243	27	6.6	44.0	99.0	108.3	355.100	9.120	2.520
244	27	6.6	44.0	99.0	108.3	220.900	11.910	1.390
245	27	6.5	47.0	102.0	112.3	130.700	3.280	0.530
246	27	6.5	47.0	102.0	112.3	117.100	3.720	0.990
247	29	5.4	90.0	29.0	94.6	94.600	3.460	1.020
248	29	5.4	90.0	29.0	94.6	90.000	2.270	0.630
249	29	4.9	60.0	25.0	65.0	57.300	1.910	0.500
250	29	4.9	60.0	25.0	65.0	66.400	1.360	0.310
251	29	5.8	54.0	25.0	59.5	152.200	5.250	0.950
252	29	5.8	54.0	25.0	59.5	164.600	7.030	1.320
253	29	5.2	49.0	31.0	58.0	84.300	2.080	0.860
254	29	5.2	49.0	31.0	58.0	112.200	2.980	0.510
255	29	5.7	53.0	30.0	60.9	52.000	1.810	0.710
256	29	5.7	53.0	30.0	60.9	90.900	3.250	0.430
257	13	6.7	35.0	168.0	171.6	66.200	4.090	0.970
258	13	6.7	35.0	168.0	171.6	75.300	8.440	0.870
259	13	6.6	44.0	134.0	141.0	76.900	5.010	0.830
260	13	6.6	44.0	134.0	141.0	95.900	9.460	1.110
261	6	7.1	130.0	50.0	139.3	167.000	15.200	3.150
262	6	7.1	130.0	50.0	139.3	169.000	10.400	2.870
263	6	7.0	119.0	108.0	160.7	76.500	5.130	1.950
264	6	7.0	119.0	108.0	160.7	66.400	4.790	0.910
265	30	7.4	40.0	249.0	252.2	27.900	3.650	2.410
266	30	7.4	40.0	249.0	252.2	26.200	4.030	1.500
267	30	7.7	14.0	107.0	107.9	219.100	27.940	11.550
268	30	7.7	14.0	107.0	107.9	235.300	24.480	10.720
269	30	6.1	23.0	113.0	115.3	63.600	5.200	1.500
270	30	6.1	23.0	113.0	115.3	49.400	3.910	1.150
271	30	6.0	14.0	115.0	115.8	75.600	2.060	0.430
272	30	6.0	14.0	115.0	115.8	43.300	2.530	0.540
273	31	7.4	40.0	345.0	347.3	31.900	4.150	1.280
274	31	7.4	40.0	345.0	347.3	30.000	3.570	1.630
275	31	6.1	70.0	18.0	72.3	99.700	11.800	1.540
276	31	6.1	70.0	18.0	72.3	161.000	12.400	2.210
277	31	6.0	72.0	38.0	81.4	30.400	4.640	1.120
278	31	6.0	72.0	38.0	81.4	55.900	8.520	1.730
279	31	6.1	78.0	30.0	83.6	72.900	4.880	0.720
280	31	6.1	78.0	30.0	83.6	75.000	8.010	1.250

M=Magnitude, D=Depth, R_e=Epicentral distance, r=Hypocentral distance
A_{max} =Peak acceleration, V_{max} =Peak velocity, D_{max} =Peak displacement

Table A-I List of Strong-Motion Records Used in This Study (Cont'd)

NO	SITE	M	D (KM)	R_e (KM)	r (KM)	A_{max} (cm/sec^2)	V_{max} (cm/sec)	D_{max} (cm)
281	31	6.7	58.0	44.0	72.8	300.700	13.250	2.340
282	31	6.7	58.0	44.0	72.8	262.700	19.400	3.910
283	8	7.4	40.0	319.0	321.5	22.100	6.120	2.650
284	8	7.4	40.0	319.0	321.5	24.600	5.820	2.600
285	8	7.7	14.0	156.0	156.6	121.500	21.810	7.680
286	8	7.7	14.0	156.0	156.6	168.000	28.770	11.680
287	8	7.1	6.0	160.0	160.1	65.500	7.540	2.790
288	8	7.1	6.0	160.0	160.1	73.700	9.550	3.390
289	9	7.7	14.0	204.0	204.5	22.600	5.480	3.590
290	9	7.7	14.0	204.0	204.5	24.000	5.260	3.970
291	32	5.0	56.0	10.0	56.9	84.700	1.460	0.050
292	32	5.0	56.0	10.0	56.9	94.500	1.500	0.100
293	32	5.0	43.0	28.0	51.3	181.100	3.280	0.130
294	32	5.0	43.0	28.0	51.3	170.500	3.590	0.070
295	32	5.8	42.0	51.0	66.1	104.100	2.590	0.290
296	32	5.8	42.0	51.0	66.1	113.300	2.980	0.340
297	32	4.6	61.0	74.0	95.9	31.100	0.780	0.030
298	32	4.6	61.0	74.0	95.9	53.100	1.000	0.060
299	32	5.2	48.0	48.0	67.9	67.300	1.240	0.080
300	32	5.2	48.0	48.0	67.9	59.300	1.060	0.120
301	32	4.8	66.0	14.0	67.5	75.200	1.460	0.060
302	32	4.8	66.0	14.0	67.5	82.900	1.760	0.090
303	32	6.6	44.0	151.0	157.3	52.600	1.610	0.460
304	32	6.6	44.0	151.0	157.3	39.100	2.340	0.600
305	32	4.9	61.5	38.0	72.3	61.400	1.100	0.050
306	32	4.9	61.5	38.0	72.3	36.500	0.570	0.040
307	32	4.7	49.0	11.0	50.2	132.400	2.740	0.150
308	32	4.7	49.0	11.0	50.2	107.800	2.670	0.170
309	26	6.8	116.0	125.0	170.5	75.200	6.940	1.150
310	26	6.8	116.0	125.0	170.5	61.500	4.830	0.970
311	26	7.1	33.0	47.0	57.4	248.800	19.740	2.470
312	26	7.1	33.0	47.0	57.4	358.200	29.050	4.850
313	33	7.4	40.0	281.0	283.8	53.400	4.190	1.830
314	33	7.4	40.0	281.0	283.8	39.100	4.500	1.370
315	33	7.0	30.0	118.0	121.8	87.600	5.000	2.000
316	33	7.0	30.0	118.0	121.8	106.500	4.820	2.080
317	33	5.6	43.0	76.0	87.3	114.200	4.100	0.720
318	33	5.6	43.0	76.0	87.3	51.600	1.710	0.710
319	33	5.0	43.0	61.0	74.6	117.700	4.090	0.740
320	33	5.0	43.0	61.0	74.6	47.700	1.450	0.420
321	33	6.1	44.0	64.0	77.7	125.800	4.870	0.450
322	33	6.1	44.0	64.0	77.7	61.300	3.500	0.740
323	33	5.8	42.0	68.0	79.9	105.700	3.790	0.530
324	33	5.8	42.0	68.0	79.9	66.700	3.740	0.700
325	33	6.7	58.0	65.0	87.1	133.100	8.600	3.180
326	33	6.7	58.0	65.0	87.1	134.600	7.010	1.960
327	33	5.6	54.0	71.0	89.2	69.200	3.870	0.370

M=Magnitude, D=Depth, R_e=Epicentral distance, r=Hypocentral distance
A_{max} =Peak acceleration, V_{max} =Peak velocity, D_{max} =Peak displacement

Table A-I List of Strong-Motion Records Used in This Study (Cont'd)

NO	SITE	M	D (KM)	R_e (KM)	r (KM)	A_{max} (cm/sec^2)	V_{max} (cm/sec)	D_{max} (cm)
328	33	5.6	54.0	71.0	89.2	56.500	2.230	0.340
329	33	4.9	42.0	12.0	43.7	87.600	2.530	0.410
330	33	4.9	42.0	12.0	43.7	34.900	1.100	0.280
331	11	6.6	72.0	27.0	76.9	231.600	9.140	2.210
332	11	6.6	72.0	27.0	76.9	230.500	9.510	1.980
333	11	7.1	0.0	95.0	95.0	183.100	7.040	1.760
334	11	7.1	0.0	95.0	95.0	137.400	5.560	1.710
335	7	7.7	14.0	270.0	270.4	39.900	2.550	1.240
336	7	7.7	14.0	270.0	270.4	30.000	2.420	1.660
337	7	7.1	6.0	201.0	201.1	70.900	4.300	0.830
338	7	7.0	119.0	164.4	202.6	56.200	3.080	0.880
339	7	7.0	119.0	164.0	202.6	127.800	4.590	0.750
340	3	7.7	100.0	401.0	413.3	47.300	2.280	1.090
341	3	7.7	100.0	401.0	413.3	64.200	2.390	1.280
342	3	6.1	60.0	85.0	104.0	41.800	2.450	0.630
343	3	6.1	60.0	85.0	104.0	62.500	3.170	0.580
344	3	5.7	84.0	42.0	93.9	61.500	2.960	1.370
345	3	5.7	84.0	42.0	93.9	96.800	3.610	1.930
346	3	7.0	119.0	42.0	126.2	150.200	8.250	3.120
347	3	7.0	119.0	42.0	126.2	197.900	5.910	1.680
348	3	6.4	92.8	48.0	104.5	81.700	2.930	0.660
349	3	6.4	92.8	48.0	104.5	116.900	3.370	0.870
350	3	6.0	78.0	106.0	131.6	54.800	2.570	0.770
351	3	6.0	78.0	106.0	131.6	74.200	3.220	1.000
352	21	7.4	40.0	374.0	376.1	26.000	3.350	0.640
353	21	7.4	40.0	374.0	376.1	18.300	1.930	0.740
354	21	6.0	22.0	60.0	63.9	110.300	6.720	0.760
355	21	6.0	22.0	60.0	63.9	68.300	3.920	0.470
356	21	6.7	58.0	77.0	96.4	115.100	8.000	2.120
357	21	6.7	58.0	77.0	96.4	74.900	8.700	2.440

M=Magnitude, D=Depth, R_e=Epicentral distance, r=Hypocentral distance
A_{max} =Peak acceleration, V_{max} =Peak velocity, D_{max} =Peak displacement

APPENDIX B

Based on Fig.9-3, we obtain the following values.

i	x_i	$N(x_i)$	$\frac{\sqrt{N(x_{i+1})}}{\frac{1}{i}\sum_{j=1}^{i}\sqrt{N(x_j)}}$
1	1.5	24	0.456
2	2.5	5	0.627
3	3.7	5	0.784
4	5.0	6	0.830
5	7.0	6	1.402
6	8.0	16	1.469
7	9.0	20	1.192
8	10.0	15	1.344
9	12.0	20	1.357
10	13.0	22	1.186
11	14.0	18	1.347
12	15.5	24	1.362
13	17.5	26	1.246
14	18.5	23	1.574
15	20.0	38	1.650
16	21.0	45	1.671
17	23.0	50	

For example for i=10

$$\frac{\sqrt{N(x_{i+1})}}{\frac{1}{i}\sum_{j=1}^{i}\sqrt{N(x_j)}} = 1.186$$

Since the maximum value of the fourth column is for i=16, that is, M=16,

$$x_M = 21.0$$

$$\frac{1}{M}\sum_{j=1}^{M}\sqrt{N(x_j)} = 4.230$$

$$\mathrm{Max}\left[\frac{\sqrt{N(x_{i+1})}}{\frac{1}{i}\sum_{j=1}^{i}\sqrt{N(x_j)}}\right] = 1.671$$

and finally

$$C_{amp} = \mathrm{Max}\left[\frac{\sqrt{N(x_{i+1})}}{\frac{1}{i}\sum_{j=1}^{i}\sqrt{N(x_j)}}\right] \times \frac{x_M}{\frac{1}{M}\sum_{j=1}^{M}\sqrt{N(x_j)}}$$

$$= 1.671 \times \frac{21.0}{4.230}$$

$$= 8.30$$

NATIONAL CENTER FOR EARTHQUAKE ENGINEERING RESEARCH
LIST OF TECHNICAL REPORTS

The National Center for Earthquake Engineering Research (NCEER) publishes technical reports on a variety of subjects related to earthquake engineering written by authors funded through NCEER. These reports are available from both NCEER's Publications Department and the National Technical Information Service (NTIS). Requests for reports should be directed to the Publications Department, National Center for Earthquake Engineering Research, State University of New York at Buffalo, Red Jacket Quadrangle, Buffalo, New York 14261. Reports can also be requested through NTIS, 5285 Port Royal Road, Springfield, Virginia 22161. NTIS accession numbers are shown in parenthesis, if available.

NCEER-87-0001 "First-Year Program in Research, Education and Technology Transfer," 3/5/87, (PB88-134275/AS).

NCEER-87-0002 "Experimental Evaluation of Instantaneous Optimal Algorithms for Structural Control," by R.C. Lin, T.T. Soong and A.M. Reinhorn, 4/20/87, (PB88-134341/AS).

NCEER-87-0003 "Experimentation Using the Earthquake Simulation Facilities at University at Buffalo," by A.M. Reinhorn and R.L. Ketter, to be published.

NCEER-87-0004 "The System Characteristics and Performance of a Shaking Table," by J.S. Hwang, K.C. Chang and G.C. Lee, 6/1/87, (PB88-134259/AS). This report is available only through NTIS (see address given above).

NCEER-87-0005 "A Finite Element Formulation for Nonlinear Viscoplastic Material Using a Q Model," by O. Gyebi and G. Dasgupta, 11/2/87, (PB88-213764/AS).

NCEER-87-0006 "Symbolic Manipulation Program (SMP) - Algebraic Codes for Two and Three Dimensional Finite Element Formulations," by X. Lee and G. Dasgupta, 11/9/87, (PB88-219522/AS).

NCEER-87-0007 "Instantaneous Optimal Control Laws for Tall Buildings Under Seismic Excitations," by J.N. Yang, A. Akbarpour and P. Ghaemmaghami, 6/10/87, (PB88-134333/AS).

NCEER-87-0008 "IDARC: Inelastic Damage Analysis of Reinforced Concrete Frame - Shear-Wall Structures," by Y.J. Park, A.M. Reinhorn and S.K. Kunnath, 7/20/87, (PB88-134325/AS).

NCEER-87-0009 "Liquefaction Potential for New York State: A Preliminary Report on Sites in Manhattan and Buffalo," by M. Budhu, V. Vijayakumar, R.F. Giese and L. Baumgras, 8/31/87, (PB88-163704/AS). This report is available only through NTIS (see address given above).

NCEER-87-0010 "Vertical and Torsional Vibration of Foundations in Inhomogeneous Media," by A.S. Veletsos and K.W. Dotson, 6/1/87, (PB88-134291/AS).

NCEER-87-0011 "Seismic Probabilistic Risk Assessment and Seismic Margins Studies for Nuclear Power Plants," by Howard H.M. Hwang, 6/15/87, (PB88-134267/AS).

NCEER-87-0012 "Parametric Studies of Frequency Response of Secondary Systems Under Ground-Acceleration Excitations," by Y. Yong and Y.K. Lin, 6/10/87, (PB88-134309/AS).

NCEER-87-0013 "Frequency Response of Secondary Systems Under Seismic Excitation," by J.A. HoLung, J. Cai and Y.K. Lin, 7/31/87, (PB88-134317/AS).

NCEER-87-0014 "Modelling Earthquake Ground Motions in Seismically Active Regions Using Parametric Time Series Methods," by G.W. Ellis and A.S. Cakmak, 8/25/87, (PB88-134283/AS).

NCEER-87-0015 "Detection and Assessment of Seismic Structural Damage," by E. DiPasquale and A.S. Cakmak, 8/25/87, (PB88-163712/AS).

NCEER-87-0016 "Pipeline Experiment at Parkfield, California," by J. Isenberg and E. Richardson, 9/15/87, (PB88-163720/AS). This report is available only through NTIS (see address given above).

NCEER-87-0017 "Digital Simulation of Seismic Ground Motion," by M. Shinozuka, G. Deodatis and T. Harada, 8/31/87, (PB88-155197/AS). This report is available only through NTIS (see address given above).

NCEER-87-0018 "Practical Considerations for Structural Control: System Uncertainty, System Time Delay and Truncation of Small Control Forces," J.N. Yang and A. Akbarpour, 8/10/87, (PB88-163738/AS).

NCEER-87-0019 "Modal Analysis of Nonclassically Damped Structural Systems Using Canonical Transformation," by J.N. Yang, S. Sarkani and F.X. Long, 9/27/87, (PB88-187851/AS).

NCEER-87-0020 "A Nonstationary Solution in Random Vibration Theory," by J.R. Red-Horse and P.D. Spanos, 11/3/87, (PB88-163746/AS).

NCEER-87-0021 "Horizontal Impedances for Radially Inhomogeneous Viscoelastic Soil Layers," by A.S. Veletsos and K.W. Dotson, 10/15/87, (PB88-150859/AS).

NCEER-87-0022 "Seismic Damage Assessment of Reinforced Concrete Members," by Y.S. Chung, C. Meyer and M. Shinozuka, 10/9/87, (PB88-150867/AS). This report is available only through NTIS (see address given above).

NCEER-87-0023 "Active Structural Control in Civil Engineering," by T.T. Soong, 11/11/87, (PB88-187778/AS).

NCEER-87-0024 "Vertical and Torsional Impedances for Radially Inhomogeneous Viscoelastic Soil Layers," by K.W. Dotson and A.S. Veletsos, 12/87, (PB88-187786/AS).

NCEER-87-0025 "Proceedings from the Symposium on Seismic Hazards, Ground Motions, Soil-Liquefaction and Engineering Practice in Eastern North America," October 20-22, 1987, edited by K.H. Jacob, 12/87, (PB88-188115/AS).

NCEER-87-0026 "Report on the Whittier-Narrows, California, Earthquake of October 1, 1987," by J. Pantelic and A. Reinhorn, 11/87, (PB88-187752/AS). This report is available only through NTIS (see address given above).

NCEER-87-0027 "Design of a Modular Program for Transient Nonlinear Analysis of Large 3-D Building Structures," by S. Srivastav and J.F. Abel, 12/30/87, (PB88-187950/AS).

NCEER-87-0028 "Second-Year Program in Research, Education and Technology Transfer," 3/8/88, (PB88-219480/AS).

NCEER-88-0001 "Workshop on Seismic Computer Analysis and Design of Buildings With Interactive Graphics," by W. McGuire, J.F. Abel and C.H. Conley, 1/18/88, (PB88-187760/AS).

NCEER-88-0002 "Optimal Control of Nonlinear Flexible Structures," by J.N. Yang, F.X. Long and D. Wong, 1/22/88, (PB88-213772/AS).

NCEER-88-0003 "Substructuring Techniques in the Time Domain for Primary-Secondary Structural Systems," by G.D. Manolis and G. Juhn, 2/10/88, (PB88-213780/AS).

NCEER-88-0004 "Iterative Seismic Analysis of Primary-Secondary Systems," by A. Singhal, L.D. Lutes and P.D. Spanos, 2/23/88, (PB88-213798/AS).

NCEER-88-0005 "Stochastic Finite Element Expansion for Random Media," by P.D. Spanos and R. Ghanem, 3/14/88, (PB88-213806/AS).

NCEER-88-0006 "Combining Structural Optimization and Structural Control," by F.Y. Cheng and C.P. Pantelides, 1/10/88, (PB88-213814/AS).

NCEER-88-0007 "Seismic Performance Assessment of Code-Designed Structures," by H.H-M. Hwang, J-W. Jaw and H-J. Shau, 3/20/88, (PB88-219423/AS).

NCEER-88-0008 "Reliability Analysis of Code-Designed Structures Under Natural Hazards," by H.H-M. Hwang, H. Ushiba and M. Shinozuka, 2/29/88, (PB88-229471/AS).

NCEER-88-0009 "Seismic Fragility Analysis of Shear Wall Structures," by J-W Jaw and H.H-M. Hwang, 4/30/88, (PB89-102867/AS).

NCEER-88-0010 "Base Isolation of a Multi-Story Building Under a Harmonic Ground Motion - A Comparison of Performances of Various Systems," by F-G Fan, G. Ahmadi and I.G. Tadjbakhsh, 5/18/88, (PB89-122238/AS).

NCEER-88-0011 "Seismic Floor Response Spectra for a Combined System by Green's Functions," by F.M. Lavelle, L.A. Bergman and P.D. Spanos, 5/1/88, (PB89-102875/AS).

NCEER-88-0012 "A New Solution Technique for Randomly Excited Hysteretic Structures," by G.Q. Cai and Y.K. Lin, 5/16/88, (PB89-102883/AS).

NCEER-88-0013 "A Study of Radiation Damping and Soil-Structure Interaction Effects in the Centrifuge," by K. Weissman, supervised by J.H. Prevost, 5/24/88, (PB89-144703/AS).

NCEER-88-0014 "Parameter Identification and Implementation of a Kinematic Plasticity Model for Frictional Soils," by J.H. Prevost and D.V. Griffiths, to be published.

NCEER-88-0015 "Two- and Three- Dimensional Dynamic Finite Element Analyses of the Long Valley Dam," by D.V. Griffiths and J.H. Prevost, 6/17/88, (PB89-144711/AS).

NCEER-88-0016 "Damage Assessment of Reinforced Concrete Structures in Eastern United States," by A.M. Reinhorn, M.J. Seidel, S.K. Kunnath and Y.J. Park, 6/15/88, (PB89-122220/AS).

NCEER-88-0017 "Dynamic Compliance of Vertically Loaded Strip Foundations in Multilayered Viscoelastic Soils," by S. Ahmad and A.S.M. Israil, 6/17/88, (PB89-102891/AS).

NCEER-88-0018 "An Experimental Study of Seismic Structural Response With Added Viscoelastic Dampers," by R.C. Lin, Z. Liang, T.T. Soong and R.H. Zhang, 6/30/88, (PB89-122212/AS). This report is available only through NTIS (see address given above).

NCEER-88-0019 "Experimental Investigation of Primary - Secondary System Interaction," by G.D. Manolis, G. Juhn and A.M. Reinhorn, 5/27/88, (PB89-122204/AS).

NCEER-88-0020 "A Response Spectrum Approach For Analysis of Nonclassically Damped Structures," by J.N. Yang, S. Sarkani and F.X. Long, 4/22/88, (PB89-102909/AS).

NCEER-88-0021 "Seismic Interaction of Structures and Soils: Stochastic Approach," by A.S. Veletsos and A.M. Prasad, 7/21/88, (PB89-122196/AS).

NCEER-88-0022 "Identification of the Serviceability Limit State and Detection of Seismic Structural Damage," by E. DiPasquale and A.S. Cakmak, 6/15/88, (PB89-122188/AS). This report is available only through NTIS (see address given above).

NCEER-88-0023 "Multi-Hazard Risk Analysis: Case of a Simple Offshore Structure," by B.K. Bhartia and E.H. Vanmarcke, 7/21/88, (PB89-145213/AS).

NCEER-88-0024 "Automated Seismic Design of Reinforced Concrete Buildings," by Y.S. Chung, C. Meyer and M. Shinozuka, 7/5/88, (PB89-122170/AS). This report is available only through NTIS (see address given above).

NCEER-88-0025 "Experimental Study of Active Control of MDOF Structures Under Seismic Excitations," by L.L. Chung, R.C. Lin, T.T. Soong and A.M. Reinhorn, 7/10/88, (PB89-122600/AS).

NCEER-88-0026 "Earthquake Simulation Tests of a Low-Rise Metal Structure," by J.S. Hwang, K.C. Chang, G.C. Lee and R.L. Ketter, 8/1/88, (PB89-102917/AS).

NCEER-88-0027 "Systems Study of Urban Response and Reconstruction Due to Catastrophic Earthquakes," by F. Kozin and H.K. Zhou, 9/22/88, (PB90-162348/AS).

NCEER-88-0028 "Seismic Fragility Analysis of Plane Frame Structures," by H.H-M. Hwang and Y.K. Low, 7/31/88, (PB89-131445/AS).

NCEER-88-0029 "Response Analysis of Stochastic Structures," by A. Kardara, C. Bucher and M. Shinozuka, 9/22/88, (PB89-174429/AS).

NCEER-88-0030 "Nonnormal Accelerations Due to Yielding in a Primary Structure," by D.C.K. Chen and L.D. Lutes, 9/19/88, (PB89-131437/AS).

NCEER-88-0031 "Design Approaches for Soil-Structure Interaction," by A.S. Veletsos, A.M. Prasad and Y. Tang, 12/30/88, (PB89-174437/AS). This report is available only through NTIS (see address given above).

NCEER-88-0032 "A Re-evaluation of Design Spectra for Seismic Damage Control," by C.J. Turkstra and A.G. Tallin, 11/7/88, (PB89-145221/AS).

NCEER-88-0033 "The Behavior and Design of Noncontact Lap Splices Subjected to Repeated Inelastic Tensile Loading," by V.E. Sagan, P. Gergely and R.N. White, 12/8/88, (PB89-163737/AS).

NCEER-88-0034 "Seismic Response of Pile Foundations," by S.M. Mamoon, P.K. Banerjee and S. Ahmad, 11/1/88, (PB89-145239/AS).

NCEER-88-0035 "Modeling of R/C Building Structures With Flexible Floor Diaphragms (IDARC2)," by A.M. Reinhorn, S.K. Kunnath and N. Panahshahi, 9/7/88, (PB89-207153/AS).

NCEER-88-0036 "Solution of the Dam-Reservoir Interaction Problem Using a Combination of FEM, BEM with Particular Integrals, Modal Analysis, and Substructuring," by C-S. Tsai, G.C. Lee and R.L. Ketter, 12/31/88, (PB89-207146/AS).

NCEER-88-0037 "Optimal Placement of Actuators for Structural Control," by F.Y. Cheng and C.P. Pantelides, 8/15/88, (PB89-162846/AS).

NCEER-88-0038 "Teflon Bearings in Aseismic Base Isolation: Experimental Studies and Mathematical Modeling," by A. Mokha, M.C. Constantinou and A.M. Reinhorn, 12/5/88, (PB89-218457/AS). This report is available only through NTIS (see address given above).

NCEER-88-0039 "Seismic Behavior of Flat Slab High-Rise Buildings in the New York City Area," by P. Weidlinger and M. Ettouney, 10/15/88, (PB90-145681/AS).

NCEER-88-0040 "Evaluation of the Earthquake Resistance of Existing Buildings in New York City," by P. Weidlinger and M. Ettouney, 10/15/88, to be published.

NCEER-88-0041 "Small-Scale Modeling Techniques for Reinforced Concrete Structures Subjected to Seismic Loads," by W. Kim, A. El-Attar and R.N. White, 11/22/88, (PB89-189625/AS).

NCEER-88-0042 "Modeling Strong Ground Motion from Multiple Event Earthquakes," by G.W. Ellis and A.S. Cakmak, 10/15/88, (PB89-174445/AS).

NCEER-88-0043 "Nonstationary Models of Seismic Ground Acceleration," by M. Grigoriu, S.E. Ruiz and E. Rosenblueth, 7/15/88, (PB89-189617/AS).

NCEER-88-0044 "SARCF User's Guide: Seismic Analysis of Reinforced Concrete Frames," by Y.S. Chung, C. Meyer and M. Shinozuka, 11/9/88, (PB89-174452/AS).

NCEER-88-0045 "First Expert Panel Meeting on Disaster Research and Planning," edited by J. Pantelic and J. Stoyle, 9/15/88, (PB89-174460/AS).

NCEER-88-0046 "Preliminary Studies of the Effect of Degrading Infill Walls on the Nonlinear Seismic Response of Steel Frames," by C.Z. Chrysostomou, P. Gergely and J.F. Abel, 12/19/88, (PB89-208383/AS).

NCEER-88-0047 "Reinforced Concrete Frame Component Testing Facility - Design, Construction, Instrumentation and Operation," by S.P. Pessiki, C. Conley, T. Bond, P. Gergely and R.N. White, 12/16/88, (PB89-174478/AS).

NCEER-89-0001 "Effects of Protective Cushion and Soil Compliancy on the Response of Equipment Within a Seismically Excited Building," by J.A. HoLung, 2/16/89, (PB89-207179/AS).

NCEER-89-0002 "Statistical Evaluation of Response Modification Factors for Reinforced Concrete Structures," by H.H-M. Hwang and J-W. Jaw, 2/17/89, (PB89-207187/AS).

NCEER-89-0003 "Hysteretic Columns Under Random Excitation," by G-Q. Cai and Y.K. Lin, 1/9/89, (PB89-196513/AS).

NCEER-89-0004 "Experimental Study of 'Elephant Foot Bulge' Instability of Thin-Walled Metal Tanks," by Z-H. Jia and R.L. Ketter, 2/22/89, (PB89-207195/AS).

NCEER-89-0005 "Experiment on Performance of Buried Pipelines Across San Andreas Fault," by J. Isenberg, E. Richardson and T.D. O'Rourke, 3/10/89, (PB89-218440/AS).

NCEER-89-0006 "A Knowledge-Based Approach to Structural Design of Earthquake-Resistant Buildings," by M. Subramani, P. Gergely, C.H. Conley, J.F. Abel and A.H. Zaghw, 1/15/89, (PB89-218465/AS).

NCEER-89-0007 "Liquefaction Hazards and Their Effects on Buried Pipelines," by T.D. O'Rourke and P.A. Lane, 2/1/89, (PB89-218481).

NCEER-89-0008 "Fundamentals of System Identification in Structural Dynamics," by H. Imai, C-B. Yun, O. Maruyama and M. Shinozuka, 1/26/89, (PB89-207211/AS).

NCEER-89-0009 "Effects of the 1985 Michoacan Earthquake on Water Systems and Other Buried Lifelines in Mexico," by A.G. Ayala and M.J. O'Rourke, 3/8/89, (PB89-207229/AS).

NCEER-89-R010 "NCEER Bibliography of Earthquake Education Materials," by K.E.K. Ross, Second Revision, 9/1/89, (PB90-125352/AS).

NCEER-89-0011 "Inelastic Three-Dimensional Response Analysis of Reinforced Concrete Building Structures (IDARC-3D), Part I - Modeling," by S.K. Kunnath and A.M. Reinhorn, 4/17/89, (PB90-114612/AS).

NCEER-89-0012 "Recommended Modifications to ATC-14," by C.D. Poland and J.O. Malley, 4/12/89, (PB90-108648/AS).

NCEER-89-0013 "Repair and Strengthening of Beam-to-Column Connections Subjected to Earthquake Loading," by M. Corazao and A.J. Durrani, 2/28/89, (PB90-109885/AS).

NCEER-89-0014 "Program EXKAL2 for Identification of Structural Dynamic Systems," by O. Maruyama, C-B. Yun, M. Hoshiya and M. Shinozuka, 5/19/89, (PB90-109877/AS).

NCEER-89-0015 "Response of Frames With Bolted Semi-Rigid Connections, Part I - Experimental Study and Analytical Predictions," by P.J. DiCorso, A.M. Reinhorn, J.R. Dickerson, J.B. Radziminski and W.L. Harper, 6/1/89, to be published.

NCEER-89-0016 "ARMA Monte Carlo Simulation in Probabilistic Structural Analysis," by P.D. Spanos and M.P. Mignolet, 7/10/89, (PB90-109893/AS).

NCEER-89-P017 "Preliminary Proceedings from the Conference on Disaster Preparedness - The Place of Earthquake Education in Our Schools," Edited by K.E.K. Ross, 6/23/89.

NCEER-89-0017 "Proceedings from the Conference on Disaster Preparedness - The Place of Earthquake Education in Our Schools," Edited by K.E.K. Ross, 12/31/89, (PB90-207895). This report is available only through NTIS (see address given above).

NCEER-89-0018 "Multidimensional Models of Hysteretic Material Behavior for Vibration Analysis of Shape Memory Energy Absorbing Devices, by E.J. Graesser and F.A. Cozzarelli, 6/7/89, (PB90-164146/AS).

NCEER-89-0019 "Nonlinear Dynamic Analysis of Three-Dimensional Base Isolated Structures (3D-BASIS)," by S. Nagarajaiah, A.M. Reinhorn and M.C. Constantinou, 8/3/89, (PB90-161936/AS). This report is available only through NTIS (see address given above).

NCEER-89-0020 "Structural Control Considering Time-Rate of Control Forces and Control Rate Constraints," by F.Y. Cheng and C.P. Pantelides, 8/3/89, (PB90-120445/AS).

NCEER-89-0021 "Subsurface Conditions of Memphis and Shelby County," by K.W. Ng, T-S. Chang and H-H.M. Hwang, 7/26/89, (PB90-120437/AS).

NCEER-89-0022 "Seismic Wave Propagation Effects on Straight Jointed Buried Pipelines," by K. Elhmadi and M.J. O'Rourke, 8/24/89, (PB90-162322/AS).

NCEER-89-0023 "Workshop on Serviceability Analysis of Water Delivery Systems," edited by M. Grigoriu, 3/6/89, (PB90-127424/AS).

NCEER-89-0024 "Shaking Table Study of a 1/5 Scale Steel Frame Composed of Tapered Members," by K.C. Chang, J.S. Hwang and G.C. Lee, 9/18/89, (PB90-160169/AS).

NCEER-89-0025 "DYNA1D: A Computer Program for Nonlinear Seismic Site Response Analysis - Technical Documentation," by Jean H. Prevost, 9/14/89, (PB90-161944/AS). This report is available only through NTIS (see address given above).

NCEER-89-0026 "1:4 Scale Model Studies of Active Tendon Systems and Active Mass Dampers for Aseismic Protection," by A.M. Reinhorn, T.T. Soong, R.C. Lin, Y.P. Yang, Y. Fukao, H. Abe and M. Nakai, 9/15/89, (PB90-173246/AS).

NCEER-89-0027 "Scattering of Waves by Inclusions in a Nonhomogeneous Elastic Half Space Solved by Boundary Element Methods," by P.K. Hadley, A. Askar and A.S. Cakmak, 6/15/89, (PB90-145699/AS).

NCEER-89-0028 "Statistical Evaluation of Deflection Amplification Factors for Reinforced Concrete Structures," by H.H.M. Hwang, J-W. Jaw and A.L. Ch'ng, 8/31/89, (PB90-164633/AS).

NCEER-89-0029 "Bedrock Accelerations in Memphis Area Due to Large New Madrid Earthquakes," by H.H.M. Hwang, C.H.S. Chen and G. Yu, 11/7/89, (PB90-162330/AS).

NCEER-89-0030 "Seismic Behavior and Response Sensitivity of Secondary Structural Systems," by Y.Q. Chen and T.T. Soong, 10/23/89, (PB90-164658/AS).

NCEER-89-0031 "Random Vibration and Reliability Analysis of Primary-Secondary Structural Systems," by Y. Ibrahim, M. Grigoriu and T.T. Soong, 11/10/89, (PB90-161951/AS).

NCEER-89-0032 "Proceedings from the Second U.S. - Japan Workshop on Liquefaction, Large Ground Deformation and Their Effects on Lifelines, September 26-29, 1989," Edited by T.D. O'Rourke and M. Hamada, 12/1/89, (PB90-209388/AS).

NCEER-89-0033 "Deterministic Model for Seismic Damage Evaluation of Reinforced Concrete Structures," by J.M. Bracci, A.M. Reinhorn, J.B. Mander and S.K. Kunnath, 9/27/89.

NCEER-89-0034 "On the Relation Between Local and Global Damage Indices," by E. DiPasquale and A.S. Cakmak, 8/15/89, (PB90-173865).

NCEER-89-0035 "Cyclic Undrained Behavior of Nonplastic and Low Plasticity Silts," by A.J. Walker and H.E. Stewart, 7/26/89, (PB90-183518/AS).

NCEER-89-0036 "Liquefaction Potential of Surficial Deposits in the City of Buffalo, New York," by M. Budhu, R. Giese and L. Baumgrass, 1/17/89, (PB90-208455/AS).

NCEER-89-0037 "A Deterministic Assessment of Effects of Ground Motion Incoherence," by A.S. Veletsos and Y. Tang, 7/15/89, (PB90-164294/AS).

NCEER-89-0038 "Workshop on Ground Motion Parameters for Seismic Hazard Mapping," July 17-18, 1989, edited by R.V. Whitman, 12/1/89, (PB90-173923/AS).

NCEER-89-0039 "Seismic Effects on Elevated Transit Lines of the New York City Transit Authority," by C.J. Costantino, C.A. Miller and E. Heymsfield, 12/26/89, (PB90-207887/AS).

NCEER-89-0040 "Centrifugal Modeling of Dynamic Soil-Structure Interaction," by K. Weissman, Supervised by J.H. Prevost, 5/10/89, (PB90-207879/AS).

NCEER-89-0041 "Linearized Identification of Buildings With Cores for Seismic Vulnerability Assessment," by I-K. Ho and A.E. Aktan, 11/1/89, (PB90-251943/AS).

NCEER-90-0001 "Geotechnical and Lifeline Aspects of the October 17, 1989 Loma Prieta Earthquake in San Francisco," by T.D. O'Rourke, H.E. Stewart, F.T. Blackburn and T.S. Dickerman, 1/90, (PB90-208596/AS).

NCEER-90-0002 "Nonnormal Secondary Response Due to Yielding in a Primary Structure," by D.C.K. Chen and L.D. Lutes, 2/28/90, (PB90-251976/AS).

NCEER-90-0003 "Earthquake Education Materials for Grades K-12," by K.E.K. Ross, 4/16/90, (PB91-113415/AS).

NCEER-90-0004 "Catalog of Strong Motion Stations in Eastern North America," by R.W. Busby, 4/3/90, (PB90-251984)/AS.

NCEER-90-0005 "NCEER Strong-Motion Data Base: A User Manual for the GeoBase Release (Version 1.0 for the Sun3)," by P. Friberg and K. Jacob, 3/31/90 (PB90-258062/AS).

NCEER-90-0006 "Seismic Hazard Along a Crude Oil Pipeline in the Event of an 1811-1812 Type New Madrid Earthquake," by H.H.M. Hwang and C-H.S. Chen, 4/16/90(PB90-258054).

NCEER-90-0007 "Site-Specific Response Spectra for Memphis Sheahan Pumping Station," by H.H.M. Hwang and C.S. Lee, 5/15/90, (PB91-108811/AS).

NCEER-90-0008 "Pilot Study on Seismic Vulnerability of Crude Oil Transmission Systems," by T. Ariman, R. Dobry, M. Grigoriu, F. Kozin, M. O'Rourke, T. O'Rourke and M. Shinozuka, 5/25/90, (PB91-108837/AS).

NCEER-90-0009 "A Program to Generate Site Dependent Time Histories: EQGEN," by G.W. Ellis, M. Srinivasan and A.S. Cakmak, 1/30/90, (PB91-108829/AS).

NCEER-90-0010 "Active Isolation for Seismic Protection of Operating Rooms," by M.E. Talbott, Supervised by M. Shinozuka, 6/8/9, (PB91-110205/AS).

NCEER-90-0011 "Program LINEARID for Identification of Linear Structural Dynamic Systems," by C-B. Yun and M. Shinozuka, 6/25/90, (PB91-110312/AS).

NCEER-90-0012 "Two-Dimensional Two-Phase Elasto-Plastic Seismic Response of Earth Dams," by A.N. Yiagos, Supervised by J.H. Prevost, 6/20/90, (PB91-110197/AS).

NCEER-90-0013 "Secondary Systems in Base-Isolated Structures: Experimental Investigation, Stochastic Response and Stochastic Sensitivity," by G.D. Manolis, G. Juhn, M.C. Constantinou and A.M. Reinhorn, 7/1/90, (PB91-110320/AS).

NCEER-90-0014 "Seismic Behavior of Lightly-Reinforced Concrete Column and Beam-Column Joint Details," by S.P. Pessiki, C.H. Conley, P. Gergely and R.N. White, 8/22/90, (PB91-108795/AS).

NCEER-90-0015 "Two Hybrid Control Systems for Building Structures Under Strong Earthquakes," by J.N. Yang and A. Danielians, 6/29/90, (PB91-125393/AS).

NCEER-90-0016 "Instantaneous Optimal Control with Acceleration and Velocity Feedback," by J.N. Yang and Z. Li, 6/29/90, (PB91-125401/AS).

NCEER-90-0017 "Reconnaissance Report on the Northern Iran Earthquake of June 21, 1990," by M. Mehrain, 10/4/90, (PB91-125377/AS).

NCEER-90-0018 "Evaluation of Liquefaction Potential in Memphis and Shelby County," by T.S. Chang, P.S. Tang, C.S. Lee and H. Hwang, 8/10/90, (PB91-125427/AS).

NCEER-90-0019 "Experimental and Analytical Study of a Combined Sliding Disc Bearing and Helical Steel Spring Isolation System," by M.C. Constantinou, A.S. Mokha and A.M. Reinhorn, 10/4/90, (PB91-125385/AS).

NCEER-90-0020 "Experimental Study and Analytical Prediction of Earthquake Response of a Sliding Isolation System with a Spherical Surface," by A.S. Mokha, M.C. Constantinou and A.M. Reinhorn, 10/11/90, (PB91-125419/AS).

NCEER-90-0021 "Dynamic Interaction Factors for Floating Pile Groups," by G. Gazetas, K. Fan, A. Kaynia and E. Kausel, 9/10/90, (PB91-170381/AS).

NCEER-90-0022 "Evaluation of Seismic Damage Indices for Reinforced Concrete Structures," by S. Rodriguez-Gomez and A.S. Cakmak, 9/30/90, PB91-171322/AS).

NCEER-90-0023 "Study of Site Response at a Selected Memphis Site," by H. Desai, S. Ahmad, E.S. Gazetas and M.R. Oh, 10/11/90, (PB91-196857/AS).

NCEER-90-0024 "A User's Guide to Strongmo: Version 1.0 of NCEER's Strong-Motion Data Access Tool for PCs and Terminals," by P.A. Friberg and C.A.T. Susch, 11/15/90, (PB91-171272/AS).

NCEER-90-0025 "A Three-Dimensional Analytical Study of Spatial Variability of Seismic Ground Motions," by L-L. Hong and A.H.-S. Ang, 10/30/90, (PB91-170399/AS).

NCEER-90-0026 "MUMOID User's Guide - A Program for the Identification of Modal Parameters," by S. Rodriguez-Gomez and E. DiPasquale, 9/30/90, (PB91-171298/AS).

NCEER-90-0027 "SARCF-II User's Guide - Seismic Analysis of Reinforced Concrete Frames," by S. Rodriguez-Gomez, Y.S. Chung and C. Meyer, 9/30/90, (PB91-171280/AS).

NCEER-90-0028 "Viscous Dampers: Testing, Modeling and Application in Vibration and Seismic Isolation," by N. Makris and M.C. Constantinou, 12/20/90 (PB91-190561/AS).

NCEER-90-0029 "Soil Effects on Earthquake Ground Motions in the Memphis Area," by H. Hwang, C.S. Lee, K.W. Ng and T.S. Chang, 8/2/90, (PB91-190751/AS).

NCEER-91-0001 "Proceedings from the Third Japan-U.S. Workshop on Earthquake Resistant Design of Lifeline Facilities and Countermeasures for Soil Liquefaction, December 17-19, 1990," edited by T.D. O'Rourke and M. Hamada, 2/1/91, (PB91-179259/AS).

NCEER-91-0002 "Physical Space Solutions of Non-Proportionally Damped Systems," by M. Tong, Z. Liang and G.C. Lee, 1/15/91, (PB91-179242/AS).

NCEER-91-0003 "Seismic Response of Single Piles and Pile Groups," by K. Fan and G. Gazetas, 1/10/91, (PB92-174994/AS).

NCEER-91-0004 "Damping of Structures: Part 1 - Theory of Complex Damping," by Z. Liang and G. Lee, 10/10/91, (PB92-197235/AS).

NCEER-91-0005 "3D-BASIS - Nonlinear Dynamic Analysis of Three Dimensional Base Isolated Structures: Part II," by S. Nagarajaiah, A.M. Reinhorn and M.C. Constantinou, 2/28/91, (PB91-190553/AS).

NCEER-91-0006 "A Multidimensional Hysteretic Model for Plasticity Deforming Metals in Energy Absorbing Devices," by E.J. Graesser and F.A. Cozzarelli, 4/9/91, (PB92-108364/AS).

NCEER-91-0007 "A Framework for Customizable Knowledge-Based Expert Systems with an Application to a KBES for Evaluating the Seismic Resistance of Existing Buildings," by E.G. Ibarra-Anaya and S.J. Fenves, 4/9/91, (PB91-210930/AS).

NCEER-91-0008 "Nonlinear Analysis of Steel Frames with Semi-Rigid Connections Using the Capacity Spectrum Method," by G.G. Deierlein, S-H. Hsieh, Y-J. Shen and J.F. Abel, 7/2/91, (PB92-113828/AS).

NCEER-91-0009 "Earthquake Education Materials for Grades K-12," by K.E.K. Ross, 4/30/91, (PB91-212142/AS).

NCEER-91-0010 "Phase Wave Velocities and Displacement Phase Differences in a Harmonically Oscillating Pile," by N. Makris and G. Gazetas, 7/8/91, (PB92-108356/AS).

NCEER-91-0011 "Dynamic Characteristics of a Full-Size Five-Story Steel Structure and a 2/5 Scale Model," by K.C. Chang, G.C. Yao, G.C. Lee, D.S. Hao and Y.C. Yeh," 7/2/91.

NCEER-91-0012 "Seismic Response of a 2/5 Scale Steel Structure with Added Viscoelastic Dampers," by K.C. Chang, T.T. Soong, S-T. Oh and M.L. Lai, 5/17/91 (PB92-110816/AS).

NCEER-91-0013 "Earthquake Response of Retaining Walls; Full-Scale Testing and Computational Modeling," by S. Alampalli and A-W.M. Elgamal, 6/20/91, to be published.

NCEER-91-0014 "3D-BASIS-M: Nonlinear Dynamic Analysis of Multiple Building Base Isolated Structures," by P.C. Tsopelas, S. Nagarajaiah, M.C. Constantinou and A.M. Reinhorn, 5/28/91, (PB92-113885/AS).

NCEER-91-0015 "Evaluation of SEAOC Design Requirements for Sliding Isolated Structures," by D. Theodossiou and M.C. Constantinou, 6/10/91, (PB92-114602/AS).

NCEER-91-0016 "Closed-Loop Modal Testing of a 27-Story Reinforced Concrete Flat Plate-Core Building," by H.R. Somaprasad, T. Toksoy, H. Yoshiyuki and A.E. Aktan, 7/15/91, (PB92-129980/AS).

NCEER-91-0017 "Shake Table Test of a 1/6 Scale Two-Story Lightly Reinforced Concrete Building," by A.G. El-Attar, R.N. White and P. Gergely, 2/28/91, (PB92-222447/AS).

NCEER-91-0018 "Shake Table Test of a 1/8 Scale Three-Story Lightly Reinforced Concrete Building," by A.G. El-Attar, R.N. White and P. Gergely, 2/28/91.

NCEER-91-0019 "Transfer Functions for Rigid Rectangular Foundations," by A.S. Veletsos, A.M. Prasad and W.H. Wu, 7/31/91, to be published.

NCEER-91-0020 "Hybrid Control of Seismic-Excited Nonlinear and Inelastic Structural Systems," by J.N. Yang, Z. Li and A. Danielians, 8/1/91, (PB92-143171/AS).

NCEER-91-0021 "The NCEER-91 Earthquake Catalog: Improved Intensity-Based Magnitudes and Recurrence Relations for U.S. Earthquakes East of New Madrid," by L. Seeber and J.G. Armbruster, 8/28/91, (PB92-176742/AS).

NCEER-91-0022 "Proceedings from the Implementation of Earthquake Planning and Education in Schools: The Need for Change - The Roles of the Changemakers," by K.E.K. Ross and F. Winslow, 7/23/91, (PB92-129998/AS).

NCEER-91-0023 "A Study of Reliability-Based Criteria for Seismic Design of Reinforced Concrete Frame Buildings," by H.H.M. Hwang and H-M. Hsu, 8/10/91, (PB92-140235/AS).

NCEER-91-0024 "Experimental Verification of a Number of Structural System Identification Algorithms," by R.G. Ghanem, H. Gavin and M. Shinozuka, 9/18/91, (PB92-176577/AS).

NCEER-91-0025 "Probabilistic Evaluation of Liquefaction Potential," by H.H.M. Hwang and C.S. Lee," 11/25/91, (PB92-143429/AS).

NCEER-91-0026 "Instantaneous Optimal Control for Linear, Nonlinear and Hysteretic Structures - Stable Controllers," by J.N. Yang and Z. Li, 11/15/91, (PB92-163807/AS).

NCEER-91-0027 "Experimental and Theoretical Study of a Sliding Isolation System for Bridges," by M.C. Constantinou, A. Kartoum, A.M. Reinhorn and P. Bradford, 11/15/91, (PB92-176973/AS).

NCEER-92-0001 "Case Studies of Liquefaction and Lifeline Performance During Past Earthquakes, Volume 1: Japanese Case Studies," Edited by M. Hamada and T. O'Rourke, 2/17/92, (PB92-197243/AS).

NCEER-92-0002 "Case Studies of Liquefaction and Lifeline Performance During Past Earthquakes, Volume 2: United States Case Studies," Edited by T. O'Rourke and M. Hamada, 2/17/92, (PB92-197250/AS).

NCEER-92-0003 "Issues in Earthquake Education," Edited by K. Ross, 2/3/92, (PB92-222389/AS).

NCEER-92-0004 "Proceedings from the First U.S. - Japan Workshop on Earthquake Protective Systems for Bridges," 2/4/92, to be published.

NCEER-92-0005 "Seismic Ground Motion from a Haskell-Type Source in a Multiple-Layered Half-Space," A.P. Theoharis, G. Deodatis and M. Shinozuka, 1/2/92, to be published.

NCEER-92-0006 "Proceedings from the Site Effects Workshop," Edited by R. Whitman, 2/29/92, (PB92-197201/AS).

NCEER-92-0007 "Engineering Evaluation of Permanent Ground Deformations Due to Seismically-Induced Liquefaction," by M.H. Baziar, R. Dobry and A-W.M. Elgamal, 3/24/92, (PB92-222421/AS).

NCEER-92-0008 "A Procedure for the Seismic Evaluation of Buildings in the Central and Eastern United States," by C.D. Poland and J.O. Malley, 4/2/92, (PB92-222439/AS).

NCEER-92-0009 "Experimental and Analytical Study of a Hybrid Isolation System Using Friction Controllable Sliding Bearings," by M.Q. Feng, S. Fujii and M. Shinozuka, 5/15/92.

NCEER-92-0010 "Seismic Resistance of Slab-Column Connections in Existing Non-Ductile Flat-Plate Buildings," by A.J. Durrani and Y. Du, 5/18/92.

NCEER-92-0011 "The Hysteretic and Dynamic Behavior of Brick Masonry Walls Upgraded by Ferrocement Coatings Under Cyclic Loading and Strong Simulated Ground Motion," by H. Lee and S.P. Prawel, 5/11/92, to be published.

NCEER-92-0012 "Study of Wire Rope Systems for Seismic Protection of Equipment in Buildings," by G.F. Demetriades, M.C. Constantinou and A.M. Reinhorn, 5/20/92.

NCEER-92-0013 "Shape Memory Structural Dampers: Material Properties, Design and Seismic Testing," by P.R. Witting and F.A. Cozzarelli, 5/26/92.

NCEER-92-0014 "Longitudinal Permanent Ground Deformation Effects on Buried Continuous Pipelines," by M.J. O'Rourke, and C. Nordberg, 6/15/92.

NCEER-92-0015 "A Simulation Method for Stationary Gaussian Random Functions Based on the Sampling Theorem," by M. Grigoriu and S. Balopoulou, 6/11/92.

NCEER-92-0016 "Gravity-Load-Designed Reinforced Concrete Buildings: Seismic Evaluation of Existing Construction and Detailing Strategies for Improved Seismic Resistance," by G.W. Hoffmann, S.K. Kunnath, J.B. Mander and A.M. Reinhorn, 7/15/92, to be published.

NCEER-92-0017 "Observations on Water System and Pipeline Performance in the Limón Area of Costa Rica Due to the April 22, 1991 Earthquake," by M. O'Rourke and D. Ballantyne, 6/30/92.

NCEER-92-0018 "Fourth Edition of Earthquake Education Materials for Grades K-12," Edited by K.E.K. Ross, 8/10/92.

NCEER-92-0019 "Proceedings from the Fourth Japan-U.S. Workshop on Earthquake Resistant Design of Lifeline Facilities and Countermeasures for Soil Liquefaction," Edited by M. Hamada and T.D. O'Rourke, 8/12/92, to be published.

NCEER-92-0020 "Active Bracing System: A Full Scale Implementation of Active Control," by A.M. Reinhorn, T.T. Soong, R.C. Lin, M.A. Riley, Y.P. Wang, S. Aizawa and M. Higashino, 8/14/92.

NCEER-92-0021 "Empirical Analysis of Horizontal Ground Displacement Generated by Liquefaction-Induced Lateral Spreads," by S.F. Bartlett and T.L. Youd, 8/17/92, to be published.

NCEER-92-0022 "IDARC Version 3.0: Inelastic Damage Analysis of Reinforced Concrete Structures," by S.K. Kunnath, A.M. Reinhorn and R.F. Lobo, 8/31/92, to be published.

NCEER-92-0023 "A Semi-Empirical Analysis of Strong-Motion Peaks in Terms of Seismic Source, Propagation Path and Local Site Conditions, by M. Kamiyama, M.J. O'Rourke and R. Flores-Berrones, 9/9/92.

50272-101

REPORT DOCUMENTATION PAGE	1. REPORT NO. NCEER-92-0023	2.	3. PB93-150266

4. Title and Subtitle
A Semi-Empirical Analysis of Strong-Motion Peaks in Terms of Seismic Source, Propagation Path and Local Site Conditions

5. Report Date
September 9, 1992

6.

7. Author(s)
M. Kamiyama, M.J. O'Rourke and R. Flores-Berrones

8. Performing Organization Rept. No.

9. Performing Organization Name and Address
Department of Civil Engineering
Rensselaer Polytechnic Institute
Troy, New York 12180-3590

10. Project/Task/Work Unit No.

11. Contract(C) or Grant(G) No.
(C) BCS 90-25010
(G) NEC-91029

12. Sponsoring Organization Name and Address
National Center for Earthquake Engineering Research
State University of New York at Buffalo
Red Jacket Quadrangle
Buffalo, N.Y. 14261

13. Type of Report & Period Covered
Technical Report

14.

15. Supplementary Notes
This research was conducted at Rensselaer Polytechnic Institute and was partially supported by the National Science Foundation under Grant No. BCS 90-25010 and the New York State Science and Technology Foundation under Grant No. NEC-91029.

16. Abstract (Limit: 200 words)
The purpose of this report is to derive a new type of semi-empirical expression for scaling strong-motion peaks in terms of seismic source, propagation path and local site conditions. Peak acceleration, peak velocity and peak displacement are analyzed in a similar fashion because they are interrelated. However emphasis is placed on the peak velocity which is a key ground motion parameter for lifeline earthquake engineering studies. With the help of seismic source theories, the semi-empirical model is derived using strong motions obtained in Japan. In the derivation, statistical considerations are used in the selection of the model itself and the model parameters. Earthquake magnitude M and hypocentral distance r are selected as independent variables and the dummy variables are introduced to identify the amplification factor due to individual local site conditions. The resulting semi-empirical expressions for the peak acceleration, velocity and displacement are then compared with strong-motion data observed during three earthquakes in the U.S. and Mexico. This comparison suggests that the proposed semi-empirical model is superior to existing models for strong ground motion peaks. The amplification factors for acceleration, velocity and displacement peaks obtained empirically by the model are found to be period-dependent and related to local soil conditions. In addition, two methods for predicting the amplification factor at a new site are proposed. Finally, a simplified method for estimating maximum soil strain is presented with the aid of the proposed semi-empirical expression for the peak velocity.

17. Document Analysis a. Descriptors

b. Identifiers/Open-Ended Terms
EARTHQUAKE ENGINEERING. SEMI-EMPIRICAL MODELS. STRONG GROUND MOTION. PEAK GROUND VELOCITY. REGRESSION ANALYSIS. SOURCE PARAMETERS. MAGNITUDE DISTANCE RELATIONSHIPS. WAVE PROPAGATION. SOIL STRAIN. LOCAL SITE CONDITIONS. SCALING RELATIONSHIPS. SITE AMPLIFICATION FACTORS.

c. COSATI Field/Group

18. Availability Statement	19. Security Class (This Report)	21. No. of Pages
Release Unlimited	Unclassified	168
	20. Security Class (This Page) Unclassified	22. Price